DISSERTATION

PERFORMANCE-BASE SEISMIC DESIGN OF WOODFRAME BUILDINGS USING NON-LINEAR TIME HISTORY ANALYSIS

Submitted by

Hongyan Liu

Department of Civil and Environmental Engineering

In partial fulfillment of the requirements

For the Degree of Doctor of Philosophy

Colorado State University

Fort Collins, Colorado

Summer 2010

COLORADO STATE UNIVERSITY

April 28, 2009

WE HEREBY RECOMMEND THAT THE DISSERTATION PREPARED UNDER OUR SUPERVISION BY HONGYAN LIU ENTITLED PERFORMANCE-BASED SEISMIC DESIGN OF WOODFRAME BUILDINGS USING NON-LINEAR TIME HISTORY ANALYSIS BE ACCEPTED AS FULFILLING IN PART REQUIREMENTS FOR THE DEGREE OF DOCTOR OF PHILOSOPHY.

Committee on Graduate Work

Marvin E. Criswell

Paul R. Heyliger

Bolivar Senior

Adviser: John W. van de Lindt

Department Head: Luis Garcia

ABSTRACT OF DISSERTATION

PERFORMANCE-BASED SEISMIC DESIGN OF WOODFRAME BUILDINGS USING NON-LINEAR TIME HISTORY ANALYSIS

Performance-based seismic design (PBSD) is a developing design methodology in the modern seismic design and research community and has already been applied to concrete and steel structures. However, the application to woodframe buildings, which represents the vast majority of the residential building stock in North America, is still under early stage of development. The total economic loss directly connected with woodframe structures was more than $20 billion after the 1994 Northridge earthquake in California. This lesson provided the impetus for both engineers and researchers to realize that seismic design should focus on system behavior during an earthquake event instead of just at the component behavior, in other words, explicitly considering system behavior and performance of a structure. The current focus in force-based design philosophy for wood looks at the component level and then makes the assumption that system performance is ensured by the component design. Because of the limitations in current design methodology and concerns of system level performance, the concept of PBSD is being adapted and applied to woodframe buildings. The ultimate goal of this study is to develop a generalized PBSD procedure that can provide a specific level of performance for woodframe buildings under prescribed earthquake loading levels.

In order to achieve this goal, this study focuses on four objectives. The first objective is to develop a conceptual PBSD procedure suitable for woodframe buildings. This includes defining the performance expectations at system level with explicit probability measures, choosing an appropriate format for the design requirements, deciding on the numerical tools and steps to determine the design that satisfies these design requirements. The second objective is to improve the existing numerical model and include base isolation device as an option to woodframe buildings for the PBSD. This task involves numerical modeling and experimental testing of friction pendulum sliding bearing base isolation devices on the shake table at CSU. The third objective is to apply the proposed design procedure to realistic building designs. This includes several design examples in this study having different floor plans from low-rise to mid-rise buildings. The examples included in this study cover several typical floor plans in the U.S. for residential buildings. The design example also includes the use of FP base isolation on a mid-rise woodframe structure. Finally, the last objective of this study is to develop a simplified design procedure that can be used by average engineers without using advanced structural models and non-linear time history analysis. This was accomplished by developing the design tables that are generated through simplified models using non-linear time history analysis. The results are checked with full simulation thereby validating the approach.

The most significant anticipated contribution of this study to the woodframe design and research communities will be the development of a generalized PBSD and is only applied to a limited number of examples in this dissertation, the format of this procedure was based on and improved from the current state-of-the-research and can be extended to many different situations including base isolation as demonstrated herein. The simplified design procedure and the format of the design table is a good candidate for incorporation of PBSD into design practice because of the prescriptive approach.

Hongyan Liu
Department of Civil and Environmental Engineering
Colorado State University
Fort Collins CO 80523
Summer 2010

Dedication

To my loved parents and son

"He has made everything beautiful in its time."

-- Ecclesiastes

Acknowledgements

I would like to acknowledge the assistance, support and advice of many people without whom this work would not have been possible. Dr. John W. van de Lindt, my advisor, provided support, assistance, advice and helped me through the about 5 years of my study in the United States. Dr. van de Lindt always encouraged me to explore new ideas and was patient with me all the way. He gave me many suggestions and encouragement throughout my research work, and showed me how to formulate scientific ideas, carry out productive research, publish scientific work and write this dissertation. My appreciation is beyond words. I would also like to thank the other members of my graduate committee, Dr. Marvin Criswell, Dr. Paul Heyliger and Dr. Bolivar Senior. Their guidance and assistance is deeply appreciated. I would also like to thank my fellow graduate students at Colorado State University for their support, encouragement, assistance, and friendship.

I would like to thank the people that encouraged me to pursue my dreams and goals. I would like to thank Dr. Michael D. Symans and Jayesh Shinde on the discussion on base isolation. I would like to thank Horacio Garza Jr. and his crew for the support on all of my lab works throughout the years. I would like to thank James M. Foreman, Frederick A. Busch, Daniel Canda, Jason Barker, Doug Allen, Poljak Jean-Baptiste, Finot Jonathan, Norer Anroine, Karthik Rechan and Sangki Park for the help on the testing woodframe buildings. I would also like to thank Weichiang Pang, Jonathan Goode, Saharat Buddhawanna, Dao Nguyen Thang, Cater Mast, Kimberly Cronin, and Rebecca Atadero for their friendship, help, and support during my studies. In particular, I would like to thank my husband Shiling Pei and my son for their patience, support, friendship, and love.

Although I only acknowledge a few people here, I express my greatest appreciation to all who have helped me along the way to get to this point.

I would like to extend my thanks to my parents and many wonderful people I had been friend with in Fort Collins for their guidance, sacrifices, support, love, and advices. Anything that I have ever or will ever accomplish is due to them.

This study was supported, in part, by the National Science Foundation under Grant No. CMMI-0529903 (NEES Research) (The NEESWood Project). Any opinions, findings, and conclusions or recommendations expressed in this material are those of the authors and do not necessarily reflect the views of the National Science Foundation.

Table of Contents

List of Figures

Figure		Page

List of Tables

Table		Page

Chapter One

Introduction

1.1 Background and Problem Definition

Natural hazards can be divided into two major categories: one that has some level of warning, such as a tsunami, volcano, or hurricane and one that has virtually no warning, such as earthquakes, landslides, or tornadoes. However, whether there is warning time or not, it is generally accepted that all natural hazards, as their name duly implies, pose a threat to human safety and can be quite costly. Some of the difficulties that must be dealt with after a natural hazard are economic loss, loss of use of a structure, loss of life, and injury. Hence the duty of a modern day civil engineer is to design structures using appropriate methodologies and principles to protect against natural hazards and to mitigate the risk of severe financial loss as a result of those hazards. The objective of life safety have been practiced in civil engineering for many decades, but only recently has engineering a building for protection of property become an objective within seismic design.

An earthquake is caused by a sudden energy release in the Earth's crust. Seismic waves are generated during the processes which result in waves within the earth's crust which cause ground shaking at a point as the waves pass. The seismic motion is transferred from the ground to the foundations of structures. Depending on the seismic mass of the structure itself and the ground motion input at the base, relative acceleration will be generated during an earthquake. In brief, this action is equivalent to adding dynamic, or inertial, forces onto a structure. Although numerous earthquakes have occurred, each one is unique, making their uncertainty a remarkable characteristic that challenges earthquake engineers worldwide. Thus, the seismic demand on structures in seismic zones must consider the probabilistic nature of these events and engineers must attempt to balance cost with user requirements within this uncertain framework.

The most popular application of light-frame wood construction in North America is for residential buildings. Light-frame wood structures are quite complex in that they have numerous contributors to seismic performance, both structural and non-structural. For example, the structure itself contains interior and exterior walls, a roof diaphragm and trusses or joists, a floor system, as well as drywall and exterior sidings. Greater than 90% of single family homes in North America are light-frame wood construction. Light-frame wood buildings posses many advantages over heavier building types such as steel and concrete frame structures. For example, the environmental benefit from using a renewable material, such as wood, makes it a "greener" material (Lippke et al., 2006). In addition, for certain applications such as one to six story buildings, the cost of the material is significantly lower and the speed of construction for light-frame wood buildings is often significantly faster. The overall cost of a light-frame wood building at these heights is lower. Finally, the repair of light-frame wood buildings is quicker and less costly than concrete and steel structures following an earthquake, if the same lack of performance was observed. The fastest growing building type in urban California is the mixed use three to four story light-frame wood building sitting on top of one story of reinforced concrete.

In the United States, the design codes for the woodframe structures are currently based on the practice of shearwall selection for either an allowable stress or load and resistance factor design, which provide the primary resistance to lateral loading. The force-based design concept can be found in current design codes such as the National Design Specification (NDS, 2005) for wood construction implementing allowable stress design (ASD) and load and resistance factor design (LRFD). Since woodframe structures has relatively ductile behavior and are light weight, it is generally considered that woodframe structure performed well under earthquake hazards and they very rarely collapse. Generally speaking, the life safety design requirements for woodframe structures can be achieved for most earthquake events. But the focus on woodframe structures seismic research changed after the 1994 Northridge earthquake. The Northridge earthquake was the highest instrumentally recorded magnitude in an urban area in North America and represented one of the costliest natural disasters in U.S. history. The report shows that this earthquake caused nearly $40 billion in losses, 72 people died and over 12,000 people were injured. Most casualties and damage occurred in woodframe buildings, particularly multi-story buildings such as two story houses and three story apartment buildings. In fact, the losses associated with the repair costs for woodframe buildings was more than $20 billion according to the survey.

Performance-based seismic design (PBSD) is a new design philosophy and methodology which was is considered to be an important development in earthquake engineering (van de Lindt et al., 2008). In this next generation design method, the seismic demands are in terms of the performance level subjected to a predefined hazard level. In brief, the structure designed using this new method is expected to achieve certain performance level when subject to a certain hazard level. ASCE 41 (2006) is the first standard to outline the procedure for PBSD and provides detailed definitions of structural performance levels and the various seismic hazard levels. The state-of-the-art of the performance-based design for structures had been summarized in Foley (2002). In this document, Foley firstly overviewed the fundamental components of performance-based design (PBD) in detail, explaining performance level and the hazard level for different loads (seismic, wind and gravity load), addressing the combination of the performance and hazard levels and the roles they played in PBD. Then the methods to quantify performance for a steel structure and a reinforced concrete structure as well as the procedure to quantify different load events within a PBD context were addressed. Finally, the fundamental optimization theory, procedure and their application within a performance-based design framework was discussed. Liu et al. (2005) stated that the design of steel special moment-resisting frame (SMRF) structures using performance-based seismic design can be approached as a multi-objective optimization problem. A detailed literature review on current codes of seismic SMRF design can be founded in Liu (2005). Also in this paper, a general seismic design optimization procedure using a multi-objective optimization formulation was presented.

Following the 1994 Northridge Earthquake, the design of woodframe structures attracted the attention of engineers and researchers. Filiatrault et al. (2002) had a thorough literature review on force-based seismic design and listed several shortcomings of this method for woodframe structures. In that paper, they also demonstrated that the inter-story drift during an earthquake was a key parameter related to the damage to woodframe structures during earthquakes. The deformation limit states were addressed by several researchers (Rosowsky 2002, van de Lindt and Walz 2003) was and have been said to be the cornerstone of PBSD (Filiatrault et al., 2002). In recent years, the application of PBSD to woodframe structures has mainly concentrating on developing design procedures to control inter-story drift so that the damage during an earthquake is kept under control. Several studies have utilized inter-story drift as the performance metric in performance-based seismic design of wood frame structures including van de Lindt et al. (2007, 2008). Most recently, Pei and van de Lindt (2008) proposed a loss based seismic design which was a new design method based on the assembly-based vulnerability procedure of Porter et al. (2001) to perform loss estimation. Recently, Pang et al. (2007) extended the direct displacement design procedure of Priestly (1998) to multi-story woodframe buildings. At present there is no universal standard for PBSD of woodframe structures beyond ASCE 41 (2007) which has many assumptions that have yet to be verified.

1.2 Expected Results and Contributions

Similar to the qualitative and quantitative definitions for structure/component performance levels and seismic hazard levels in ASCE 41, a format for building performance targets will be proposed in this dissertation. The remarkable difference between the performance levels proposed here and in ASCE 41 is that other generalized performances such as the floor acceleration will also be included and be considered as design control parameters as well as the inter-story drift. A practical PBSD procedure for woodframe buildings will be summarized in this dissertation and will be demonstrated through numerical simulations using the SAPWood software (Pei and van de Lindt, 2007). This procedure will be applied in the example buildings to control displacement and acceleration of woodframe structures under seismic loads and achieve the specified targets.

The application of base isolation systems to woodframe structures has by no means been extensive in civil engineering (Symans et al, 2002). In this dissertation, the base isolation system will be treated within the design process as an option for woodframe design in high seismic zones. The hysteric behavior of base isolation system will be modeled in SAPWood software. The overall numerical performance of the base isolation system and woodframe structure will be verified through a shake table experiment to ensure the accuracy of the numerical model. In addition, some constructability issues related to the isolation level floor system will be addressed during the construction and detailed herein.

With the help of the numerical simulations, incorporation of base isolation devices into PBSD will be conducted based on in the ability of the devices to reduce damage/losses.

The numerical examples in this dissertation include three single family houses with different floor plans, a three-story condominium, and the six-story Capstone woodframe building. The preliminary design of these structures will based on the current design codes ASCE 7 (2006) and the International Building Code (2006). In other words the size, nail pattern, materials and location of the shearwalls of these buildings will first be determined by the traditional force-based design procedure. The SAPWood numerical models will then be set up based on the preliminary design and the numerical simulations will be executed using a series of recorded earthquake records at different seismic hazard level. These numerical structural models will be modified using the generalized PBSD procedure proposed in this study. If the performance level does not satisfy the design target, a re-design of the structure will be carried out until the design targets are achieved. Moreover, if the re-designed structure still cannot satisfy the design target, a base isolation system may be applied as another option to ensure the structure achieve the design performance target defined in this study.

The practical PBSD procedure on woodframe structure proposed in this study requires step-by-step modifications based on nonlinear numerical simulations. This can be very tedious for engineers in design practice. Simplified models for one- and two-story woodframe building are built and analyzed with an earthquake ground motion suite for each hazard level defined in the design target curve and design tables were summarized in this study. These design tables can comprise a simplified version of the PBSD design procedure for woodframe structures. This will allow practical implementation/application of the complex time history analysis results discussed herein without the need for doing the analysis. The procedures to use the design tables will be suitable for simplified performance-based design of one- to two-story woodframe buildings.

This dissertation work will contribute to the state of the art in seismic analysis of woodframe structures and seismic design in four ways. Firstly, a general practical PBSD procedure is proposed that can be used to design woodframe structures. The procedure will be applied to different woodframe structure examples in this dissertation which can serve as design examples for engineers using this PBSD procedure. Secondly, a refined set of performance targets as combinations of structural responses and seismic hazard level is proposed in this dissertation, which is more general compared to existing PBSD literatures. In case of base isolation design, the isolation device performance will also be considered within the performance levels. Thirdly, the application of base isolation systems to woodframe structures is included in this dissertation and serves as an option for woodframe buildings in high seismic zones. Finally, a simplified PBSD procedure was proposed in the form of design charts and tables which will benefit the engineering profession by providing a viable and practical way to conduct PBSD.

1.3 Overview of Chapters

The remaining chapters of this dissertation lead the reader through the practical PBSD procedure for woodframe structures, the generalized performance targets for the structures and the earthquake hazard levels, the SAPWood software package for numerical simulation, one of base isolation system applied to light-frame wood structure, Friction Pendulum System (FPS), numerical model for FPS in SAPWood software, design of FPS using the PBSD procedure, experimental investigation and verification of numerical analysis, simulation of several different woodframe structures at different locations and finally the simplified design tables for design professionals. Subsequent chapters also provide the numerical and experimental results and discussions for the PBSD procedure on woodframe structure with or without FPS devices. Finally, conclusions and recommendations based on the results from this study are provided for the reader, for potential future research fields and for design professionals.

The summary of each chapter below provides a brief overview of the remaining sections in this dissertation:

Chapter 2: Performance-Based Seismic Design

Chapter 2 mainly discusses the next generation design philosophy, Performance-based Seismic Design (PBSD), for woodframe structures. Firstly, the history of PBSD and current practice on woodframe structure was reviewed in Section 2.1. Then the performance expectations on woodframe buildings in traditional force-based seismic design, ASCE 41, NEESWood project were introduced in Section 2.2. Based on the previous study, a more generalized performance expectation had been proposed which will be used throughout this dissertation for the PBSD examples in this study. The inter-story drift and floor acceleration had been chosen as the design target in this study. After the performance expectations are defined, a generalized practical PBSD procedure for woodframe structures is presented in Section 2.3 in the form of a flowchart. Thus, the steps of designing woodframe structures are systematically specified in this chapter. Finally, an existing numerical tool, the SAPWood software package, is introduced in Section 2.4. This software can execute nonlinear dynamic analysis on woodframe structures and will be used to perform the numerical analysis for the design examples in Chapter 5 and 6.

Chapter 3: Incorporation of FPS in PBSD

Chapter 3 presents the application of FP bearings in woodframe structures. The literature review on base isolation system was covered in Section 3.1. In Section 3.2, the performance of FP bearings was discussed. Based on the behavior of the FP bearings during an earthquake, a numerical model was programmed into the SAPWood software to incorporate the effects of FP bearings in time history analysis. FP bearings can be an option (sometimes might be the only option) in high seismic hazard level regions if a very strict performance target is required by the owner/user. The generalized PBSD procedure had been modified to include FP bearings and these changes were listed in

Section 3.4. An example of such situation was illustrated in Chapter 6 by imposing a strict performance level, especially for mid-rise woodframe buildings.

Chapter 4: Experimental investigation of a half-scale woodframe building on friction pendulum slider bearings

Chapter 4 provides the setup and discussion of the experimental study on FP bearing system and verification of numerical model through test results and numerical simulation comparison. In Section 4.1, the derivation of the scaling procedure for the woodframe building is presented. Then, in Section 4.2, a typical small California style single family house was designed and scaled to half size and was built in the Structural Engineering Laboratory (SEL) at Colorado State University. The uni-axial shake table tests of half-scale woodframe structure with FP bearings were conducted. The comparison between the experimental results and numerical prediction using SAPWood software package were conducted to verify the numerical model of the FP bearing developed in SAPWood. The application of FP bearing to woodframe buildings requires a stiff isolation level floor diaphragm to transfer shear force and support superstructure during an earthquake event. Therefore, in Section 4.4, the possibility of construct the full scale prototype of the foundation using a steel-wood combined diaphragm was discussed.

Chapter 5: Design examples using PBSD procedure

Chapter 5 presents in detail the proposed PBSD procedure of designing different woodframe structures at different locations. Three types of floor plan shape for single family houses were included in the design examples, namely rectangular, square and L-shape. The purpose of the different shapes of the woodframe building was to include as many variations of the representative buildings in practice as possible to verify the versatility of the design procedure. A three-story condominium building was also selected as the design example to illustrate the PBSD procedure on the typical multi-unit residential buildings in North America. A suite of recorded earthquake ground motion records from ATC 63 project were used as earthquake input in the numerical simulations. The formula of defining PNE value at each performance expectation segments in the design target curve was proposed in Section 5.2.5 which allows the end users' inputs to be considered in the design. Once the design target was defined, the application of the generalized PBSD procedure proposed in this dissertation, including the numerical simulation and revision steps, is executed and illustrated in detail through the design examples in this chapter.

Chapter 6: Mid-rise woodframe design example using PBSD procedure

Chapter 6 presents the generalized PBSD procedure applied to a mid-rise woodframe building used for the NEESWood project. The NEESWood Capstone structure is a six-story apartment building which will be tested on the world largest shake table in Japan in 2009. The preliminary design of the Capstone building was conducted using a PBSD procedure developed within the NEESWood project, namely direct displacement design (DDD) for woodframe structure. The numerical model corresponding to this design was built in SAPWood for numerical simulations in PBSD procedure. Numerical simulations were performed with ATC 63 earthquake records and the system performance, inter-story drift and floor acceleration, had been examined with the performance expectations calculated for mid-rise building in Los Angeles area. In order to control acceleration in addition to inter-story drifts, an alternative revision method, applying FP bearings under Capstone building, was conducted and investigated.

Chapter 7: Simplified Design Procedure

Chapter 7 presents the simplified procedure for PBSD of woodframe structures which provides a designer with the ability to directly utilize the results of nonlinear time history analysis without performing the simulation procedure. The simplified procedure was based on a great amount of the numerical simulation results on a simplified one-story and two-story woodframe assembly and was presented in the form of design tables. Two examples were performed using the simplified procedure to examine the feasibility of the simplified procedure and the final design results were verified using time history analysis. Practitioners may benefit from this simplified procedure if they want to adopt the requirements in PBSD to design woodframe structures.

Chapter 8: Summary, Conclusions and Contributions

Chapter 8 presents the conclusions, contributions and recommendations as a final result for this study. These conclusions and contributions are obtained based on numerical simulations and the application of the PBSD procedure to the illustrative design examples conducted in this dissertation. The recommendations for future research based on the work in this study are also suggested.

Chapter Two

Performance-based Seismic Design

2.1 State of the practice for woodframe buildings

Performance-based seismic design (PBSD) is a new design philosophy felt by the vast majority of researchers and many practitioners to have the potential to improve seismic design. PBSD explicitly considers both the performance expectations of the structure and the seismic hazard level to ensure that the owner's expectations are met. In addition, a key feature of this philosophy is the explicit consideration of structural and non-structural components' impact on performance since models of the structural behavior are considered and not simply stresses or forces. The application of PBSD can be found in reinforced concrete and steel buildings as well as bridge structures. For woodframe buildings this new design philosophy is still under development within the worldwide research community. Several researchers around the world have preliminarily investigated the PBSD procedure for woodframe structures. It has been demonstrated from research and experiments that the damage to woodframe structures and their components are strongly correlated with inter-story drift primarily due to shear deformation during earthquakes (Filiatrault and Folz, 2002). In their paper, Filiatrault and Folz also proposed a direct displacement procedure for woodframe structures. Several advantages and disadvantages of the direct displacement approach to PBSD were discussed. Rosowsky and Ellingwood (2002) proposed another approach which utilized a fragility analysis methodology. A neural network approach was developed by Foschi (2003) to identify the optimal nail spacing for a wood shearwall to reach a given reliability index for a single transient drift requirement. Later, several general examples of implementing performance-based seismic design which applied the neural network was presented by Zhang and Foschi (2004). In 2004, Ellingwood et al. (2004) presented a new approach to woodframe structural analysis which is applicable to wind and earthquake loads. Their procedure directly adopted the drift related performance levels proposed in FEMA 356 (2000) and later in ASCE-41 (2006) as the target for the design. On the other hand, direct use of damage indices within PBSD may also be a viable option (see e.g. van de Lindt, 2005) or even monetary loss as the result of an earthquake (Pei and van de Lindt, 2008).

Currently, the majority of woodframe structures are somewhat limited to low-rise configurations (1 to 3 stories) which may be attributed to a lack of understanding of the way taller mid-rise light-frame wood buildings perform. The NEESWood project is a five-university collaborative research effort on woodframe structures funded by the U.S. National Science Foundation. The ultimate purpose of the NEESWood project (van de Lindt et al., 2006) is to develop PBSD procedures to help safely increase the height of woodframe buildings as well as mitigate damage to existing low-rise structures. There are several tasks within the NEESWood project that will be fulfilled between 2005 to 2009. The first step is to have a full-scale two-story woodframe benchmark townhouse tested on a shake table. This experiment had already been carried out using the twin shake tables at the State University of New York at Buffalo NEES facility. Seismic protective systems, specifically damping devices, were also installed in some shearwalls in the benchmark structure to investigate the efficiency of the protective system during those shake table tests (Shinde et al., 2008). The purpose of this test was to study the effect and behavior of interior and exterior walls with finish materials, as well as to benchmark the performance of a force-based designed building designed to a recent design code (1998 UBC). At the same time the test results could be used as a benchmark for woodframe performance and as a database to improve nonlinear numerical models for seismic analysis of woodframe buildings. The benchmark test was completed in 2006 and the report (Christovasilis et al. 2007) for the benchmark structure test released at the end of 2007 and can be downloaded at the NEESWood website. Then, a full-scale mid-rise multi-family residential woodframe condominium building will be built and tested on the E-Defense (Miki) shake table in Japan, which is currently the largest 3-D shake table in the world. This mid-rise building was designed using the PBSD philosophy which was part of the NEESWood project. The first tier of the PBSD procedure which is termed direct displacement design (DDD) can be applied to select wood shearwalls within a building (Pang and Rosowsky, 2007). The second tier of the design philosophy utilizes nonlinear time history analysis. In order to perform the this type of numerical analysis of a woodframe building, a sub-task within the NEESWood project was to develop a software package Seismic Analysis Package for Woodframe structures (SAPWood) which is a numerical tool to model the seismic behavior of woodframe buildings. The SAPWood software and the user's manual can be downloaded at http://www.engr.colostate.edu/NEESWood/sapwood.html. Within the project, the study of passive protective systems applied to woodframe structures is being investigated by research teams at Rensselaer Polytechnic Institute (RPI) and Colorado State University (CSU). Although the damper systems were installed in the benchmark structure during one test phase and tested at UB, shake table tests of shearwalls installed with improved damper systems are being conducted at RPI. Another shake table test which will focus on the application of friction pendulum (FP) base isolation for a half-scale woodframe residential building will be conducted on the uni-axial shake table at the CSU structural laboratory. These tests can provide valuable information on the application of damage control systems to woodframe buildings, especially to residential structures. One focus of these base isolation tests will be on constructability of the first story base at prototypical scale. The societal impact of this new design philosophy (economic and risk impact) is being investigated at the University of Delaware (UD) with simulation on the potential seismic induced loss to the region after the new design procedures were followed at large scale.

2.2 Performance expectations

Current seismic design procedure is a force-based design philosophy. In this traditional design approach, the designer/practitioner concentrates on ensuring the structural components meet the strength requirements which are often expressed in the form of an inequality between load demand and component capacity. Various factors (load factor, resistance factor, etc.) will be applied on a side of the inequality in order to attempt to take into account uncertainties associated with the resistance and the loading. However, force-based design does not explicitly consider loading which is associated with damage, only with capacity. Neither the overall system performance nor the probability of failure is explicitly checked in this force-based design framework. The force-based seismic design on woodframe structures in Allowable Stress Design (ASD) code should follow the procedure outlined below: firstly, depending on the region of the structure, the spectral acceleration which will be used for the seismic load calculation will be obtained from seismic hazard maps; secondly, the lateral seismic base shear force is calculated based on the provided design condition, such as the dead load, the live load, the soil type, the approximate fundamental period of the structure, the building type etc.; thirdly, the lateral seismic force will be statically distributed to each level and the force on each shearwall line will be obtained at this step; fourthly, if the diaphragms are not flexible, the effect of torsion should be considered in the design procedure; fifthly, based on the distributed seismic force on each shearwall line, the shearwall can be designed following the design charts in ASD, where the designer chooses the wall configuration details so that the shear capacity of the wall exceed the shear demand; finally, the deflection should be checked. One can see from the typical design procedure stated above, force-based building design procedures focus on individual component capacity with only implicitly considered system behavior. As a result, a designer using a force-based approach can over design, but still little will be known as to exactly how this affects the system behavior and subsequent performance during an earthquake.

However, force-based design techniques are relatively easy to understand and practice; enabling the engineers to accomplish safe designs that protect the lives of the building occupants. The design of structures can often be formalized into a procedure involving tables and charts and using automated tools such as excel spreadsheets, making it an appealing methodology.

On the other hand, performance-based seismic design has a goal that is quite different from force-based design. The difference between performance-based seismic design (PBSD) and force-based seismic design is that PBSD explicitly targets particular performance levels under specific seismic intensity levels. To do that requires careful consideration of system-level behavior since this has a critical effect on damage.

The 1994 Northridge earthquake resulted in substantial damage to light-frame wood buildings which were designed with force-based design codes over the last 50 years. This inadequate performance revealed one of the limitations in current force-based seismic design. Namely, that in the vast majority of cases life safety is well provided, but very significant and costly damage may result during a strong earthquake. Due to the uncertainties in the seismic events themselves and structures' own properties, the structural response will be considered as a random variable during earthquake in PBSD. Comparing to force-based design, this can be a great improvement since it gives the designer the freedom to set any level of performance desired instead of using predefined safety margins set by force or resistance factors. These considerations make the requirements (or expectations) for performance-based design to take a very different form compared to those in force-based design. Conceptually, the performance based design requirement should be a probabilistic statement on the desired performance under certain loading circumstances, which is also probabilistic.

2.2.1 Performance expectations in ASCE 41

Minimum Design Loads for Buildings and Other Structures (ASCE 41, 2006) defined the seismic intensity levels in the terms of their return period. These hazard levels are associated with the probability of exceedance of 50% in 50 year, 20% in 50 year, 10% in 50 year and 2% in 50 year which correspond to the average number of years between events of that intensity of 72, 225, 474 and 2475 years, respectively. In ASCE 41, the performance level for a building is divided into two main categories: discrete structural performance levels and intermediate structural performance ranges. There are four levels in the discrete structural performance level and they are Immediate Occupancy (IO), Life Safety (LS), Collapse Prevention (CP) and Not Considered. The intermediate structural performance ranges includes the Damage Control Range and the Limited Safety Range. With the target performance level and hazard level defined, the performance requirements in ASCE 41 can be any combination of these levels. These combinations, listed in Table 2-1, represent all possible design targets in the PBSD procedure articulated in ASCE 41 and the designer can customize the desired performance level of their design based on the owner's requirements.

Table 2-1 Rehabilitation objectives in ASCE 41

		Target Building Performance Levels			
		Operational Performance Level	Immediate Occupancy Performance Level	Life Safety Performance Level	Collapse Prevention Performance Level
Earthquake Hazard Level	50%/50 year	a	b	c	d
	20%/50 year	e	f	g	h
	BSE-1 (~10%/50 year)	i	j	k	l
	BSE-2 (~2%/50)year	m	n	o	p

Currently, it is felt by many researchers and practitioners that inter-story drift is the best indicator of structural damage for woodframe structures. Thus a combination of performance level and earthquake hazard level for woodframe structures can be summarized in Table 2-2, which was developed as part of FEMA 356 (2000) requirements and later adopted by ASCE 41 (2006) as well, and has been widely used by many researchers (e.g. Filiatrault et al. 2002, van de Lindt et al. 2007). From this table, one can see that the operational performance level at a seismic intensity of 20% in 50 years has not been considered for woodframe structure, primarily because most woodframe buildings are residential and operational is not as critical provided occupancy is possible.

Table 2-2 Relationship between performance levels and seismic hazard levels for woodframe buildings (ASCE 41)

		Target Building Performance Levels		
		Immediate Occupancy Performance Level	Life Safety Performance Level	Collapse Prevention Performance Level
Earthquake Hazard Level	50%/50 year	Drift Limits: 1% transient 0.25% permanent		
	BSE-1 (~10%/50 year)		Drift Limits: 2% transient 1% permanent	
	BSE-2 (~2%/50 year)			Drift Limits: 3% transient or permanent

2.2.2 Performance expectation in the NEESWood project

The inter-story drifts assigned to various structural performance levels in ASCE 41 were based primarily on component and sub-assembly testing around the world as well as expert judgment. However, based on observations of recent full-scale shake table test, the behavior of whole woodframe structures, including uni-axial shake table test of one-story woodframe structure at Colorado State University (van de Lindt et al, 2007) and the three-dimensional shake table testing of the NEESWood benchmark structure at the University at Buffalo (Christovasilis et al. 2007), the drift levels listed with the corresponding hazard levels in Table 2-2 were not felt to be accurate. This was particularly evident at the CP performance level, which in ASCE 41 aligns with a 3% drift. The NEESWood benchmark structure had inter-story drift nearing 4% and was not near collapse thus indicating that 3% may be too low for collapse prevention. In addition, collapse testing of wood buildings in Japan has indicated that collapse occurs well in excess of 10% inter-story drift for two-story single family homes, although those were not light-frame wood constructions. Therefore, new drift performance expectations were proposed within the NEESWood project and the damage description for both structural and non-structural components of woodframe structure at each seismic intensity level/performance expectation are listed in Table 2-3. The seismic hazard level 1, 2, and 3 in this table are adopted to represent ordinary ground motions with different probabilities of exceedance similar to the ASCE 41 hazard levels. The level 4 was adopted to represent near-field ground motion hazard where the location of the structure is near the fault, which has very different ground motion characteristics. The inter-story drift for each hazard level has been adjusted to 1%, 2%, 4% and 7%.

Table 2-3 Damage control and building performance levels (NEESWood project)

Performance Expectations	Corresponding Peak Inter-story Drift (%)	Wood Framing and OSB/Plywood Sheathing	Gypsum Wall Board (GWB)
Level A	0.1 – 1.0%	Minor Splitting and cracking of sill plates (some propagation) Slight sheathing nail withdraw	Slight cracking of GWB Diagonal propagation from door/window openings Partial screw withdraw Cracking at ceiling-to-wall interface
Level B	1.0 – 2.0%	Permanent differential movement of adjacent panels Corner sheathing nail pullout Cracking/splitting of sill/top plates	Crushing at corners of GWB Cracking of GWB taped/mud joints
Level C	2.0 – 4.0%	Splitting of sill plates equal to anchor bolt diameter Cracking of studs above anchor bolts Possible failure of anchor bolts	Separation of GWB corners in ceiling Buckling of GWB at openings
Level D	4.0 – 7.0%	Severe damage across edge nail lines, separation of sheathing Vertical posts uplifted Failure of anchor bolts	Large pieces separated from framing Entire joints separated and dislodged

2.2.3 Performance expectations in this study

PBSD approaches currently take the form of one or more combinations of earthquake hazard level (i.e. seismic intensity level) and performance level, i.e. inter-story drift requirement. Keeping aligned with this approach, a performance target curve is proposed in this dissertation. In order to make PBSD more general, a generalized performance expectation formulation is proposed herein. Initially, the hazard level and structure performance level should be defined. In general, a number of hazard levels should be defined as H_1, H_2, …, H_m, with H_1 representing the most statistically frequent seismic events and H_m representing the most statistically rare event. Then a number of building performance levels should be established as S_1, S_2, …, S_n, with a similar order of significance as that of the hazard levels. Note that the total number of seismic events m and the total number of building performance level n need not necessarily be equal for the general case. Finally, the PBSD expectation in this study is defined as a ladder type curve within a P-H (performance vs. seismic hazard event) plot with the acceptable probability of non-exceedance (PNE) values assigned to each segment of this curve. The procedure for generating a performance expectation curve for any structure can be summarized as follows:

1. Based on the desired combinations of seismic hazard level and performance level (such as the owner's desire for additional protection beyond force-based design code minimums, the designer's suggestion, etc.), establish the combinations of performance/hazard (P/H) for P-H plot;

2. For different hazard levels, select the acceptable performance level associated with a particular probability of exceedance. Mark the points corresponding to the choice on the P-H plot;
3. A common consideration in making the decision as to an acceptable performance level at each hazard level is that the higher hazard level will always result in more severe performances. These points are plotted into a ladder curve, one need to double check the final performance curve to make sure that there is no conflict between the points of choice. For example, the performance level corresponds to a higher hazard level will always be equal or greater than those corresponds to lower hazard levels;
4. Draw a horizontal line to the right of the points in between the hazard levels, then vertically connect the ends of these horizontal lines to form a "ladder" like curve;
5. Finally, select a predefined probability of non-exceedance (PNE) value on the horizontal line to the right of the points. The median is often used provided enough earthquakes are used in the analysis to provide reasonable representation of the uncertainty in seismic demand.

This concept discussed above can be easily illustrated in Figure 2-1. For example, the shaded area in Figure 2-1 indicates that the performance level should be at least level S_3 with an acceptable probability of non-exceedance of PNE_3 when the prescribed hazard level is between H_2 to H_3. The advantage of this new proposal for performance expectation is that by generalizing the performance expectation one can associate it with the structure's drifts, accelerations, or even financial loss etc. Similarly, the hazard level can be spectral acceleration (S_a), peak ground acceleration (PGA), or return period (T_r) etc. Note that any performance targets defined in existing PBSD documents can be represented by a particular curve or a segment of the curve in this formulation, and thus this is simply providing for a generalization. Need to be mentioned that there are several factors affecting the selection of the predefined PNE value in the generalized procedure, such as the hazard condition (location) of the building and the expectation of the building performance during earthquakes from the owner/user. These influence factors need to be considered in defining the design target. It is usually hard (if not impossible) for the owner to design the design target in form of Figure 2-1 alone without the help of design engineers due to the lack of background knowledge on performance level and hazard level. Thus it is envisioned in this study that the engineer is to provide predefined performance and hazard levels while the owner's input is to be reflected on the PNE levels. For woodframe buildings, inter-story drifts are commonly used to characterize performance in the PBSD studies. However, no studies to date have included acceleration as a performance requirement.

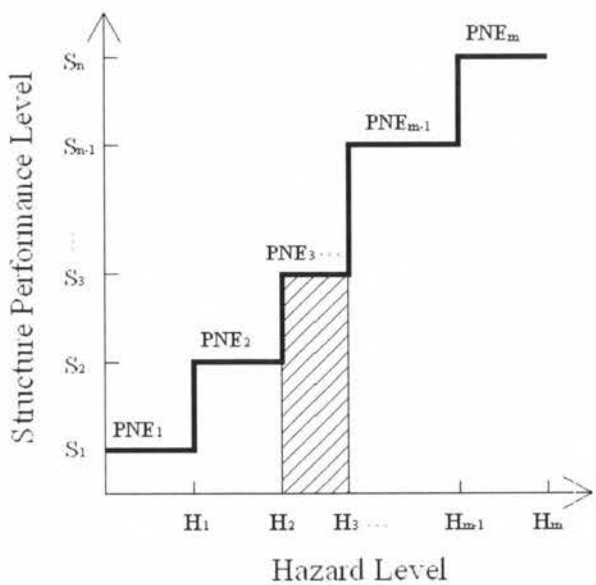

Figure 2-1 Proposed design expectation for PBSD in this study

However, in order to illustrate the use of this conceptual framework with real applications, S_a at 0.2 second has been selected to be the indicator of the seismic hazard level, then drift and acceleration have been chosen to represent the performance expectation for some hypothetical building. Note that consideration of acceleration did not appear in ASCE 41 and has only been considered in a few studies for loss estimation (e.g. Pei and van de Lindt, 2008). The reason that acceleration needs to be considered as another performance indicator as well as the inter-story drift is two-fold. First, excessive accelerations that can occur in the upper stories of buildings can cause severe contents damage as well as severe personal injury during earthquakes and thus need to be controlled. Secondly, the acceleration requirements as a performance expectation can help to introduce ductility in the design. Considering acceleration reduction as a performance in PBSD can prevent the over-design of the stiffness in lower story levels resulting from the inter-story drift requirements. Note that the purpose of including acceleration requirements is to help control the damage from movable contents in the building especially in higher story. Generally speaking, a sudden acceleration at some point in loading history and only last a very short period will not cause the contents to move or fall. The damage of the movable contents requires enough momentum gathered under a significant level of acceleration persisted over certain time period. Thus the acceleration requirements indicated in PBSD should be the moving average acceleration over a short period (e.g. 0.1 sec) rather than the numerical peak acceleration. In generalized PBSD procedure described above, the procedure to determine the predefine PNE value while defining the design expectation is not specified in order to leave that freedom to the end user (with the help of the engineer). In this dissertation, four design examples at three different locations will be severed as illustrative design cases using proposed generalized PBSD procedure in Chapter 5. Thus a recommended procedure to define PNE value in this study will be discussed in Chapter 5. In order to make the generalized PBSD procedure more specific for the examples in current study, the hazard level (S_a) and the performance levels of drift and acceleration were determined/chosen as shown in Figure 2-2 and 2-3. The exact PNE value at each level will later be determined in Chapter 5. These expectations are to be satisfied/exceeded simultaneously in the final design. Moreover, for the convenience of the reader who is more familiar with incremental dynamic analysis (IDA) (Vamvatsikos et al., 2002) curves, the hazard and performance level axis were switched and shown in Figure 2-2(b) and 2-3(b) so that the figure is compatible with a typical IDA curve.

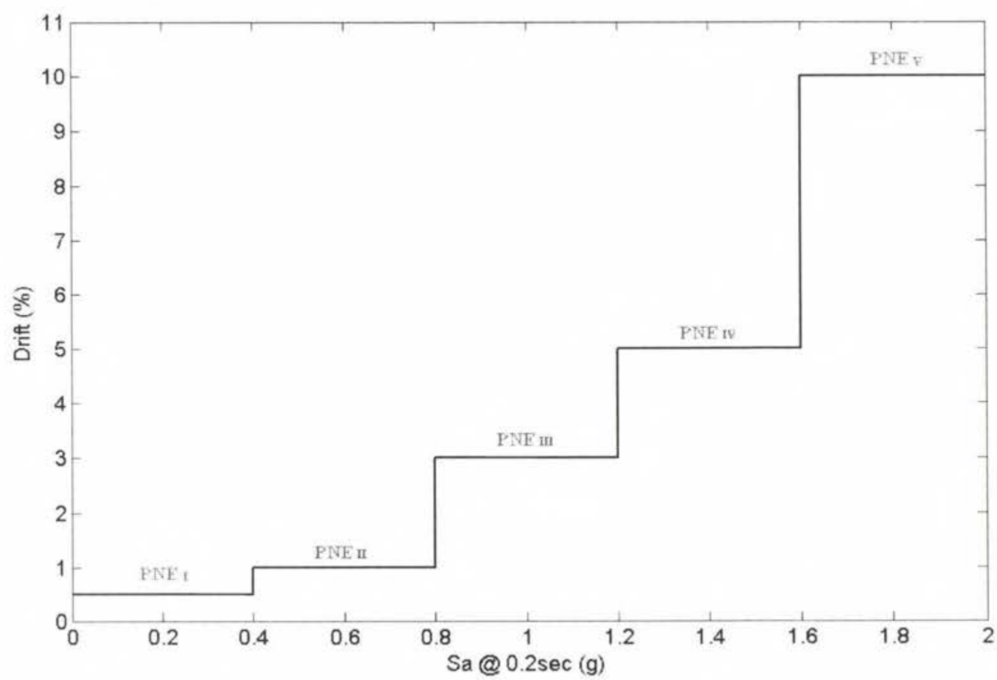

Figure 2-2(a) Performance expectation for inter-story drift in this study

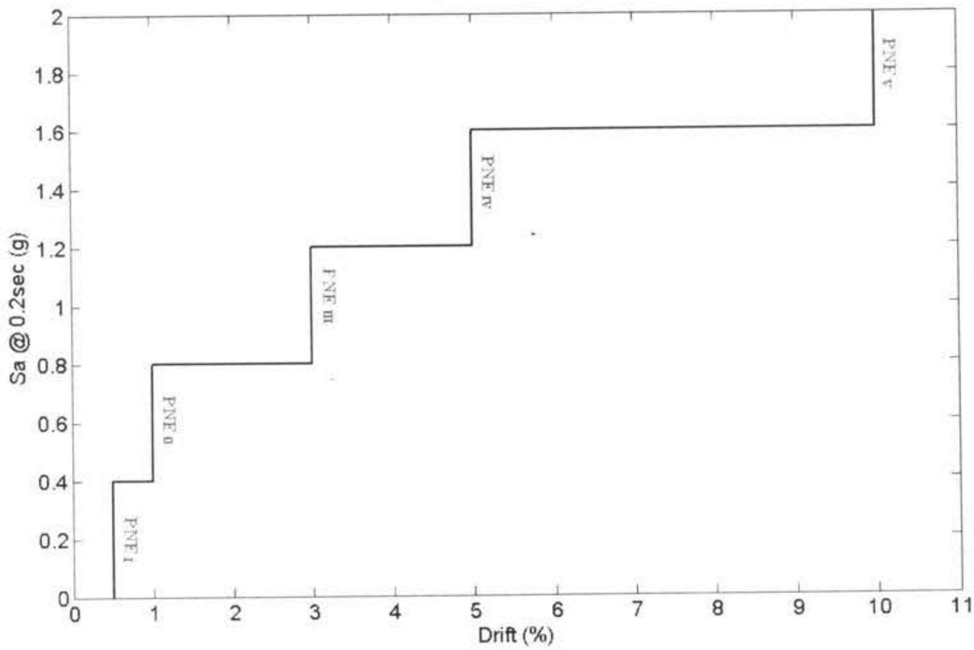

Figure 2-2(b) Performance expectation for inter-story drift in this study (IDA version)

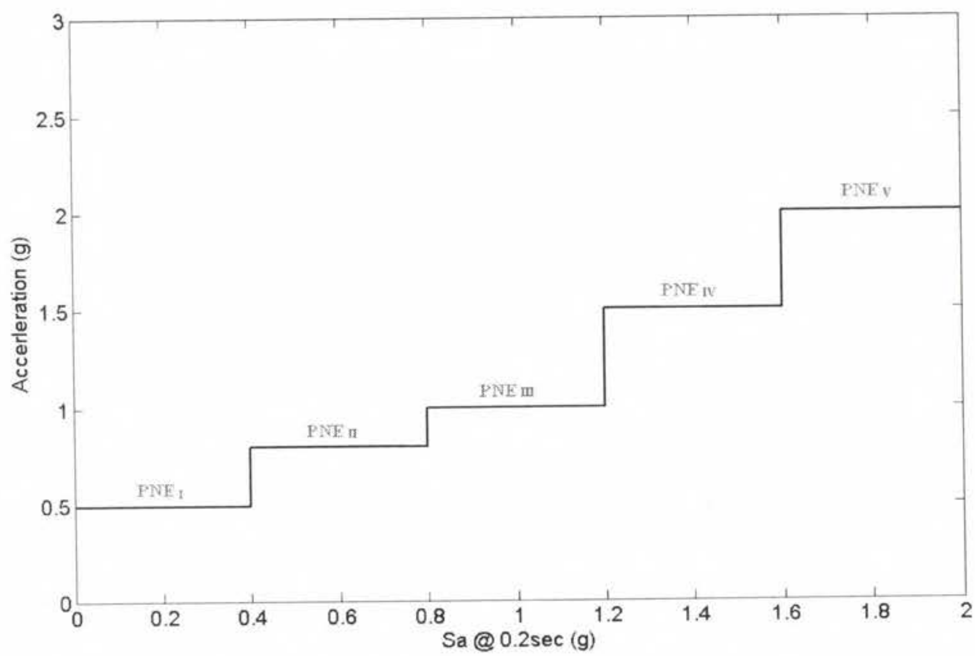

Figure 2-3(a) Performance expectation for acceleration in this study

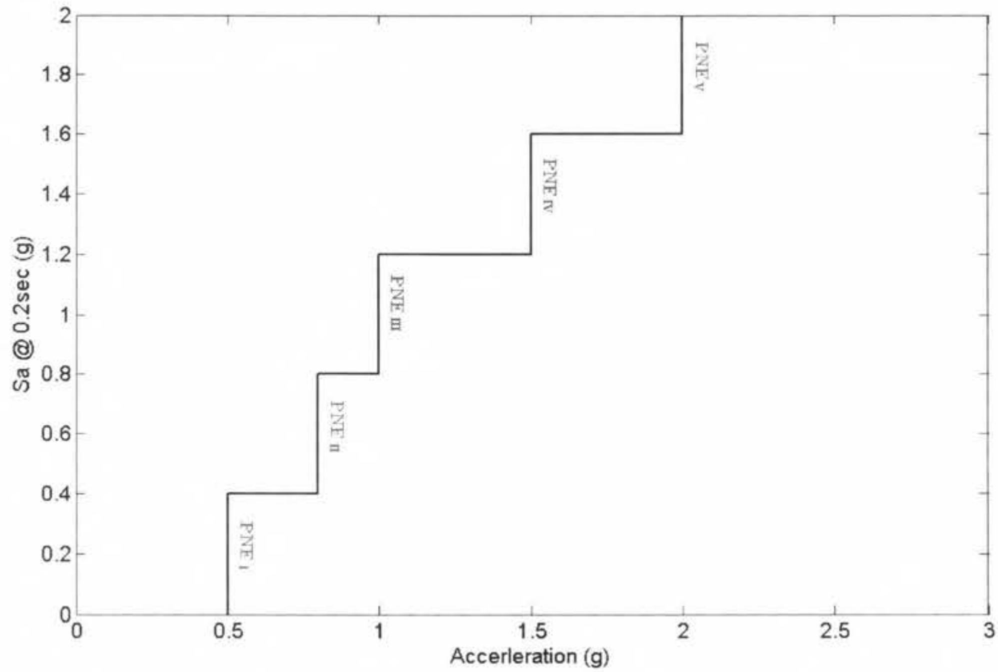

Figure 2-3(b) Performance expectation for acceleration in this study (IDA version)

2.3 Design and simulation procedure

Before discussing the PBSD procedure in this study, consider the shortcomings of traditional force-based design in the beginning of this section. First, the seismic load is not a deterministic force acting on the structure but a random dynamic force induced by the acceleration of the ground. The calculation of seismic force is considered in current force-based seismic design approximately with an elastic response spectrum and ductility related safety factors. Uncertainty sources such as resistance, material, loading, and construction have never been explicitly considered in force-based design, instead the force and resistance factors are used to insure a predefined level of safety which the designer has no control over. Using predefined force and resistance factors during design procedure often causes the final design to be conservative which obviously wasting construction materials and increasing the total cost. The negative effect of reduction factor R had been discussed in the shortcomings of force-based seismic design of wood buildings (Filiatrault et al., 2002). However, it is important to point out that force-based seismic design does have merits. First and foremost it is simple and efficient.

In contrast to force-based design, the new design philosophy, PBSD, allows the engineering design team to explicitly select performance targets, whereas the design team is not left too many choices in force-based design. If the design team or owner seeks to go beyond the design code minimum, the only choice is to increase the load or resistance. In this study, probabilistic uncertainty was considered explicitly in the design procedure proposed. The design procedure was based on the fact that the response (such as inter-story drift, floor acceleration, financial losses, etc.) of the building during an earthquake should be considered to be a random variable due to the uncertainties in the seismic events themselves, the structural properties, and the cost of construction materials. Hence, Monte-Carlo simulation will be used in this study to obtain the numerical samples so that the structural responses can be characterized as a statistical distribution based on these numerical simulations. In this process, it is fairly straightforward to represent the uncertainties in earthquake events and structures with appropriate probabilistic models. Finally, the statistical distribution of performance indicators, such as drift probability curves or floor acceleration fragilities, can be used directly for the PBSD check against the desired performance levels, i.e. the expectation described earlier. For different geographical locations and different structure types, these distributions likely will be different due to the uncertainties discussed before. Therefore, the drift/acceleration probability curve which will be used in this study should vary for different geographical locations and different design plans. As most researchers agree, PBSD benefits greatly from numerical analysis tools, especially time-history analysis software. A software package named SAPWood had been developed within the NEESWood project (Pei and van de Lindt, 2007) and will be used to check the PBSD procedure presented in this dissertation. Additional information on this numerical tool will be presented in Section 2.4.

The general procedure proposed for PBSD is presented in flowchart form in Figure 2-4. From this flowchart, one can see that the first step in this proposed PBSD procedure is to conduct a traditional force-based seismic design in order to identify a lower bound for the design that will provide life safety to the occupants as is currently done. At this stage, the purpose of using PBSD should be to explicitly achieve the desired performance which cannot be obtained through force-based seismic design rather than completely replacing force based design. Once the force-based design was completed, wall models should be built according to the designed configuration as lateral load resisting elements. Then these elements should be assembled into a system level model in software program which can perform the dynamic time-domain analysis for structures. In this study, SAPWood program was selected as the numerical tool to execute the numerical simulations. A SAPWood Nail Pattern (SAPNP) model can be built in SAPWood according to the provided preliminary wall configurations. Hysteric parameters for individual walls can be obtained through quasi-static pushover analysis on the SAPNP model. With the wall parameters calculated in SAPNP and wall location known from the preliminary floor plan, the system level numerical model can be built in SAPWood. Then the system model will be subjected to a ground motion suite scaled to the predefined hazard levels. This process is termed a Multi-case IDA (M-IDA) since it is simply a multiple record incremental dynamic analysis (IDA) (Vamvatsikos et al., 2002). The results from numerical simulations (maximum inter-story drift and floor acceleration in this study) will be recorded to construct the conditional distributions of these performance indicators at each hazard level. If the long-term performance related to earthquake occurrence is the performance requirement (such as life time financial loss), based on building location information, one can find the hazard curve information from the United States Geological Survey (USGS) website and combine these uncertainties together using statistical methods. The hazard curve will also be needed if the hazard levels were defined with indicators such as return period or annual exceedance of probability in this procedure. All the simulation results corresponding to the PNE value on the design target curve can then be graphically expressed as a function of the corresponding hazard level and compared to the design target curve. The design target curve is assumed to be "satisfied" when the PNE of structural performance level at designed hazard level is within the required/acceptable PNE for the design target curve. If the target curve is not satisfied, design modifications need to be performed to the preliminary design, such as changes in nail patterns, adding/removing shearwalls, adding base isolation, dampers, etc. The modified system model will then be analyzed with the same procedure described above until the design target curve is satisfied.

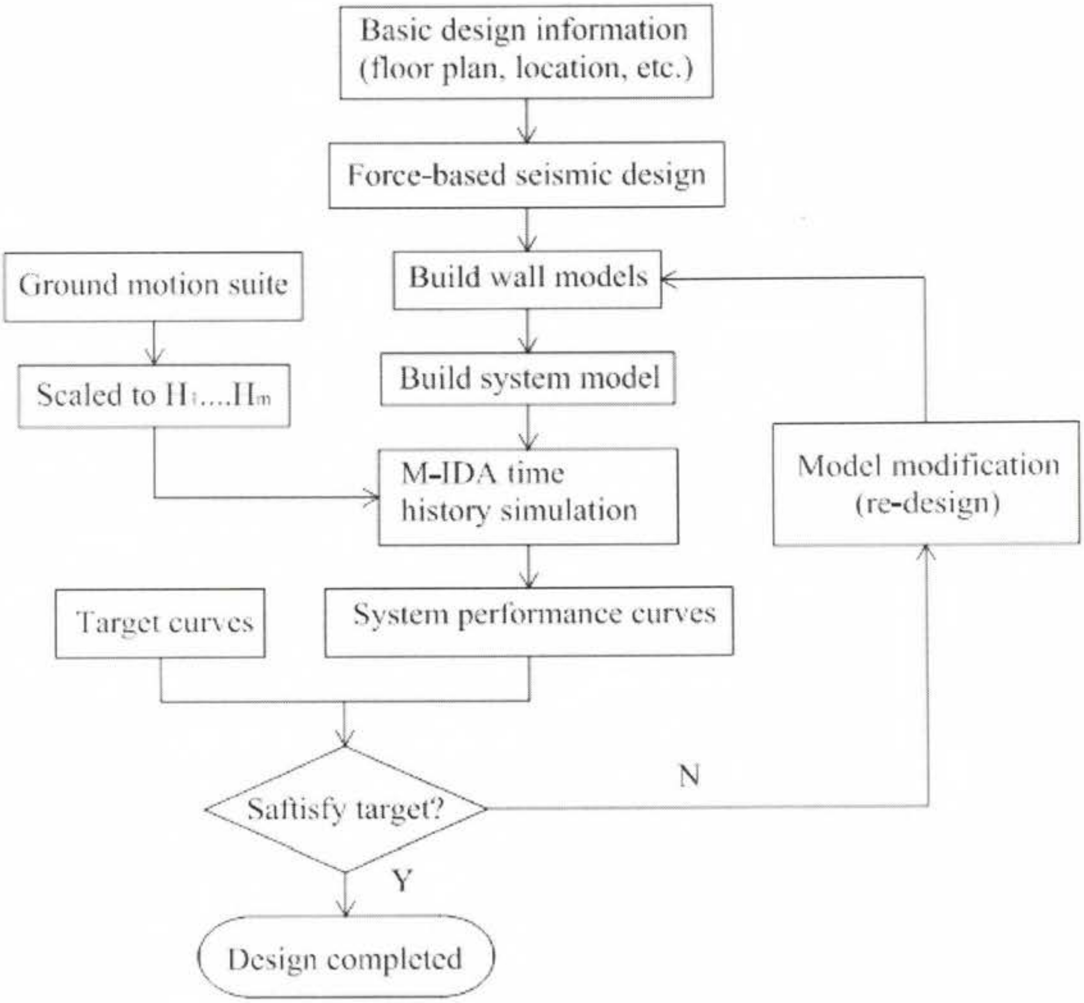

Figure 2-4 Probabilistic performance-based seismic design procedure in this study

2.4 Numerical tool for the design

The Seismic Analysis Package for Woodframe Buildings (SAPWood) software package was developed during the NEESWood project in 2007 and will be used as the tool for the numerical simulations in this study. The PBSD procedure proposed in this study will be applied in example buildings to dictate the performance (displacement and acceleration) of woodframe structures under seismic loads. The SAPWood software was capable of performing time domain analysis on woodframe structures. Currently, there are four types of spring models in this program to describe the behavior of each individual wall, namely the linear model, bilinear model, ten-parameter CUREE model (Filiatrault and Folz, 2002) and a sixteen-parameter Evolutionary Parameter Hysteretic Model (EPHM) (Pang et al., 2007). The application of EPHM model in SAPWood program is an improvement in extending the accurate prediction on woodframe structure in large displacement region. The Nail Pattern (NP) analysis in SAPWood is the module that allows the user to set up the wall model from the most basic configuration: studs, sheathing and nails. Different from the CASHEW (Folz and Filiatrault, 2001) model, both the panel nails and framing connectors are considered in NP analysis. The hysteresis results after the quasi static analysis of the NP model can be plotted and the hysteretic model parameters can be obtained in four hysteretic models. In SAPWood, there is also an option to "check nail" which can plot the hysteresis of every nail/framing connector after the reversed cyclic analysis. The loss estimation methods developed in Pei's dissertation (Pei, 2007) have been programmed into the SAPWood program.

With all these features, the time domain numerical tool SAPWood, will be used to perform the numerical simulations in this dissertation work. The current version of SAPWood did not consider the application of the base isolation system, the numerical model of Friction Pendulum System (FPS), one of the base isolation systems, will be programmed into SAPWood. The more details about FPS numerical model will be discussed in Section 3.3. There will one more new feature in SAPWood program after adding the FPS numerical model.

Chapter Three

Incorporation of Friction Pendulum Bearings in Performance-based Seismic Design

3.1 Literature review on base isolation system

It is well understood that horizontal earthquake ground motion causes the majority of the damage to engineered and non-engineered structures. Excessive inter-story drift of the structure in the horizontal direction causes cracking within the drywall, broken and cracked studs, pullout and shearing of sheathing-to-framing nails, and can even cause global collapse of a building. Generally speaking, the concept of seismic isolation is to place isolation equipment that either has a relatively low horizontal stiffness between the structure and the ground or that allows the building to slide on a surface with some level of friction to increase the building period, thereby reducing the floor accelerations and related inter-story drifts. Either type of base isolation system decreases the horizontal seismic force transferred to the structure and thereby significantly reduces the damage to the structure during an earthquake. In regions of high seismic intensity, the use of a base isolation system represents one approach to significantly reducing structural and non-structural damage.

There are two common types of base isolation systems: rubber bearings and friction pendulum slider bearings. For the rubber bearing base isolation system, the most popular isolator is made from multilayered laminated rubber bearings with steel reinforcing layers in which the rubber bearings are soft in the horizontal direction while the reinforced steel plates could provide high stiffness in the vertical direction for gravity support. The Foothill Communities Law and Justice Center in Rancho Cucamonga California, completed in 1985, was the first building with a base isolation system in United States (Naeim et al. 1999). This four-story steel building is 12 miles from San Andreas fault and there are 98 isolators making up the base isolation system. The isolators are the multi-layered natural rubber bearings reinforced with steel plates. Field data along with experimental test results and numerical simulations have clearly demonstrated that the seismic response of buildings (e.g., inter-story drift and floor acceleration) can be substantially reduced with the installation of either type of base isolation system.

A numerical analysis and shake table test of a five-story steel model with and without a rubber bearing base isolation using different strong earthquake records was performed in Australia (Wu et al. 2002). This steel structure was designed by Samili (1999) and was adopted by the International Association for Structural Control (IASC). Both the numerical analysis and the shake table test results showed that the efficiency of the rubber bearing base isolation system on steel frame structure strongly depends upon the type and nature of the earthquake ground motion. The numerical analysis and shake table test results indicated that the isolation system was able to reduce both the maximum acceleration and inter-story drift at each story level. However, this reduction was strongly dependent on the earthquake ground motion used in the numerical analysis and the shake table tests.

The application of base isolation systems is becoming more and more common for concrete and steel structures. Application in woodframe structures is quite rare. Symans et al. (2002) provides an extensive literature review on the use of base isolation and supplemental damping systems for woodframe structures. In that paper, it was shown that it is quite difficult to install base isolation and supplemental damping systems in woodframe buildings, because the floor diaphragms in woodframe buildings typically do not have high enough in-plane stiffness to transfer the force to the base isolation system and keep all the bearings displacing in unison. Furthermore, flexible utility connections are also required if base isolation systems are installed which means these flexible connections need to cross the plane of the isolation. In addition, in the case of low friction sliding isolation bearings, the low weight of woodframe buildings can result in undesirable sliding at low levels of wind or seismic excitation. Thus, a wind restraint system may be needed. In spite of these practical limitations, the paper still concluded that seismic protective systems, such as base isolation and supplemental damping systems can help achieve better performance for woodframe structures during strong earthquake ground motion.

As a result of the investigation of base-isolated residential houses built in Japan, researchers have pointed out that there exists several difficulties in the application of base isolation to wood structures, including the expense of the base isolation systems themselves relative to the cost of the building, and the effectiveness of base isolation due to the structure's light weight. Laminated rubber bearings are mostly used to isolate buildings, but new isolation configurations need to be developed to improve the efficiency of the base isolation system (Iiba et al. 2001) and its application.

3.2 Performance expectation for the FPS

The Friction pendulum system (FPS) is a bearing/slider with a spherical concave sliding surface which is shown in Figure 3-1.

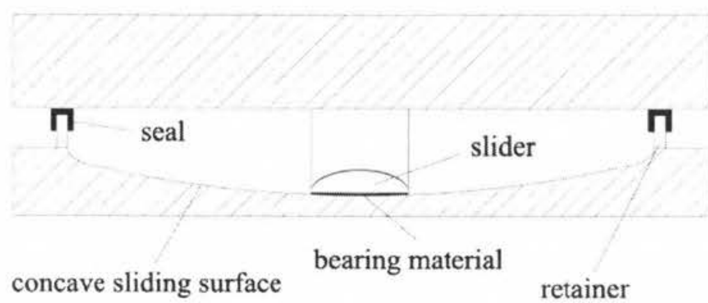

Figure 3-1 Typical configuration of friction pendulum system bearing

Generally, the lentil-shaped bearing/slider is covered by a Teflon-based high bearing capacity composite material and the spherical surface is made of stainless steel.

Therefore, the sliding friction coefficient will be in the range of approximately 0.05 to 0.2, although recent procedures can reduce the friction coefficient to 0.03. The FP bearing begins to work once the earthquake force overcomes the static value of friction. Then the lateral force developed during this process is equal to the combination of the mobilized frictional force and the restoring force provided by the spherical surface. The spherical sliding surface provides both a restoring force and a friction force while the bearing is sliding. The restoring force during the process ensures that the structure is automatically self-centered after an earthquake which is considered a unique feature of the FPS whereas the friction force provides energy dissipation during the cyclic response. It needs to be emphasized that the structural period of the building is only related to the radius of the curvature of the spherical surface which means that it is unrelated to the mass/weight of the structure above. The lateral resistance of an FPS isolation system is intentionally designed to be low so as to decouple the ground motion from the stiffer structure above. The bearing includes a retainer around its perimeter which provides a hard stop, or displacement limit, should it move too much. The design of the FPS in this study will mainly concentrate on this characteristic as well as the FPS radius. The force-deformation constitutive relation of the FPS and the details of numerical model in SAPWood will be discussed in Section 3.3.

Based on the brief introduction of the FPS bearings above, the qualitative performance expectation of the FPS during earthquake is to reduce damage of the building without exceeding the displacement limit of the FP bearing and thus hitting the stop. As previously mentioned, part of the earthquake energy is dissipated by the friction during the cyclic movement of the FP bearing, so the FPS is considered a passive seismic protective system to protect the super-structure installed above. Obviously, significantly smaller inter-story drifts and accelerations are expected once the FPS is installed. In other words, the implementation of an FPS is usually the result of a drift and acceleration expectation that cannot be satisfied simultaneously with basic structural design such as stiffening the lower stories of a building. Therefore, almost by default, the performance expectations on the super-structure in this case will be more restrictive compared to the expectations discussed in Chapter 2. The generalized format for performance expectations (Chapter 2) is also applicable to the super-structure here.

Based on a large amount of previous numerical analysis done in the preliminary stages of research, it is apparent that an inter-story drift limit of 1% when FP bearings are present is generally satisfied with proper selection of the FPS. Hence, for the design examples in this study, the performance expectation on the inter-story drift is selected as less than 0.5% and the floor accelerations are selected as 0.3g, 0.5g and 0.8g for different hazard levels. For the FPS device itself, a failure (device displacement exceeds its capacity) probability is also assigned to each hazard level as the performance expectation. In other words, the performance expectations after installing the FP bearing must include three parts at the same time: one is that the FP bearing has not exceeded the displacement limit, the second that the inter-story drift limit is satisfied, and the third that the floor acceleration of the super-structure is within the expectation.

Although FP bearings can substantially reduce inter-story drifts within a super-structure and play a very important role in seismic protection, the price of the equipment itself and the installation are quite expensive. In addition, the installation of FP bearings in woodframe buildings requires substantial stiffening of the diaphragm which substantially increases the material and construction cost of the base diaphragm. Although application of FP bearing to woodframe buildings will clearly raise the initial cost, if the long-term savings from earthquake events is accounted for, it may very likely be considered an economically viable solution.

3.3 FPS numerical model in SAPWood

3.3.1 Mathematical model of FPS

There are several mathematical models in research field to describe the behavior of the FP bearing. For small deformations, the classical force-deformation relationship of the FPS (Almazan et al., 1998) is depicted in Figure 3-2.

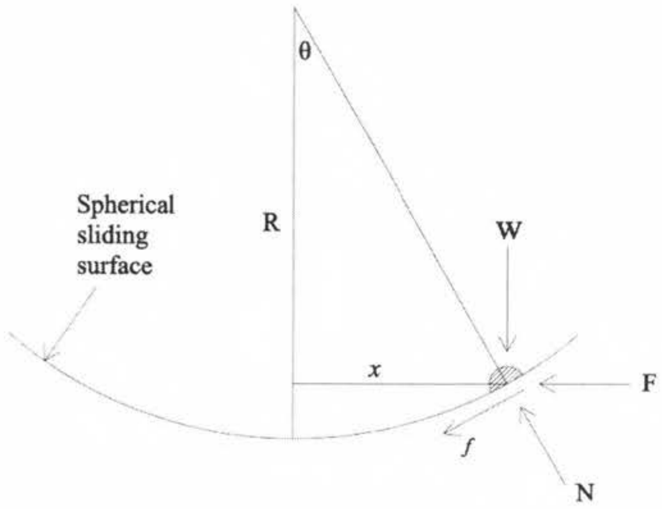

Figure 3-2 Force diagram of friction pendulum system bearing

Based on this figure, the forces that act on the bearings are W, the weight of the structure acting on the isolator, F, the horizontal restoring force and the reaction forces at the sliding surface are N, the normal contact force, f, the friction force. For geometry, R is the radius of the FPS, x, is the lateral displacement of the bearing and θ is the central angle which usually is very small. It is assumed the friction force is modeled as Coulomb friction and f is equal to μN, where μ is the friction coefficient. Since θ is assumed to be small, the cosine of the angle θ is equal to 1 and the normal contact force N is equal to W ($N = W\cos(\theta)$). From the horizontal equilibrium of the bearing, the force-deformation relationship can be expressed as

$$F = \frac{W}{R}x + \mu W \operatorname{sgn}(\dot{x}) \tag{3-1}$$

where $\operatorname{sgn}(\dot{x})$ is the sign function which equals -1 or +1 depending on whether the velocity is negative or positive relative to the ground. This relationship is confined only in one plane and the vertical component of ground motion is neglected.

For bidirectional motion, Equation (3-1) can be expressed as

$$\vec{F} = \frac{W}{R}\vec{X} + \mu W \frac{\dot{\vec{X}}}{\left\|\dot{\vec{X}}\right\|} \tag{3-2}$$

where, $\vec{F} = \left[F_x\, F_y\right]^T$ is the horizontal restoring force of the bearing, F_x and F_y are the Cartesian components of this force in the *x*- and *y*- direction; $\vec{X} = \left[X_x\, X_y\right]^T$ is the horizontal deformation of the bearing relative to the ground, X_x and X_y are the *x*- and *y*-direction displacement component; $\dot{\vec{X}} = \left[\dot{X}_x\, \dot{X}_y\right]^T$ is the horizontal velocity of the bearing and $\dot{X}_x$ and $\dot{X}_y$ are the velocity components in the *x*- and *y*- direction; the direction of the velocity is determined by $\frac{\dot{\vec{X}}}{\left\|\dot{\vec{X}}\right\|}$. Both equation (3-1) and (3-2) are valid only when the velocity of the slider is not zero, i.e. after the static friction force is exceeded and the FP bearing begins to slide.

3.3.2 Numerical model of FPS in SAPWood

There are a number of numerical models adopted to simulate the behavior of FP bearing during earthquake excitation in earlier studies (e.g. Ryan et al., 2004 and Mosqueda et al., 2004). One of the most commonly used models is the bilinear model developed based on test results of the FP bearing. Figure 3-3 shows the hysteretic response of an FP bearing during dynamic excitation. The similarity of this hysteretic loop to an ideal bilinear oscillator is apparent.

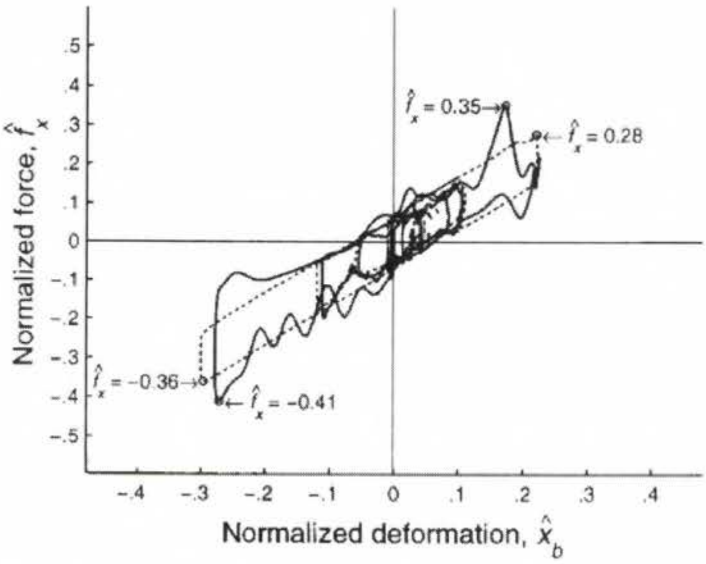

Figure 3-3 FPS hysterical response (excerpted from Almazan et al., 1998)

Ryan et al. (2004) pointed out that it is convenient to use the bilinear force-displacement to model an FP bearing. The rigid-plastic force-displacement relationship comes from the initial slip motion of the FP bearing which can be approximated using a very small pre-slip deformation in the bilinear model. Typically, the pre-slip deformation of the bearing is of the order of 0.02 inch (0.05 cm). Based on Equation (3-1), the post-yield stiffness is described by the pendular stiffness $\frac{W}{R}$ and the yield strength is set to μW. The bilinear numerical model is depicted in the Figure 3-4.

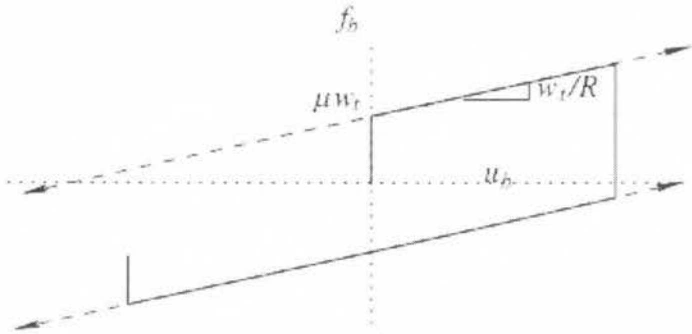

Figure 3-4 Rigid-plastic force-displacement relation of the isolator for uniaxial excitation (excerpted from Ryan et al., 2004)

Although the bilinear model is easy and convenient to implement, there also exist some limitations for the model. First, it is obvious that the bilinear model can only model the movement of the FP bearing in one direction. In reality, the FPS is allowed to slide approximately in the horizontal plane in any direction. Second, as previously mentioned, the restoring force from the mathematical model is related to the vertical force/component, which will change during an earthquake. In extreme cases, the overturning effect may even cancel out the weight acting on the FPS which will definitely change the model behavior. However, in the bilinear model, the parameters (radius *R*, weight *W*) remains the same once the model is set up independent of the actual vertical force during the loading process. Finally, Constantinou et al. (1990) discovered that the friction coefficient between the slider/bearing and stainless steel surface can change with different sliding velocity and is thus velocity dependent. This effect cannot be considered in the bilinear model. Typically, two bilinear models must be used in both the x- and y-direction in order to approximately simulate the in-plane movement of an FP bearing.

The behavior of an FP bearing with a rigid body super-structure under multiple components of excitation was studied by Mosqueda et al. (2004) with both a displacement controlled test and dynamic excitation test. Different numerical models were compared in that paper including an uncoupled bilinear model with and without varying vertical force, a coupled model with and without varying vertical force, and also a model with varying friction coefficient. It was concluded based on the comparison to test results that the coupled model with the varying vertical force component is the most accurate model among the ones studied. Therefore this is the model adopted in this dissertation study. The displacement and the corresponding force in the horizontal plane of this FP bearing model were programmed into the SAPWood program and are shown in the Figure 3-5.

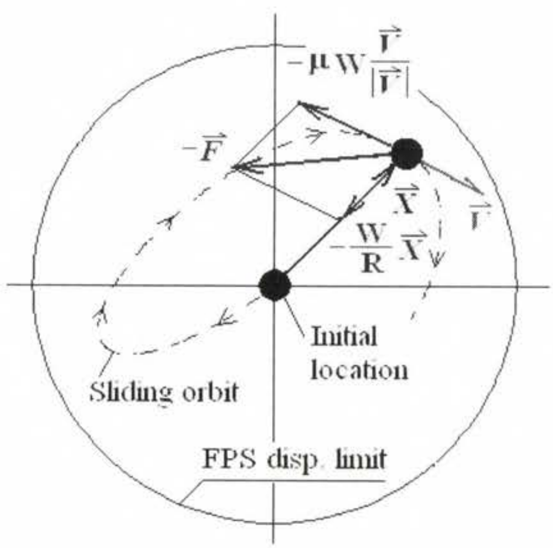

Figure 3-5 Displacement in the horizontal plane of the FPS

The FP bearing element was modeled as a special element with stiffness and restoring force in three directions. The vertical stiffness was set to be linear and very large in compression and virtually non-existent in tension to simulate the uplift of the device. The compression force (W) at each FP bearing element can then be obtained from the vertical spring element at each time step during earthquake excitation. Hence, the compression force (vertical force) acting on the bearing, W, is a function of time. For in-plane movement, two states were used to simulate the stick situation and slide behavior of the system. Similar to the pre-slip displacement concept for the one dimensional bilinear spring model, a concept termed yielding range was used to distinguish sticking and sliding in this study. Initially, the FPS slider was at the origin and a very large stiffness K_0 was assigned to the horizontal movements. The value of K_0 was selected such that the static friction will be reached at a displacement D_y relative to the origin. When the slider movement relative to the origin exceeded D_y, the program automatically switches to the slide situation by using an equation similar to Equation (3-2) to update the restoring force and horizontal stiffness at each time step. The sticking location, X_0, was initially set to be at the origin. It will also be updated as the velocity of the sliding motion reaches zero or is reversed to simulate the possibility that the slider can come to a temporarily stop at any place in the horizontal plane during earthquake loading. The element behaves as a generalized bilinear model in two-dimension, with the vertical compression force updated constantly during loading. The force and stiffness of the FP bearing element is updated at every time-step based on the following equations

The stick situation:

$$\vec{F} = \frac{W}{R}\vec{X} + K_0(\vec{X} - \vec{X}_0) \qquad \left|\vec{X} - \vec{X}_0\right| \le D_y \tag{3-3}$$

The slide situation:

$$\vec{F} = \frac{W}{R}\vec{X} + \mu W\frac{\vec{V}}{\left|\vec{V}\right|} \qquad \left|\vec{X} - \vec{X}_0\right| > D_y \tag{3-4}$$

In which, $\vec{F}$ is the horizontal restoring force vector, R is the radius of the FPS, W is the vertical compression load acting on the bearing, $\vec{X}$ is the horizontal displacement vector relative to the ground, μ is the coefficient of friction, which will also change during the time history analysis (will be discussed later), $\vec{V}$ is the horizontal velocity vector , $\vec{X}_0$ is the sticking location, and D_y is the radius of the yielding range, it should typically be a very small value and be calculated as

$$D_y = \frac{\mu W}{K_0} \tag{3-5}$$

The vertical load W on the FP bearing can be updated by the vertical force in the numerical model spring element. Note that if the spring force is in tension, W will be set to 0. K_0 is set to be a large number, in SAPWood, it was chosen when the D_y is 0.05 inch given the initial compression force W.

As mentioned earlier, the friction coefficient of the FPS device is not constant. Constantinou et al. (1990) performed a series of experiments on the FPS friction coefficient with different combinations of velocity, pressure and Teflon material. One of the experiments results is shown in the Figure 3-6. Based on the test results, they also proposed an empirical relationship between the friction coefficient and sliding velocity as:

$$\mu_s = f_{\max} - Df \exp(-a|\dot{U}|) \tag{3-6}$$

in which $f_{\max}$ is the coefficient of friction at large sliding velocities, Df is the difference between $f_{\max}$ and $f_{\min}$ which is the coefficient of friction at very low velocity, a is a constant for given bearing pressure and condition of interface.

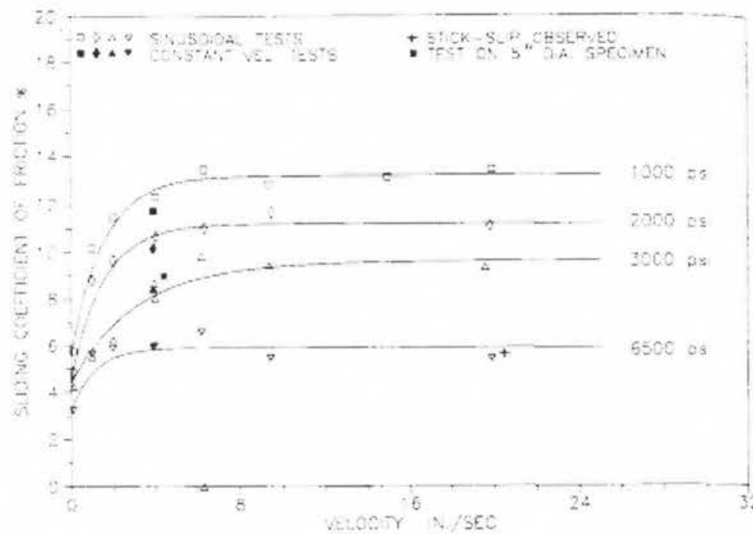

Figure 3-6 Variation of sliding coefficient of friction with velocity of glass-filled Teflon at 25% for sliding parallel to lay (excerpted from Constantinou et al., 1990)

The effect of a velocity dependent friction coefficient was also included in SAPWood program and applied in this dissertation work.

3.4 Design procedure for the FPS

The design procedure for using the FP bearing with a woodframe structure is not very different from the generalized PBSD procedure outlined in Section 2.3. However, there are three steps that should be modified to include the effect of the FP bearing devices.

(1) The FPS devices should be included in the system model for numerical simulation. The number and location of the FP bearing should be reflected in the model.

(2) Determination of whether or not performance expectations are achieved should be evaluated based on the following considerations. As discussed in Section 3.2 of this dissertation, the performance expectation after installing the FP bearing should consider more than simply drift. First, the displacement limit of the FP bearing can not be exceeded which causes the damage to the FPS devices itself and can also result in high accelerations in the superstructure with the sudden stop; Second, the response of the super-structure should be reduced significantly for large earthquakes to satisfy the performance expectations proposed for the wood structure. Third, the economic impact of the inclusion of FPS device should be evaluated after the final design for the long-term hazard mitigation. Several options with different size of the FPS devices can be listed by the total construction cost. This step can give the owner or engineering team an idea whether use the FPS device or not or which FP bearing is going to be used in the final construction.

(3) The modification step in the generalized PBSD procedure should be focused on the modifications of the FP bearing system since the properties of the FP bearing control the response of the structure. The radius of the FPS devices greatly affects the period of the isolate system. It should be increased when the response of the super structure is large. The displacement limit of the FPS devices can be increased when necessary, but will result in a more expensive design since the size of the FPS device will increase accordingly. The adjustment on the number and location of FP bearings can be applied to provide uniform support over the base layer and suit the design of the base frame. The user can also modify the super-structure above and keep the FPS devices configuration as the same. However, the change in system behavior from modifying the super-structure is not as significant as that from modifying the FPS devices itself. Three options to modify the FPS which can be considered at current stage have been illustrated in Figure 3-7.

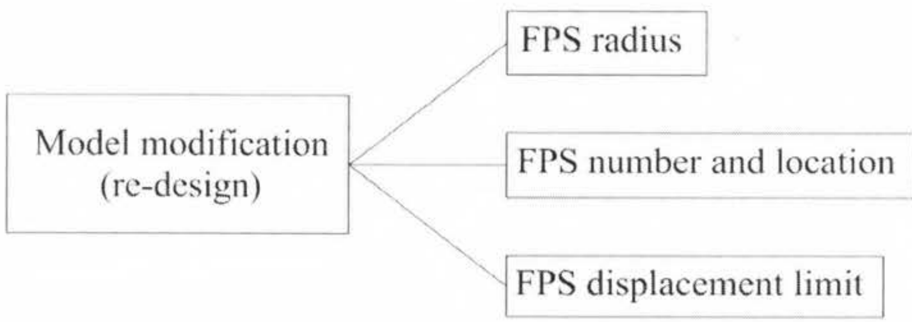

Figure 3-7 FPS devices design modification

Chapter Four

Experimental Investigation of a Half-scale Woodframe Building on Friction Pendulum Slider Bearings

4.1 Scaled woodframe building

4.1.1 Scaled model test literature review

In recent years, valuable information on the dynamic behavior of structures, especially concrete structures, has been made available by research studies performed at moderate to small scales. This is typically because either laboratory space is limited or costs associated with full scale testing are excessive, or both. Zarnic et al. (2001) tested one-fourth scaled models with different shapes of masonry in-filled reinforced concrete frame buildings of various shapes on a shake table. A composed sine wave with acceleration amplitudes in different magnitude was used as the input for the shake table. The author concluded that the scaled models had comparable dynamic characteristics to the prototype based on the observed damage. The comparison of the response to the full size prototype showed that the scaled model replicated well when the applicable scaling rules were followed and the scaled models could provide valuable information. The conclusion from a series shake table tests state that the prototype buildings are able to sustain high dynamic excitations. Also, the author pointed out that the scaled modeling of the local behavior of structural elements is less reliable owing to the limitations of modeling properties.

Bertero et al. (1985) conducted a one fifth scaled model of a reinforced concrete structure at the University of California, Berkeley. His research showed that it is difficult to get similarity between the scaled model behavior and the prototype without the proper similitude for the material during the pseudo-dynamic test on the shake table. In another later case, a 1:32 scaled model (Caccese et al. 1990) test of isolated precast shearwalls was carried out at Drexel University. These two studies showed that to obtain more knowledge of the seismic behavior of reinforced concrete structures, experimental studies are very important and that scaled models using earthquake simulation is an acceptable way to investigate seismic behavior of full scale structures.

Van de Lindt (2008) applied energy-based similitude for woodframe structure at the connector level. Both full-scale and half-scale one-story woodframe buildings with rectangular floor plan were tested on the shake table at CSU. The test results verified that the scaled test of woodframe structures can be performed to investigate the prototype behavior following the energy-based similitude procedure.

4.1.2 Fundamental theory of a scaled model

In scaling a structure for dynamic testing a number of parameters/variables as well as the governing equations should both be carefully considered during the selection of the scaling procedure. In order to design a scaled experiment which will replicate the response of interest in the full scale structure, the scale factors for the boundary condition, material properties, dimensions, and time must follow certain fundamental rules of similitude. In the present study, the Buckingham's π - theorem was used to derive the scaling factor (see Noor et al. 1998 for details).

Buckingham's π - theorem

Buckingham's π - *theorem* states that if X_1, $X_2 \ldots X_n$ are physical quantities related by some functional form

$$f(X_1, X_2 \ldots X_n)=0 \tag{4-1}$$

may be further expressed as

$$\Phi(\pi_1, \pi_2, \ldots \pi_m) = 0 \tag{4-2}$$

in which the π *-terms* (i.e. π_1, etc.), are dimensionless products of the physical variables X_1 to X_n. Then in order to find these π terms, one can express X_1 as a multiple product of the others, i.e.

$$X_1 = KX_2^a X_3^b X_4^c \text{, etc.} \tag{4-3}$$

in which K is a constant and a, b, c are to be determined. Then, by introducing the relevant dimensions of X_1 to X_n on either side of Equation (4-3), a sufficient number of equations are generated which allow meaningful relationships between the constants a, b, c etc. to be determined. Finally the m, π*-terms*, where $m=n-r$, can be obtained by grouping them with the r fundamental quantities such that all groups are dimensionless.

After finding the π*-terms* for the interested physical equation, the model and prototype can achieve complete similarity if all the dimensionless π*-terms* are the same in both model and prototype. The scaling factors for the scaled test can then be derived from the equations established through the π*- terms*.

4.1.3 Woodframe structure scaling techniques

Woodframe structures are very popular for residential construction in North America, comprising more that 90% of new homes. The main lateral force resisting assemblies for light frame wood structures are wood shearwalls which are made from dimensional lumber, plywood or oriented strand board (OSB), and nails. Different from reinforced concrete structures, the primary lateral resistance of the shearwall is provided by the interaction of framing studs and sheathing panels through nail or screw connections. The nonlinear load resisting behavior at the connector level, such as the pulling out of the sheathing nails and crushing of the wood around the nails, provides the majority of the shear resistance to the forces induced by the earthquake ground motion. Therefore one can conclude that the damage to shearwalls occurs, or at least begins, at the nail level during earthquakes. A one-story full scale woodframe uni-axial shake table test at Colorado State University (CSU) showed this damage characteristic (van de Lindt and

Liu, 2007, van de Lindt, Liu and Pei, 2007). After a series of several earthquakes at different intensity levels, some nails which connected the frame and sheathing were pulled out and crushing of wood around nails was also observed, especially around the corner fasteners. Based on these observations and the nonlinear behavior/mechanics of a shearwall, it can be seen that if the fasteners can be scaled, then the wall and subsequently the entire building should behave similarly to the prototype. For woodframe structures, it is difficult to simply use a dimensional scale factor to scale the prototype because the woodframe structure itself is a complicated dynamic system whose energy dissipation behavior is controlled by every sub-assembly component/connector which means that each component/connector has its own nonlinear behavior. In this study, scaling will begin at the nail level based on a series of reversed cyclic tests, and the appropriate scaling method for woodframe structures will be determined and applied.

The size of the uni-axial shake table at Colorado State University (CSU) is 8 ft x 16 ft and the height from the surface of shake table to roof is about 13 ft. Due to this size limitation, it was impossible to perform the shake table test with a full scale woodframe structure resembling realistically sized residential construction, thus a scaled test was selected for this study. On the other hand, the selection of the correct scaling factor for woodframe structures must also consider the constructability, which means the nail, sheathing panel, and dimensional lumber size must be available for the scaled construction. Hence, in order to make the most of the space on the shake table at CSU, a dimensional scaling factor of ½ was selected. At the same time other details should also be considered under the similitude theorems when dealing with the scaling of wood. These details include the choice of framing studs, sheathing panels, nails and, of course, added seismic mass which will be put on the scaled model. For practical reasons and compression capacity, dimensional lumber 1x3 (0.75" x 2.5") was selected as the scaled studs to be representative of the 2x4 (1.5" x 3.5") prototype studs and ¼" thick three-ply plywood was used as scaled sheathing panels in the half-scale woodframe model.

Therefore the scaling procedure in this study will focus on the choice of the governing equations, nail type, the scaling factors for seismic mass and the time scale of the earthquake input while given the dimension scaling factor is equal to ½. For the scaling factors used in this study, we define

$$S_x = \frac{x\,of\ model}{x\,of\ prototype} = \frac{x_m}{x_p} \tag{4-4}$$

where x can be a physical property of the prototype and the model, such as length l, time t, mass m, dissipation energy E, or restoring force F; the subscript m stands for model and p stands for the prototype.

The scaling factor for acceleration was selected to be 1 in this study ($S_{acc} = 1$) which means that the absolute acceleration is the same both for both the scaled input and the prototype. Then the time scaling factor for earthquake input can be obtained based on a dimensional factor equals to ½ ($S_l = \frac{1}{2}$). Based on the unit of acceleration, the time scaling factor is the computed as

$$S_{acc} = \frac{a_m}{a_p} = \frac{l_m}{t_m^2} \bigg/ \frac{l_p}{t_p^2} = 1 \qquad \Rightarrow \qquad (\frac{t_m}{t_p})^2 = S_t^2 = \frac{l_m}{l_p} = S_l$$

$$\Rightarrow \qquad S_t = \sqrt{S_l} = \frac{1}{\sqrt{2}}$$

Since the materials for the half-scale woodframe structure have been selected and the scaling factor for the acceleration has been set to unity, the scaling factor for seismic mass will only depend on the nail type in this study. Based on the fundamental theorems of similitude and the characteristics of energy dissipation in woodframe components, two governing equations have been selected to drive the scaling factors for seismic mass. Namely, Newton's second law

$$ma + F = 0 \tag{4-5}$$

in which, m is the seismic mass, a is the acceleration and F is the nail restoring force, and conservation of energy which can be expressed as

$$\int xFdx = \frac{1}{2}mv^2 + E_{diss} \tag{4-6}$$

in which, x is drift level, F is the force, m is the mass, v is the velocity and E is the dissipated energy dissipated during excitation.

Using Newton's second law (Equation (4-5)), the governing equations for the model and the prototype are as below:

$$m_m a_m + F_m = 0 \tag{4-7}$$

$$m_p a_p + F_p = 0 \tag{4-8}$$

Based on the definition of the scaling factor (Equation (4-4)) and $S_{acc} = 1$, we have $a_m = S_{acc} a_p = a_p$, $m_m = S_m m_p$ and $F_m = S_F F_p$. Hence, Equation (4-7) can be written as:

$$\frac{S_m}{S_F} m_p a_p + F_p = 0 \tag{4-9}$$

In order to make Equation (4-8) and (4-9) equivalent:

$$\frac{S_m}{S_F} = 1$$

Using the conservation of energy (Equation (4-6)), the governing equations for the model and the prototype are written as:

$$\int x_m F_m dx = \frac{1}{2} m_m v_m^2 + E_m \tag{4-10}$$

$$\int x_p F_p dx = \frac{1}{2} m_p v_p^2 + E_p \tag{4-11}$$

Similarly, using scaling factors, the Equation (4-10) can be rewritten as:

$$S_l S_F \int x_p F_p dx = S_m S_v^2 \frac{1}{2} m_p v_p^2 + S_E E_p \tag{4-12}$$

In order to make Equation (4-11) and (4-12) equivalent, the following relationship must be satisfied:

$$S_l S_F = S_m S_v^2 = S_E$$

in which, the dimensional scaling factor $S_l = \dfrac{1}{2}$ and the velocity scaling factor

$S_v = \dfrac{S_l}{S_t} = \dfrac{1}{2} \Big/ \dfrac{1}{\sqrt{2}} = \dfrac{1}{\sqrt{2}}$, hence, we get:

$$\frac{S_m}{S_E} = 2$$

For a standard North American one- or two-story residential structure it is typical to use 8d common nails for the wood shearwalls in woodframe buildings. In order to find the appropriate nail type for the scale model, a series of reverse cyclic loading tests on small nails was carried out at the CSU lab for three different types of nails: 4d common nail (4d), 4d-finish (4df) and 3d-finish (3df). The finish nails have smaller heads than the common nails and are usually used in non-structural applications (attaching finishing material such as trim board, etc). For robustness of the comparison, three different load protocols were used in the cyclic test and are shown in Figure 4-1. Based on the nail hysteresis from the nail cyclic tests, the restoring force F, the dissipation energy E under different loading protocols, the scaling factor S_F and S_E for each type of nail were obtained and listed in Table 4-1.

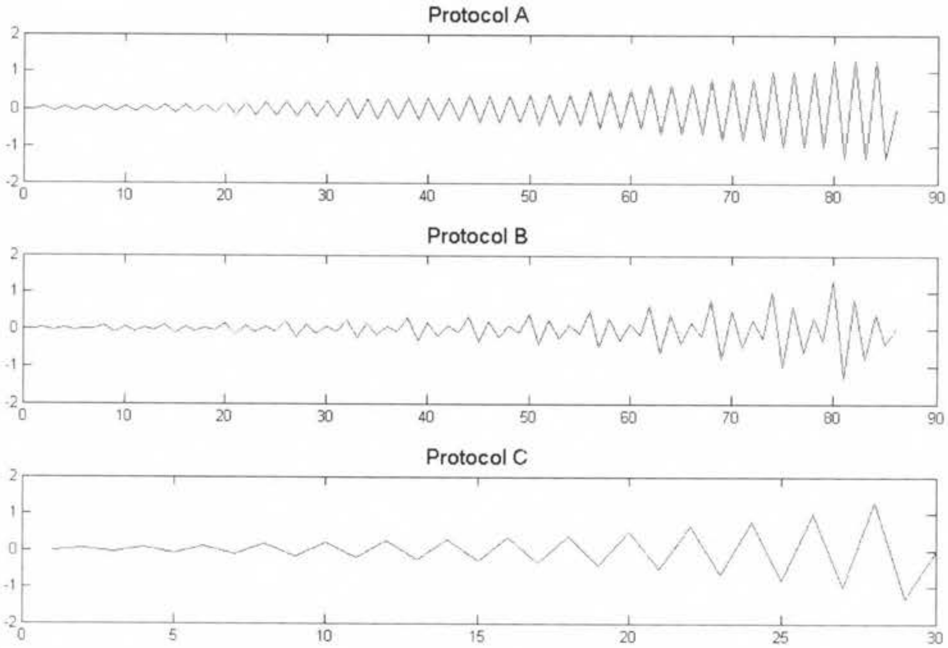

Figure 4-1 Protocols in nail cyclic test

Table 4-1 Restoring force scaling factor S_F and energy dissipation scaling factor S_E

Nail type	Protocol	Force (lb)	S_F	Energy (J)	S_E
8d	A	300		920.67	
	B	240		1020.30	
	C	250		837.72	
4d	A	100	0.33	120.41	0.13
	B	80	0.33	188.12	0.18
	C	155	0.62	65.78	0.08
4df	A	55	0.18	78.82	0.09
	B	100	0.42	131.04	0.13
	C	55	0.22	73.45	0.09
3df	A	90	0.30	104.26	0.11
	B	90	0.37	100.07	0.10
	C	110	0.44	72.13	0.09

Since the sheathing to framing nails dissipate most of the energy during earthquake shaking for woodframe buildings as previously discussed, it was appropriate to use conservation of energy in the scaling procedure along the lines of van de Lindt (2007). There are several nail options for a half-scale woodframe building. However, for convenience of construction, a 4df nail was selected to simulate an 8d nail at scale. Thus, the mass scaling factor can be determined based on the energy scaling factor and the relationship between mass and energy scaling factor (from 0.18 to 0.26). In this study, the mass scaling factor has been selected to be equal to 0.25 ($S_m = \frac{1}{4} = 0.25$).

4.1.4 Verification of scaling factors on half-scale woodframe structure

In order to verify the scaling techniques for woodframe structures in this study, the comparison between a full-scale and a half-scale woodframe shake table test was performed. A similar study was performed by van de Lindt (2007) but that building was relatively small and rectangular, so it is believed that it should be checked with a more realistic building configuration. A two-story full-scale woodframe townhouse, hereafter referred to as the benchmark structure, was tested on the twin shake tables at State University of New York at Buffalo (UB) in 2006 (Christovasilis et al. 2007). The floor plan of benchmark structure tested at UB is shown in Figure 4-2 and it was approximately 22 ft x 58 ft. A scaled version of the benchmark structure was built at CSU to determine the accuracy of scaling a woodframe building. The size of shake table at CSU is approximately 8 ft x 16 ft, thus a scaling factor of 1:2 for dimension was selected. Due to the size limitation of the uni-axial shake table at CSU, the shearwalls only in the N-S direction of benchmark structure were built at half-scale for the woodframe structure. In order to fit all scaled shearwalls on the shake table at CSU, the shearwalls were compactly installed. The floor diaphragm was assumed to be rigid in both the half-scale model and the prototype. This assumption was not accurate for the prototype but a necessity. The number of nails used at every nail line is the same and the quantity of anchor bolts and the hold-downs of each shearwall are also the same as the benchmark structure tested at UB. Figure 4-3 shows the actual half-scale benchmark structure tested on the uni-axial shake table at CSU. Sand bags were used to simulate the seismic mass on each story, which was 12 kips for the first-story and 4.8 kips for the roof level as calculated earlier (e.g. ¼ the mass of the prototype).

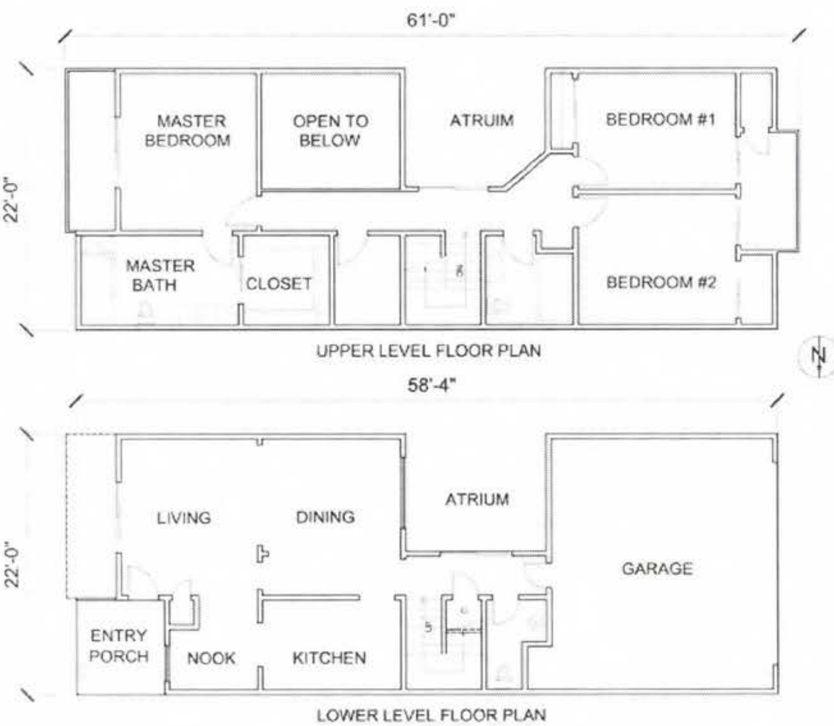

Figure 4-2 Two-story benchmark structure floor plan

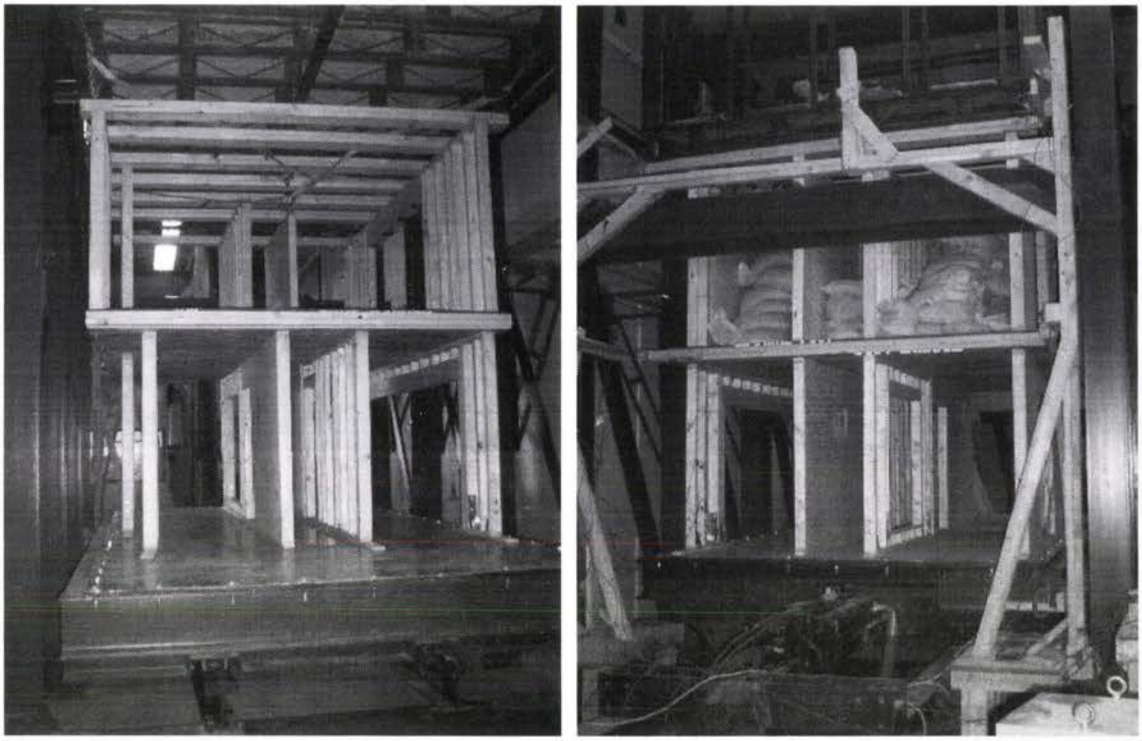

Figure 4-3 Half-scale woodframe structure experiment setup

The response of the scaled model and the prototype at the level 2, S06 earthquake are shown in Figure 4-4 and 4-5. From these plots, it is quite obvious that the period of the scale model and the prototype agrees well, which shows that the scaling method in this study can reasonably represent the woodframe prototype.

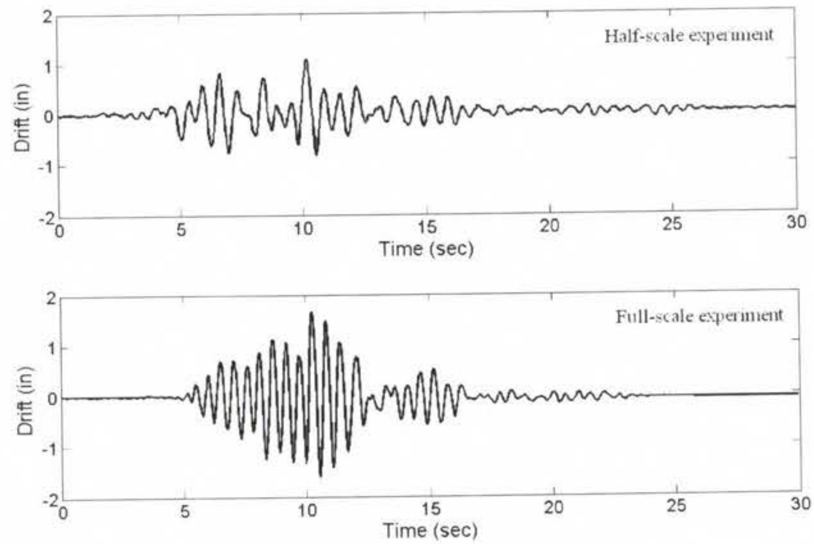

Figure 4-4 1st-story left side (garage side) wall inter-story drift comparison

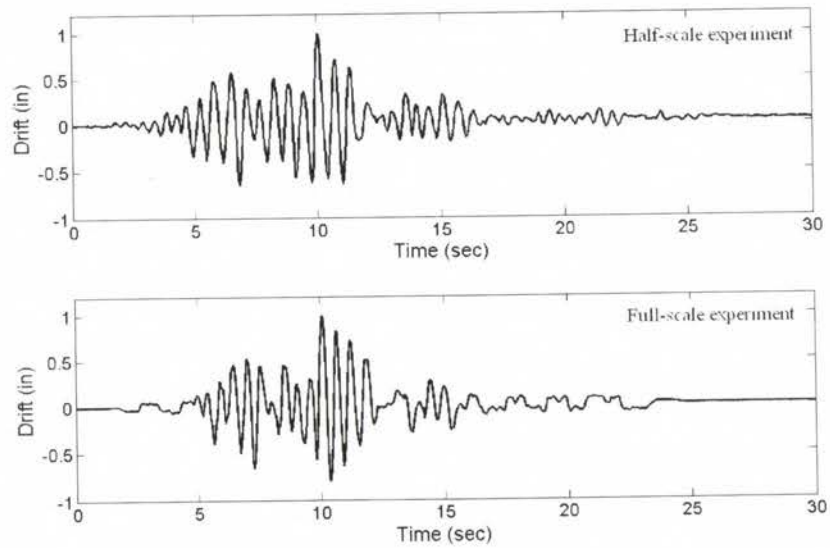

Figure 4-5 1st-story right side (non-garage side) wall inter-story drift comparison

4.2 Half-scale woodframe building experiment setup

The practicability of the half-scale experiment on woodframe structure had been discussed in the previous Section. In order to verify the numerical model and design procedure discussed in Chapter 3, the half-scale woodframe building with the FP bearings were built and tested on the uni-axial shake table at CSU. This is also the first time that the FP bearings applied to woodframe structure in United States.

4.2.1 Experiment building

It was mentioned previously that the size of the shake table at CSU is 8 ft x 16 ft. Hence, a western style woodframe residential building in California was designed based on the footprint of the shake table at CSU. The 1^{st}-story of the prototype was designed to be a rectangular shape and take full advantage of the steel shake table surface. However in order to provide realistic architecture to the building, and introduce the possibility of a slight torsional response mode (even with uni-axial excitation) the 2^{nd}-story was not a regular shape. The floor plan for the prototype is shown in Figure 4-6. This typical single family home has three bedrooms, two and half bathrooms, and a one-car attached garage. The total area for the prototype is about 1,150 square feet which is relatively small for North America but not atypical for urban areas in California. The solid model for this residential structure is shown in Figure 4-7. The half-scale model was built at CSU the structural lab based on this prototype.

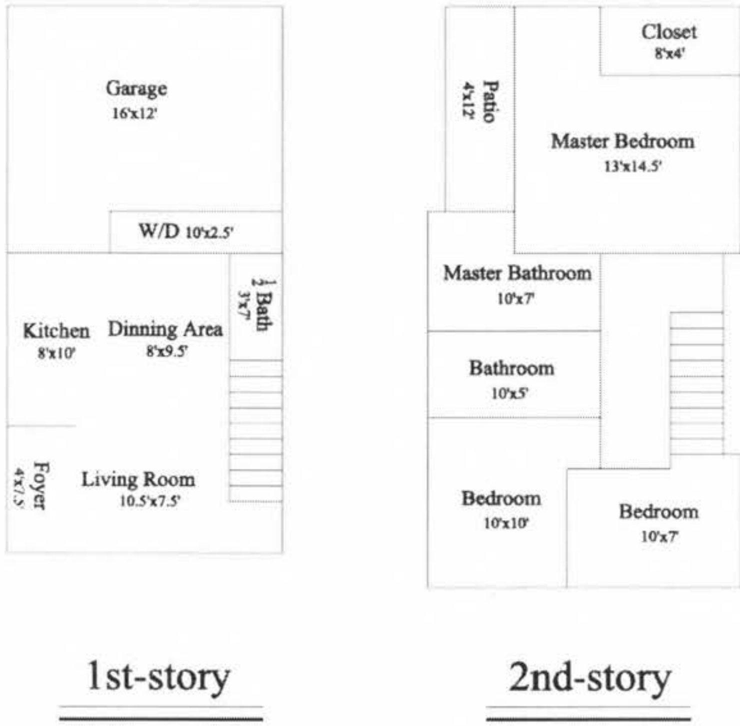

Figure 4-6 Two-story western-style woodframe structure floor plan

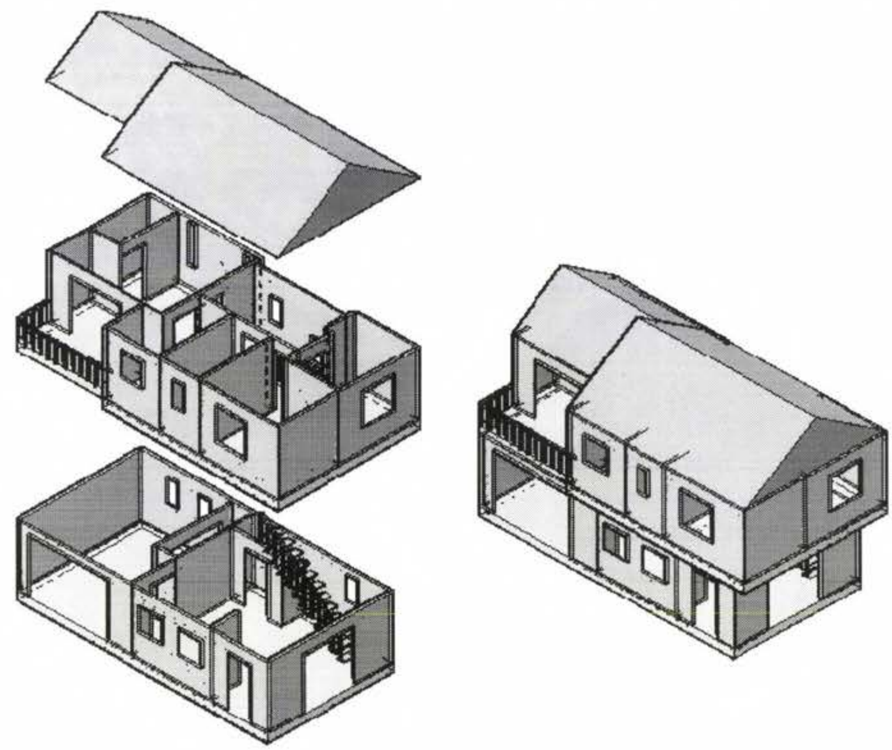

Figure 4-7 Two-story western-style woodframe structure solid model

4.2.2 Foundation configuration

The difficulties in applying the FP bearing to a woodframe structure were discussed in Chapter 3. In order to make the FP bearings applicable for the half-scale woodframe model, designing a foundation with significantly high in-plane stiffness and strength was the key issue in the shake table tests conducted in this study. Since the first floor is rectangular and four FP bearings will be used in the shake table test, the location of the bearings was kept symmetrical so that the vertical force acting on each FP bearing is equal to the reaction of each FP bearing and tends to be uniform for the shake table test. The placement of the bearings was designed to minimize the bending stiffness demand on the floor diaphragm. In order to increase the rigidity and out-of-plane stiffness of the foundation diaphragm, steel beams (W6x9) were integrated into the design and are shown in Figure 4-8. The area between the steel beams was filled with wood diaphragm. The connection details, such as steel to steel, wood to steel etc., were shown in Figure 4-9.

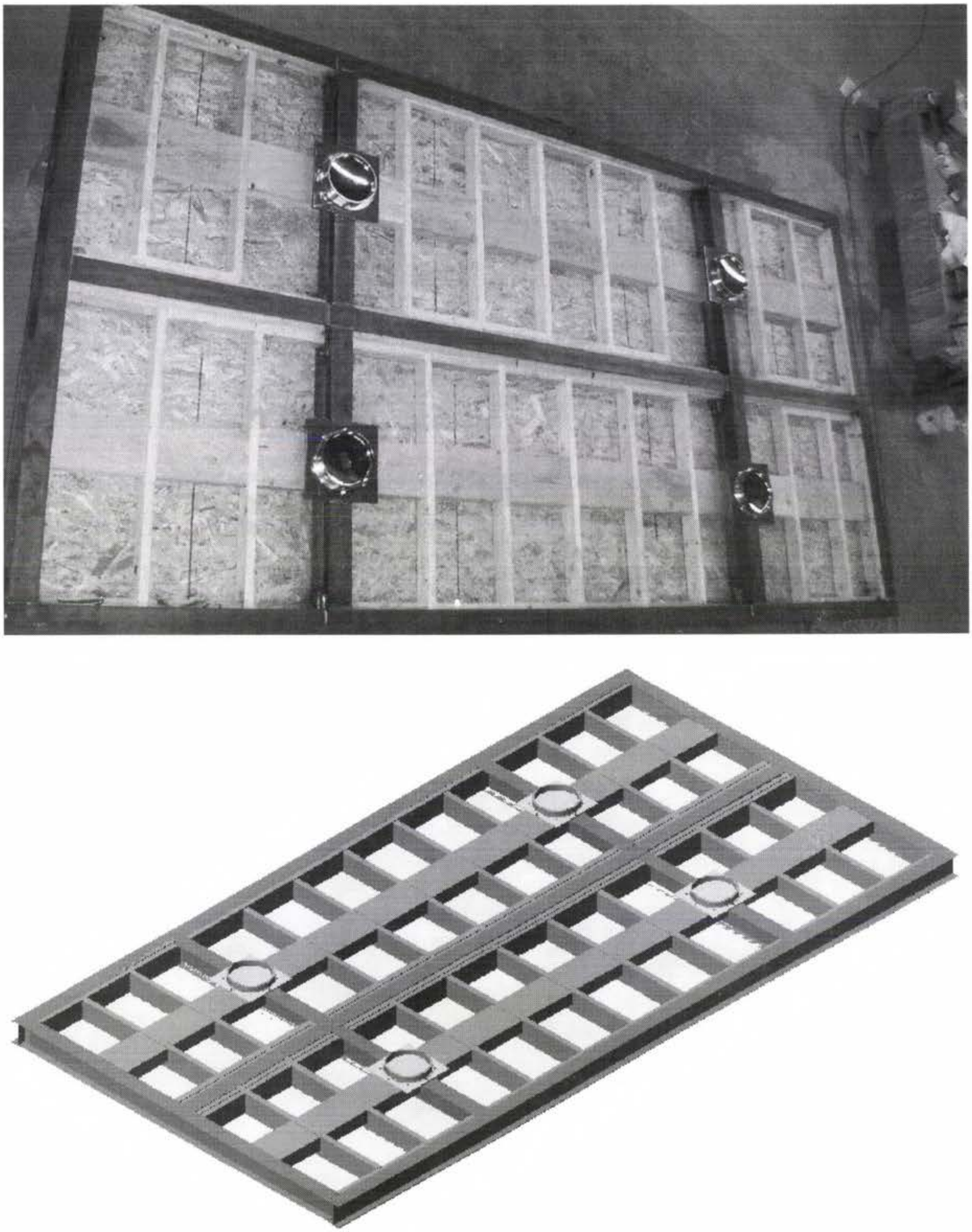

Figure 4-8 Foundation configuration of the half-scale woodframe building

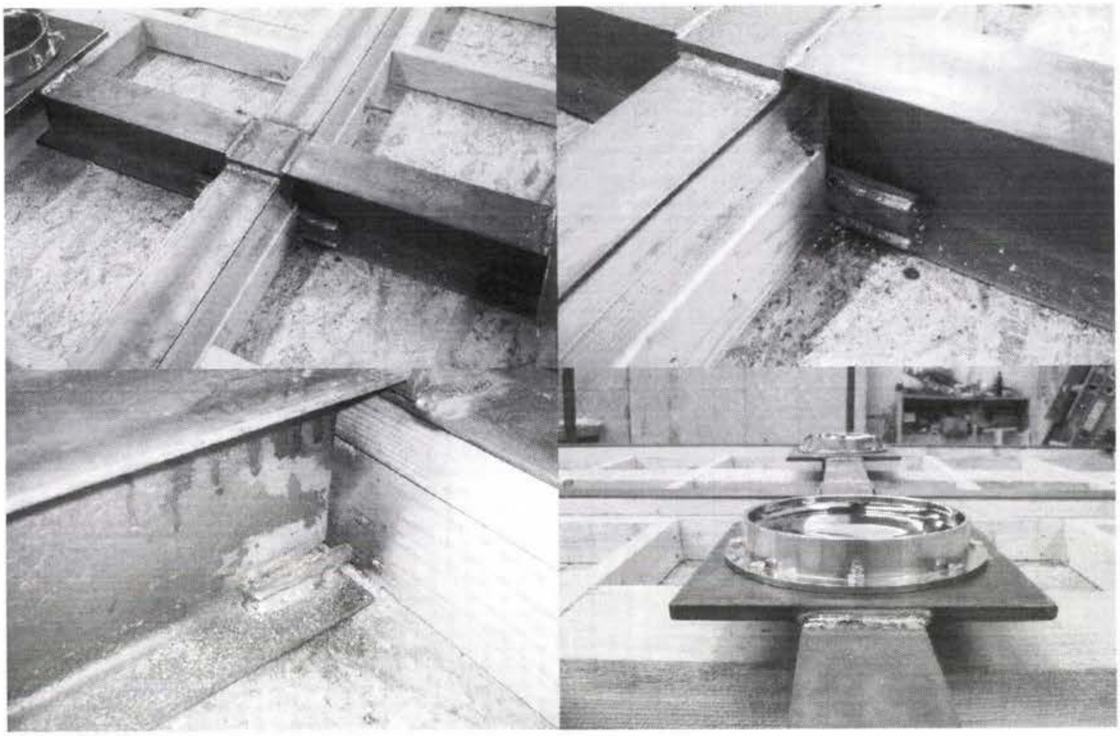

Figure 4-9 Foundation connection details

4.2.3 Experiment set up

As mentioned in Section 4.1.3, dimensional lumber 1x3 (actual size is 0.75 inch x 2.5 inch) was selected as the scaled studs, ¼ inch thick three-ply plywood panels was used as scaled sheathing panels, 6d common nails were used for framing and recall 4d-finish nails were selected in sheathing connection in building half-scale California residential building. Simpson hold-down HD2A (the smallest off-the-shelf shear wall hold down available) were used at the corner of each shearwall line in the 1^{st}-story and 3/8'' steel bolts were used for the anchor bolts along the sill plate of the shearwalls. Since the seismic mass scaling factor was ¼ and the floor area of the scaled model is already a quarter of the prototype, the distributed seismic weight (psf) value is the same for both the prototype and the half-scale model. The distributed seismic mass for the first, the second floor level and the roof level is 25 psf, 35 psf and 25 psf respectively. Considering the weight of shearwalls and floor diagram itself, the additional seismic mass (concrete paving blocks) placed at each level was 2,200 lb, 3,700 lb and 2,500 lb.

Two string potentiometers were installed to measure the displacement of the roof and second story diaphragm during earthquake excitation. Two LVDT gages were installed for the measurement of the table displacement and the isolated base motion. Three accelerometers were installed on the roof, second story diaphragm, and the isolated base to measure the acceleration at these locations during earthquake excitation.

4.3 Numerical model verification with experiment results

4.3.1 Numerical analysis

The SAPWood software was used for the numerical analyses in this study. It was mentioned in Chapter 2 that in this software package, the user has the ability to set up the wall model first at the sub-assembly level using the nails and studs. Hence the SAPWood Nail Pattern (SAPNP) models for the shearwalls in the half-scale western style California building were built in SAPWood according to the preliminarily designed wall configuration. These wall models were then subjected under predefined cyclic loading protocols (quasi-static pushover analysis) to obtain the wall hysteresis parameters. Once the wall parameters were identified for each wall, the system level numerical model for the structure is then developed in SAPWood based on wall location known from the preliminary architectural floor plan. In addition to shearwall hysteretic springs, the FP bearing model should also be included in the system numerical model. It was discussed in Chapter 3 that the element that characterize the behavior of the FP bearing model in SAPWood are controlled by the radius R, initial stiffness K_0, the friction coefficient at maximum and minimum velocity f_{max} and f_{min} and the constant for the given bearing pressure and condition of the interface a. The properties of the FP bearing used in the experiment are: radius of curvature equal to 47.35 cm (18.64 inch), a displacement capacity of +/- 8.22 cm (3.24 inch), and a maximum and minimum friction coefficient of 0.1 and 0.06 which was recommended by Constantinou (Constantinou 1994). The constant a was set equal to 0.508.

Once the numerical model with base isolation elements was established, a suite of twenty ground acceleration records developed by Krawinker et al. (2000) were scaled to the 2%/50 hazard level (defined as having a 2% probability of being exceeded over a 50 year period) and applied to the structure in the numerical analysis in order to determine which ground motions could be used in the half scale shake table test. The displacement capacity of the FP bearing is the most important criterion in this selection process since the bearings can be damaged if their motion exceeds the capacity during the test. This could also severely damage the building since there is a hard stop on the building. On the other hand, the test was intended to prove the effectiveness of isolation system under seismic excitation to some degree. Thus, the response of the FP bearings needs to be significant enough for the ground motion records selected. In this study, there are two criteria to select the earthquake record: one is that if the displacement of FP bearing in the numerical simulation is greater than the displacement capacity of the bearing, the earthquake record is not selected, and the second is that if the displacement of FP bearing is less than 50% of the displacement capacity of the bearing, the earthquake record will not be selected. Therefore, after twenty numerical simulations, there are three earthquake records that had been selected, namely the 1994 Northridge earthquake recorded at the LA-Hollywood storage station (nor5), the 1989 Loma Prieta earthquake recorded at the Capitola station (lp1), and the 1987 Superstition Hills earthquake recorded at the Plaster city station (sup3). At the 2%/50 hazard level, the peak ground acceleration (PGA) of these three earthquake records were 0.643g (nor5), 0.683g (lp1) and 0.778g (sup3) respectively.

Since the 2%/50 level ground motions selected above can be used without damaging the FP bearings, these ground motions can also be scaled down to lower intensity levels to perform the shake table test. So the shake table tests with three 10%/50 level motions were also conducted in order to thoroughly study the impact of the incorporation of FP bearing devices under different levels of earthquake intensity. The peak ground acceleration at 10%/50 level was 0.482g (nor5), 0.423g (lp1) and 0.398g (sup3) respectively. Together with the collapse prevention (CP) hazard level records, a total of six ground motions were used in the series of shake table tests. For model verification purpose, the recorded shake table motion during earthquake excitation was used as the earthquake input in the numerical analysis. The maximum displacement of FP bearing and the inter-story drift at the 1st-story and 2nd-story in the numerical simulations were listed in Table 4-2. The time history of the responses are shown in Figures 4-10, 4-11 and 4-12.

Table 4-2 Numerical analysis result

Earthquake	Hazard level	Maximum displacement of FP bearing (in)	Maximum inter-story drift at 1st-story (in)	Maximum inter-story drift at 2nd-story (in)
lp1	10%/50	0.92	0.13	0.12
	2%/50	1.63	0.15	0.14
nor5	10%/50	0.93	0.14	0.11
	2%/50	1.93	0.17	0.15
sup3	10%/50	1.32	0.17	0.16
	2%/50	2.41	0.19	0.18

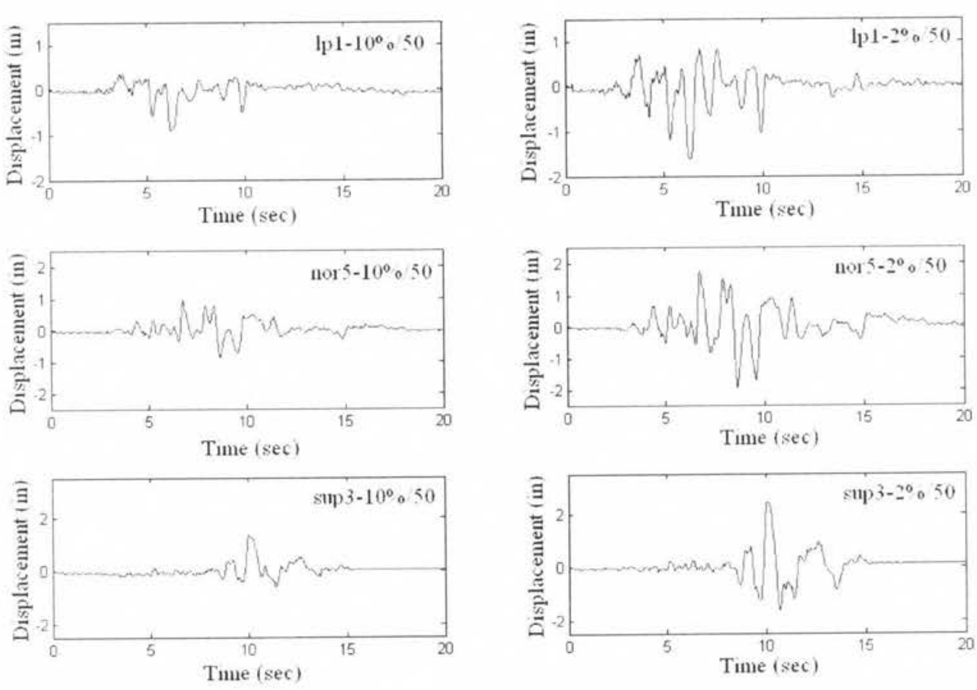

Figure 4-10 FPS displacement numerical results

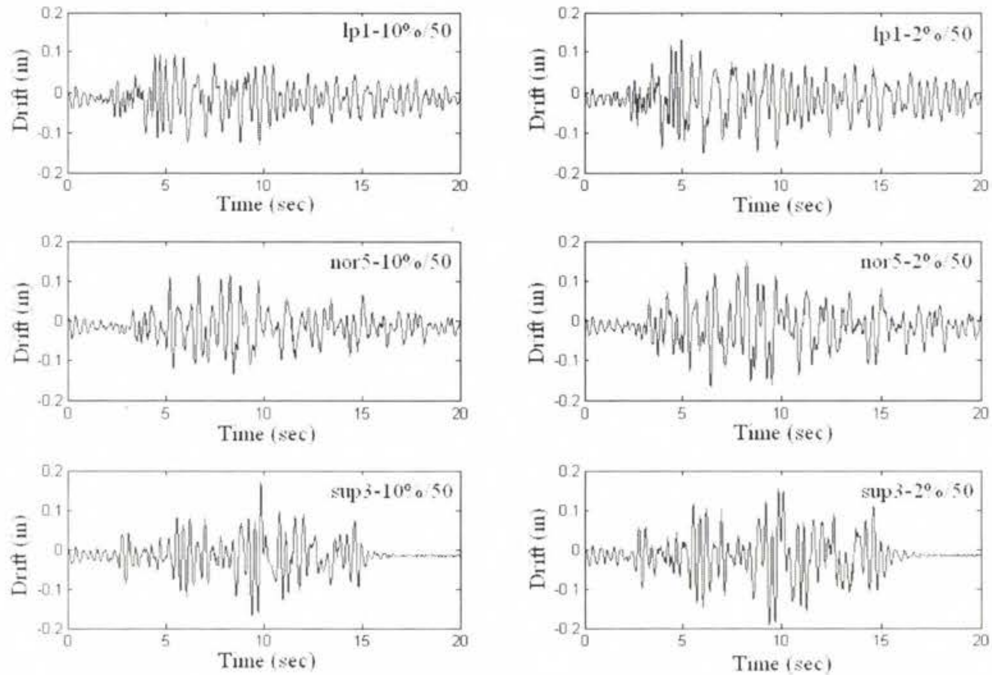

Figure 4-11 1st-story inter-story drift numerical results

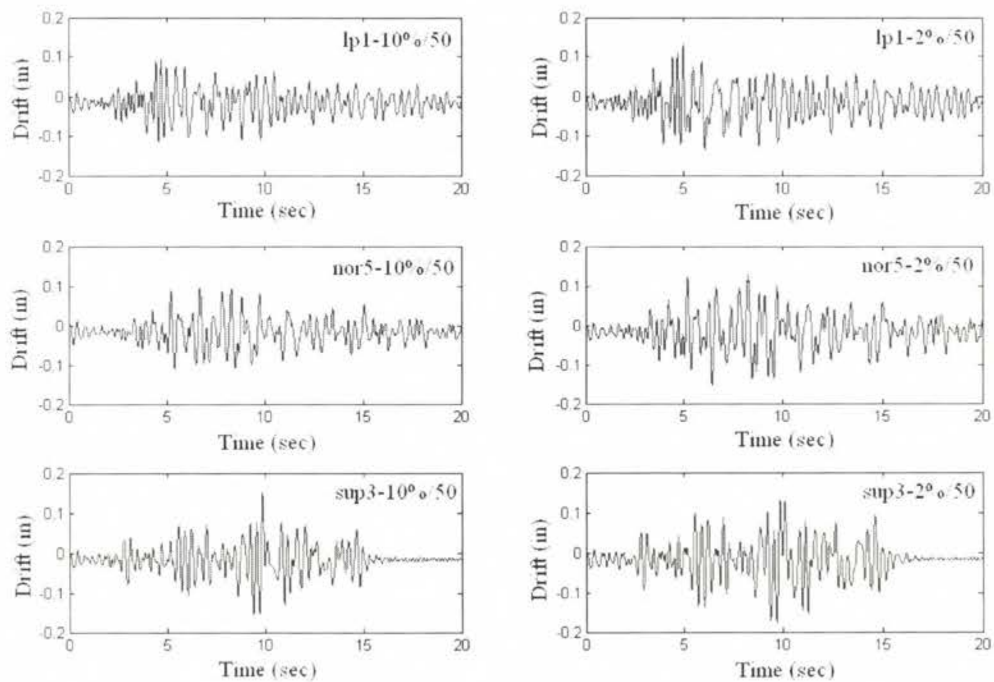

Figure 4-12 2nd-story inter-story drift numerical results

4.3.2 Experiment and numerical analysis comparison

Following the construction of half-scale woodframe structure, installation of the base isolation system and displacement and acceleration gage set up, a series of uni-axial shake table test were conducted at the structural lab of CSU in September 2008. In order to verify the numerical model of FP bearing in the SAPWood software (discussed in Chapter 3), the responses during earthquake excitation, such as the displacement of the FP bearing and the inter-story drift at each story, are compared in this section. The comparison of the maximum displacement of the FP bearing and the inter-story drift at the 1^{st}-story and 2^{nd}-story between are listed in Table 4-3. The comparisons of time history for the responses of FPS bearings are shown from Figure 4-14 to 4-15.

Table 4-3 Experiment and numerical analysis comparison

Earth quake	Hazard level	Maximum displacement of FP bearing (in)		Maximum inter-story drift at 1st-story (in)		Maximum inter-story drift at 2nd-story (in)	
		Test	Numerical model	Test	Numerical model	Test	Numerical model
lp1	10%/50	0.97	0.92	0.26	0.13	0.16	0.12
	2%/50	1.68	1.63	0.83	0.15	0.24	0.14
nor5	10%/50	0.99	0.93	0.14	0.14	0.19	0.11
	2%/50	2.09	1.93	0.21	0.17	0.24	0.15
sup3	10%/50	1.53	1.32	0.17	0.17	0.14	0.16
	2%/50	3.12	2.41	0.34	0.19	0.24	0.18

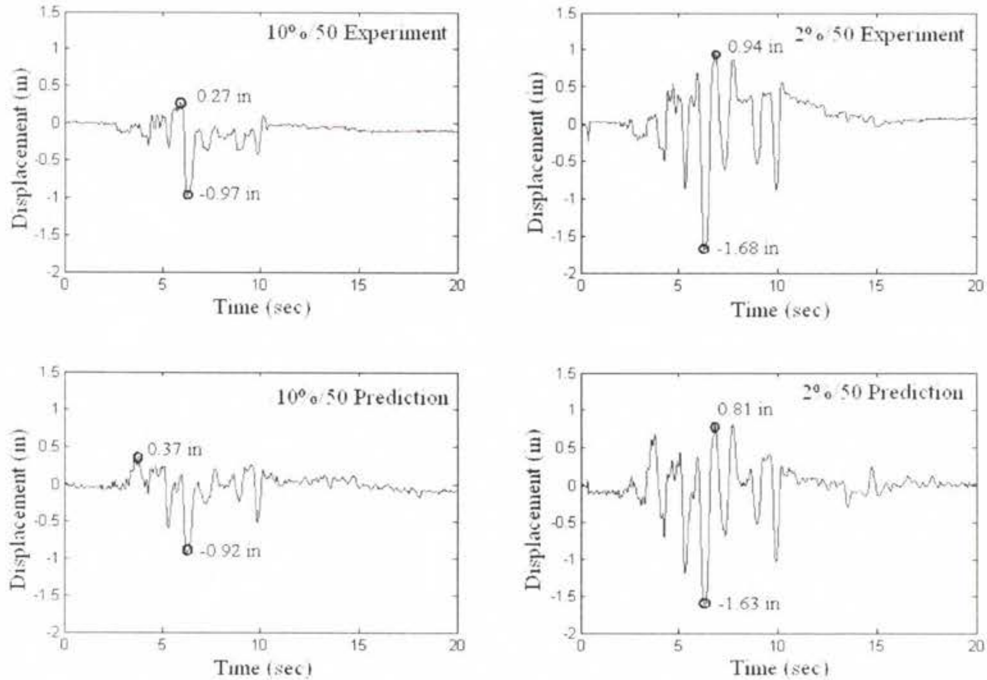

Figure 4-13 FPS bearing response comparison with lp1 earthquake record

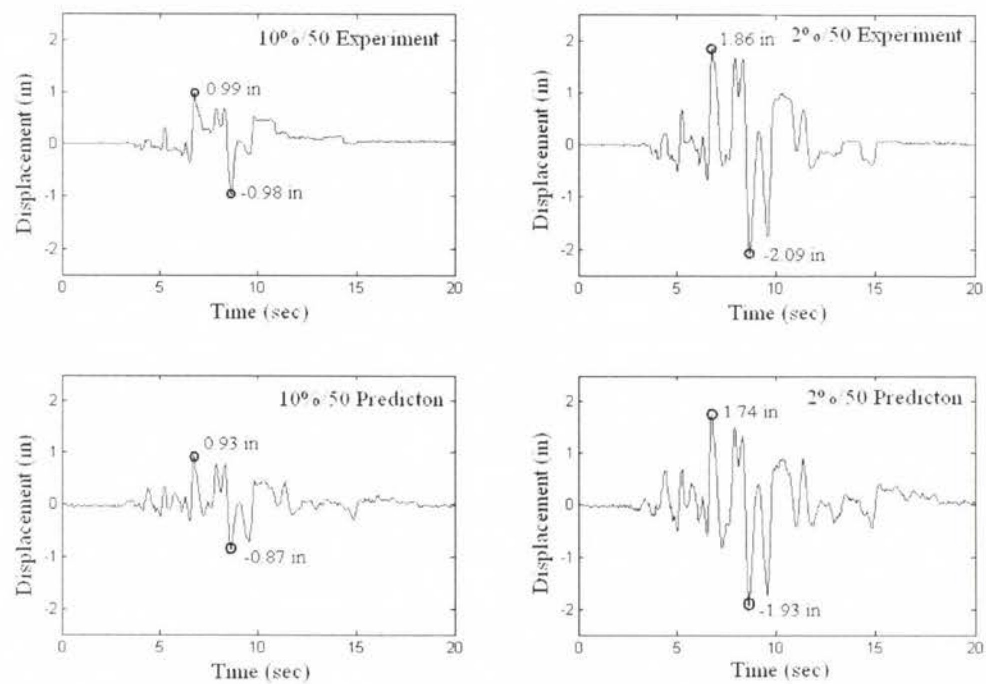

Figure 4-14 FPS bearing response comparison with nor5 earthquake record

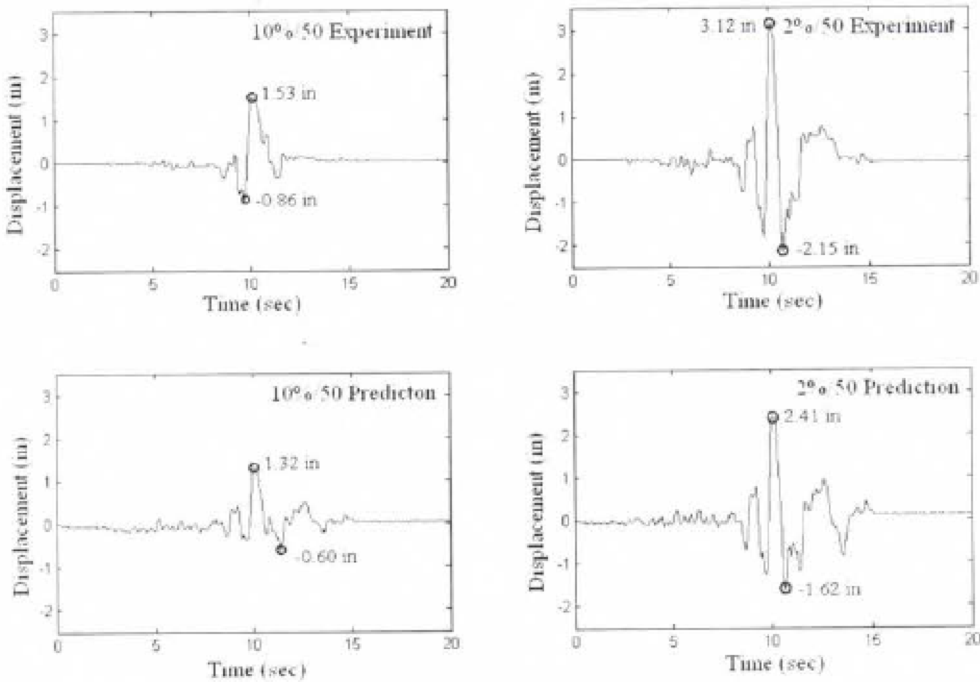

Figure 4-15 FPS bearing response comparison with sup3 earthquake record

The comparison of the results showed that the numerical model is capable of capturing the time history behavior of the system, but the maximum response of the FPS bearing was under-predicted. The inter-story response of the wood structure is very small and will not govern the design.

4.4 Foundation and FP bearing at prototype scale

Since the foundation diaphragm design is a key feature in the application of base isolation for woodframe structures, the full-scale foundation of the prototype was discussed in this section. As it discussed in Section 4.1.3 of this dissertation, the half-scale model tested on the shake table at CSU had a geometric scaling factor equal to ½ and the seismic mass scaling factor was set equal to ¼. The main concern in bringing the half-scale foundation frame back to full-scale is to be able to control the stiffness of the foundation both in- and out-of-plane so that the deflection will not be excessive and shear forces are adequately transferred. It was assumed herein that the layout of the foundation frame is rectangular. Thus the deflection of the half-scale model will be proportional to that of the prototype following the similitude theory. In general, the deflection of a frame can be related to the load and the properties of the members as

$$\Delta \propto \frac{Fl^3}{EI} \tag{4-13}$$

where Δ is the deflection of any member in the frame, F is the load acting on the member, l is the length of the member, E is the material elastic modulus, and I is the cross-section moment of inertia.

In order to achieve the same level of rigidity in the prototype base frame as the scaled model, the ratio of prototype base deflection to the scaled model deflection should be less than ½, which is

$$S_\Delta = \frac{\Delta_m}{\Delta_p} \geq \frac{1}{2}$$

$$\Rightarrow \quad \frac{F_m l_m^3}{E_m I_m} \Big/ \frac{F_p l_p^3}{E_p I_p} \geq \frac{1}{2} \quad \Rightarrow \quad \frac{F_m}{F_p} \cdot \left(\frac{l_m}{l_p}\right)^3 \Big/ \frac{E_m}{E_p} \cdot \frac{I_m}{I_p} \geq \frac{1}{2}$$

Since steel beams were used to build the stiff foundation in both the half-scale model and the prototype, the properties of steel will be the same which means the elastic modulus scaling factor equals to 1 ($S_E = \frac{E_m}{E_p} = 1$). The ratio of the magnitude of force on the frame should be ¼ since the gravity and seismic force is proportional to the mass ($S_F = S_M = \frac{M_m}{M_p} = \frac{1}{4}$). The dimensional scaling factor equals to ½ ($S_l = \frac{1}{2}$). Therefore

$$S_I = \frac{I_m}{I_p} \leq \frac{S_F S_l^3}{\frac{1}{2} S_E} = \frac{\frac{1}{4} \cdot (\frac{1}{2})^3}{\frac{1}{2} \cdot 1} = (\frac{1}{2})^4 = \frac{1}{16}$$

In half-scale model, the steel beam is using W6x9 whose moment inertia (x-x) is equal to 16.4 in^4. In order to achieve the same out of plane stiffness provided in the half-scale shake table test for the prototype, the moment inertia of the steel member needs to be greater than 262.4 in^4. Based on the moment inertia criteria and the height of typical floor joist products, W 12x35 was selected for the foundation in prototype building.

For the FP bearing used in prototype, the displacement capacity needs to be twice as large as the one used in the half-scale model. However, the change in the radius of the FP bearing does not necessarily follow similitude theory since its impact involves nonlinear response of the structure, which means it is not just a linear similitude relationship. The design of FP bearing at full scale should follow the performance-based seismic design procedure with FP bearing included, which will be discussed in later chapters.

Chapter Five

Low-rise Woodframe Design Examples Using Performance-based Seismic Design Procedure

5.1 Building configurations for design examples

In this Chapter, the methodology and procedures proposed in Chapter 2 were applied to the generalized performance-based seismic design (PBSD) of typical woodframe buildings. Four woodframe buildings with realistic configurations and floor plans served as the illustrative examples. Although the selection did not incorporate all types of woodframe construction style in current design practice, it was believed to be a good representative subset of the current woodframe building inventory. The validity of the generalized PBSD concept and design procedure using non-linear time history analysis is believed to be well illustrated through the numerical simulations and analysis and results presented herein.

The example buildings used in this study included three two-story single family dwellings (SFD) with different characteristic shapes and a three-story condominium building, i.e. a multi-family dwelling (MFD). All of these buildings were light frame wood construction and each only considers wood shearwalls as the lateral force resisting mechanism. The architectural floor plans for the design examples are presented in Figures 5-1 to 5-4. In order to consider the effect of seismicity, three locations were selected for these design examples, namely Los Angeles (Lat/Lon: 34° N 118.2° W), Sacramento (Lat/Lon: 38.6° N 121.5° W) and Portland (Lat/Lon: 45.4° N 122.5° W). The preliminary design for the examples at different locations were based on the seismic design provision (Section 12.8 Equivalent Lateral Force Procedure) in ASCE 7 (2006) and wood shearwall design in NDS (2001). Later, the numerical model parameters for structural sheawalls as well as non-structural partition walls sheathed using gypsum wall board (GWB) were obtained using the SAPWood wall database. With the numerical model established, the PBSD procedure outlined earlier was followed. It is worth mentioning that the non-structural walls were included even though they are not part of traditional force-based design. They are part of the PBSD procedure because these walls can significantly affect the performance of the structure system.

5.1.1 Design example I: SFD with rectangular shape

This design example is a two-story SFD with a rectangular shape. The total area of the house is approximately 2,694 sq. ft. The building has four bedrooms, two and half bathrooms, and a two-car attached garage. The architectural floor plan is shown in Figure 5-1.

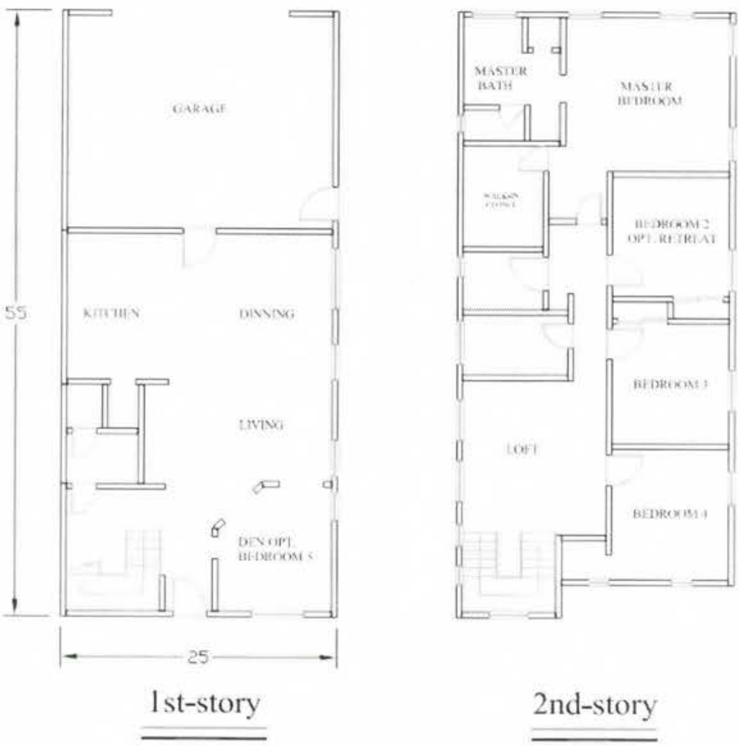

Figure 5-1 Design example I (rectangular shape) floor plan (unit: ft)

5.1.2 Design example II: SFD with 'L' shape

This design example is a two-story SFD with an 'L' shape. The total area of the house is approximately 2,760 sq. ft. This building has four bedrooms, two and half bathrooms, and an attached two-car garage. The architectural floor plan is shown in Figure 5-2.

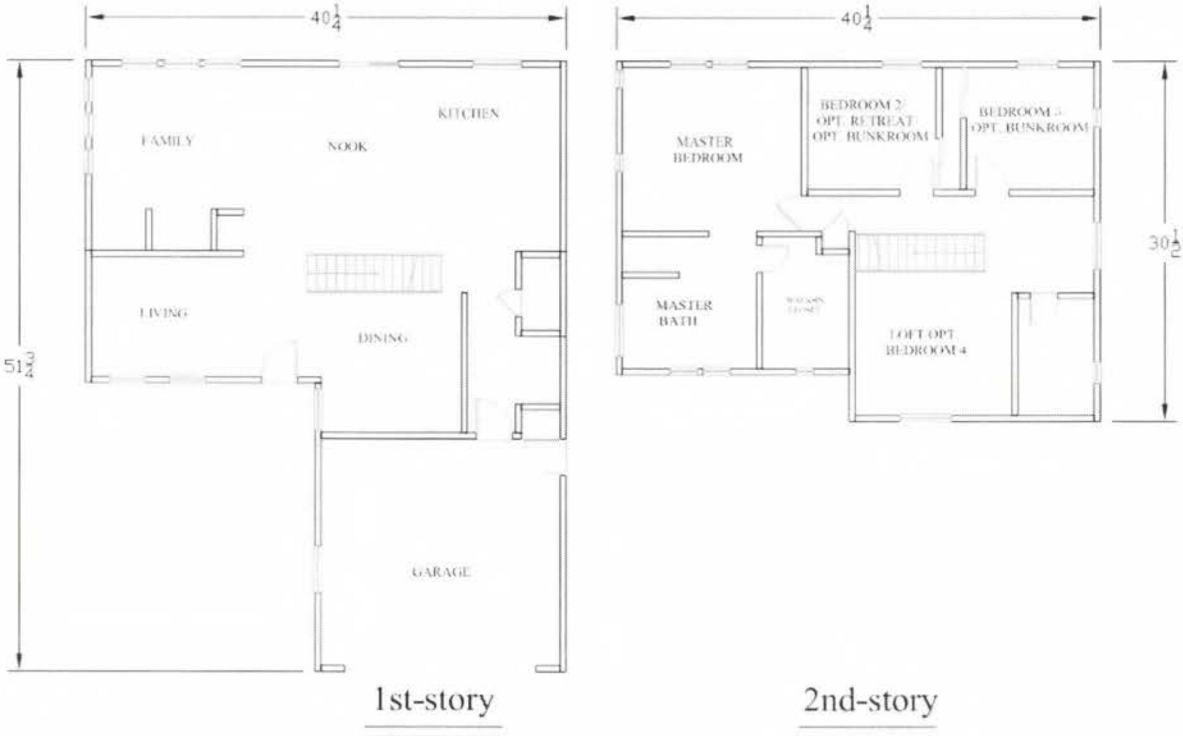

Figure 5-2 Design example II ('L' shape) floor plan (unit: ft)

5.1.3 Design example III: SFD with square shape

This design example is a two-story SFD with a square shape. The total area of the house is approximately 3,175 sq. ft. This building has five bedrooms, two and half bathrooms, and an attached three-car garage. The architectural floor plan is shown in Figure 5-3.

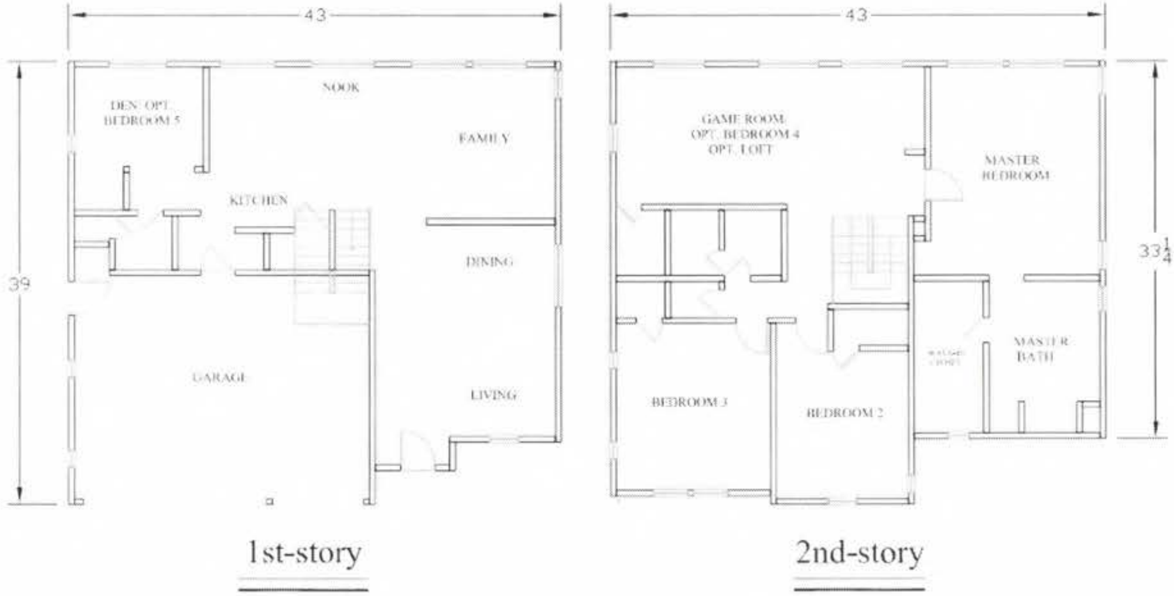

Figure 5-3 Design example III (square shape) floor plan (unit: ft)

5.1.4 Design example IV: Condominium

This design example is a three-story condominium building. The total area of each unit is approximately 2,175 sq. ft. Each unit has three bedrooms and three bathrooms. The architectural floor plan is shown in Figure 5-4.

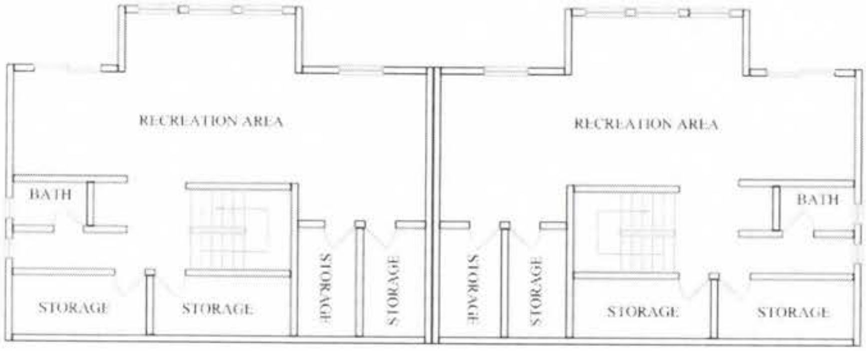

Lower Level

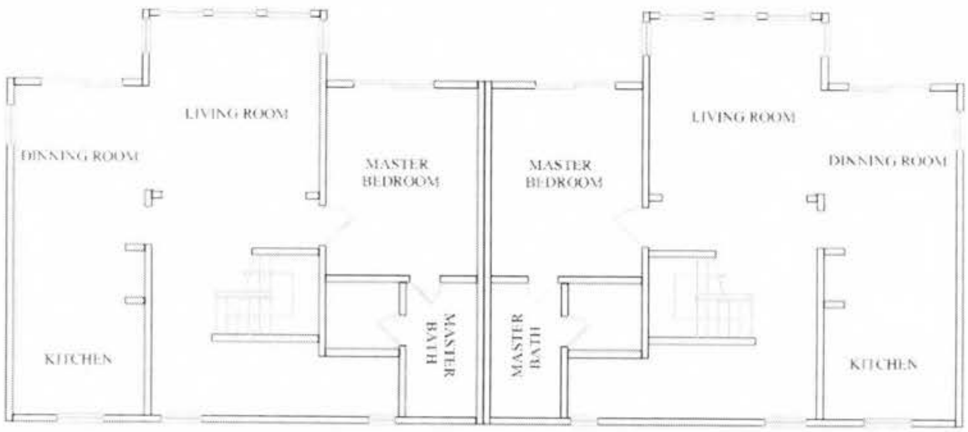

Main Level

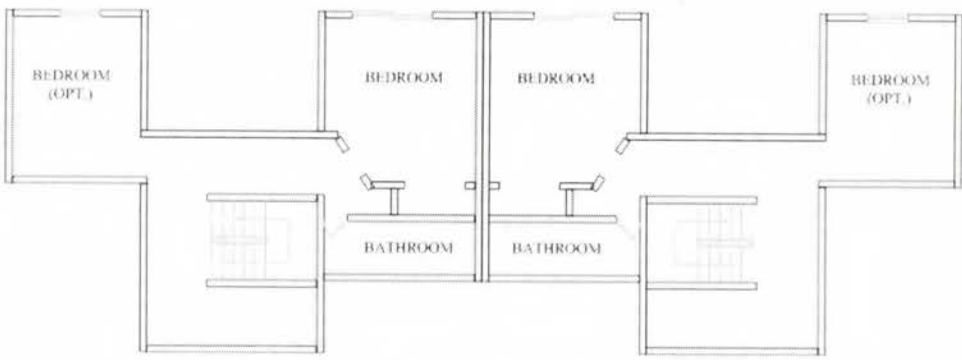

Upper Level

Figure 5-4 Design example IV (Condominium) floor plan (unit: ft)

5.2 PBSD procedure of design examples

In this section, the design and simulation procedure proposed in Section 2.3 is performed using the design example buildings illustrated above at three different locations. Herein let us firstly review the generalized PBSD procedure proposed in Chapter 2. First, the traditional force-based seismic design is performed for each of these woodframe buildings based on the basic information provided (floor plan, location, etc.) of the building. Whether the force-based design is over-designed or not enough, no matter what, the preliminary design can provide a good start point for the PBSD procedure. Second, once the force-based seismic design is completed, the individual wall model and system level numerical model for the woodframe building can be built based on the preliminary result. In this study, the processing of the building numerical model for individual walls and system models were executed using existing software: the SAPWood program. For individual walls, the SAPNP model was set up according to the preliminary wall configurations provided in the first step. Then through reversed-cyclic analysis on the SAPNP model, the hysteric parameters for each wall can be obtained. Assembling the system model for the entire woodframe building is based on the wall location known from floor plan and the wall hysteric parameters obtained from SAPNP analysis. Third, as was mentioned, the time-history analysis for the system model was executed using the SAPWood program. Here, in this study, multiple incremental dynamic analysis (M-IDA), time history simulation is performed to provide the data needed to implement the PBSD procedure. In this step, the performance of the numerical model at different hazard levels with a suite of earthquake records will be recorded. Fourth, construct the conditional distributions of the recorded performance at each hazard level and compare the performance curve with the predefined target curve. If the target curve is satisfied, the design is complete. If it is not, the preliminary design based on the force-based design result needs to be revised and the newly modified model must be re-analyzed and go through the steps above until the performance targets are satisfied. The entire PBSD procedure using SAPWood software in this Section is illustrated in Figure 5-5.

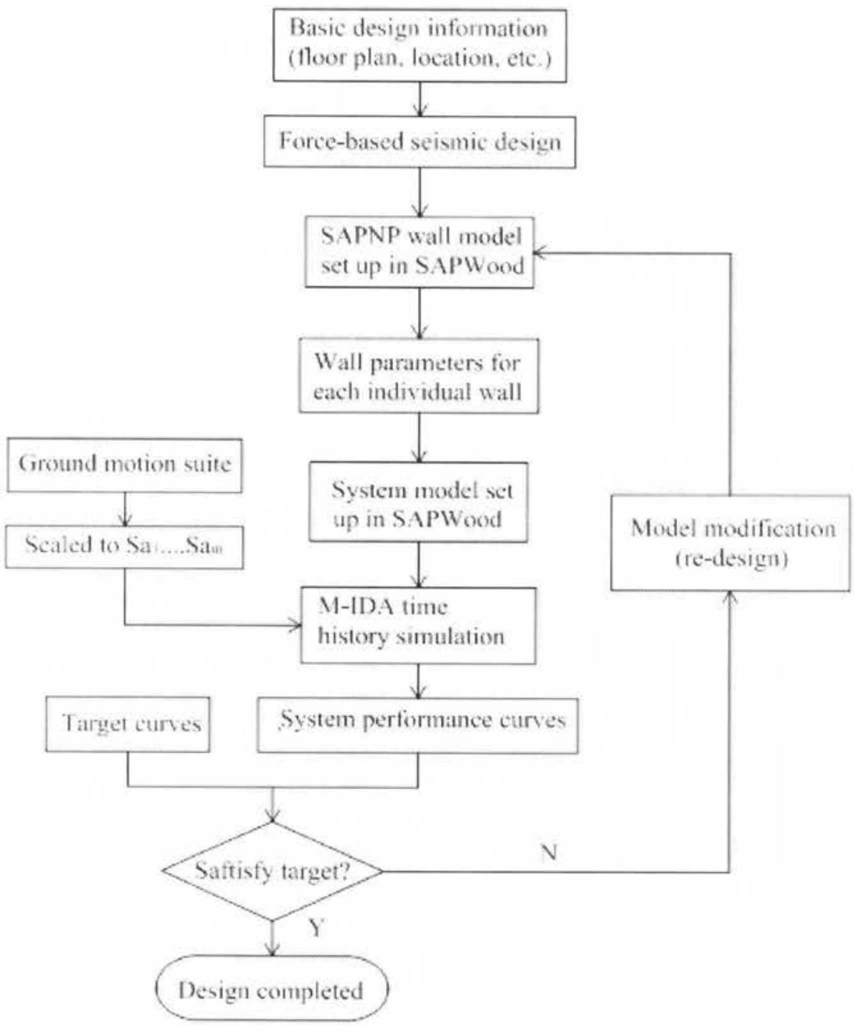

Figure 5-5 PBSD procedure using SAPWood program proposed in this dissertation

5.2.1 Force-based seismic design using current code

In this section, the force-based seismic design of the example buildings is conducted using current code requirements. First the seismic loads were calculated using the equivalent lateral force procedure (ELFP) as outlined in ASCE 7 (2006). Based on the force calculation, the length of the shearwalls in each direction, nail type and the panel thickness are selected. This was done using Table 4.1B in the NDS supplements (2001) which was used to determine the nail pattern for each shearwall. In this study, Douglas fir was selected for framing, 8d common nail (length: 2.5 inch, diameter: 0.131 inch) is chosen for sheathing to framing connector and the thickness of sheathing panel is 15/32''. As mentioned, three different locations were selected to represent different seismic zone, namely Los Angeles (Lat/Lon: 34° N 118.2° W), Sacramento (Lat/Lon: 38.6° N 121.5° W) and Portland (Lat/Lon: 45.4° N 122.5° W). Among these locations, Los Angeles represents a high seismic zone and Portland represents a low seismic zone.

The seismic mass for each story is assumed to be equivalent to 45 psf evenly distributed over the floor diaphragm. Following the ELFP design procedure in ASCE 7, the distributed vertical seismic force on each story of the example buildings are listed in Table 5-1.

Table 5-1 ELFP design result

		Example I			Example II		
	Cs	V	V_1	V_2	V	V_1	V_2
Los Angeles	0.18	21.59	9.82	11.77	22.11	11.50	10.61
Sacramento	0.06	7.27	3.31	3.96	7.46	3.88	3.58
Portland	0.09	11.16	5.08	6.08	11.43	5.94	5.49
	Example III			Example IV			
	V	V_1	V_2	V	V_1	V_2	V_3
Los Angeles	25.43	11.44	13.99	39.14	9.39	14.09	15.66
Sacramento	8.58	3.86	4.72	13.20	3.17	4.75	5.28
Portland	13.15	5.92	7.23	20.23	4.86	7.28	8.09

Note: C_s is the seismic response coefficient; V is the total design lateral force or shear at the base of the structure (kip); V_i is the portion of the seismic base shear induced at ith-story (kip).

Based on the shearwall design Table 4.1B in NSD supplement (2001), the nail pattern for the shearwalls in example buildings are shown from Figure 5-6 to Figure 5-9. The numbers inside the geometric symbols beside the walls represent the edge nail spacing used in shearwalls, for example, 6 means 6"/12" nail pattern (6" edge spacing and 12" field spacing). The nail spacing value in the circle is for the force-based seismic design in Los Angeles, the value in the triangle is for the design in Sacramento and the value in the square is for the preliminary design in Portland.

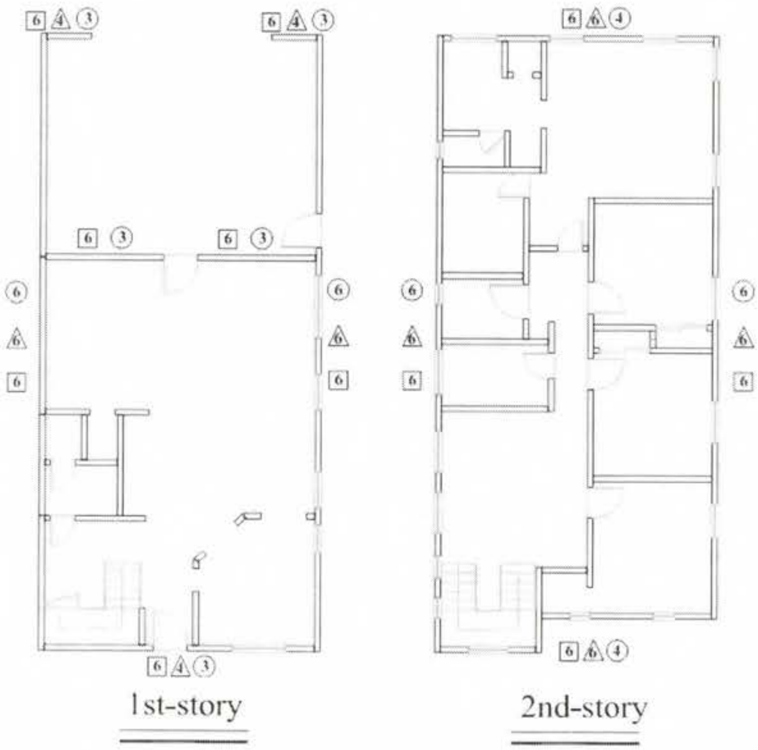

Figure 5-6 Force-based design nail pattern for design example I (rectangular shape)

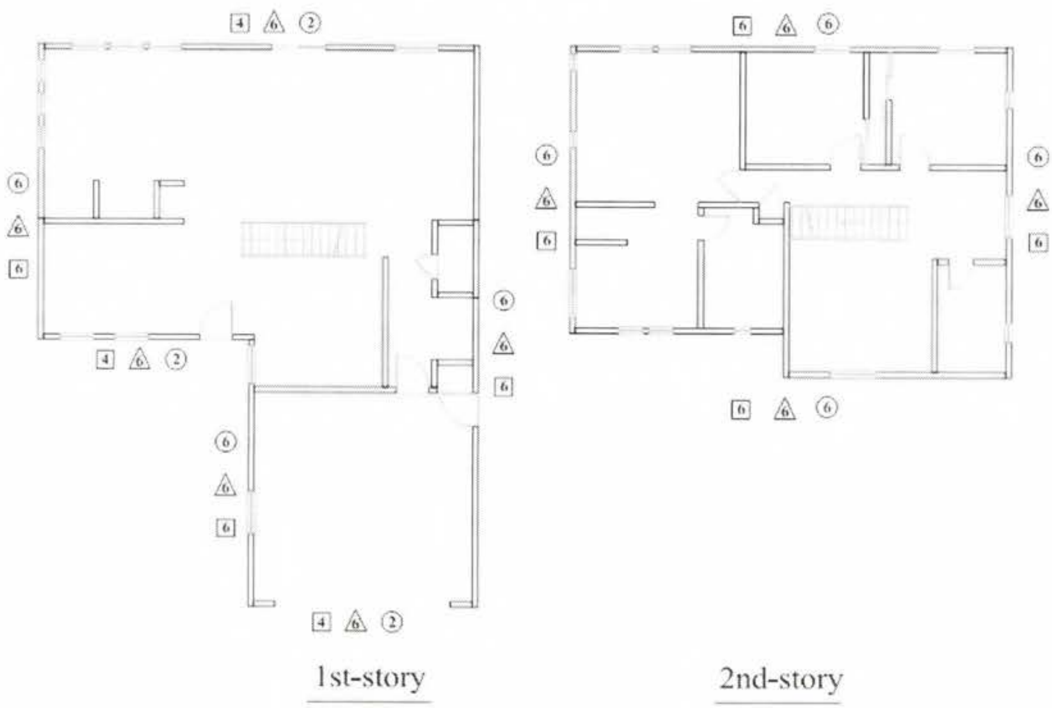

Figure 5-7 Force-based design nail pattern for design example II ('L' shape)

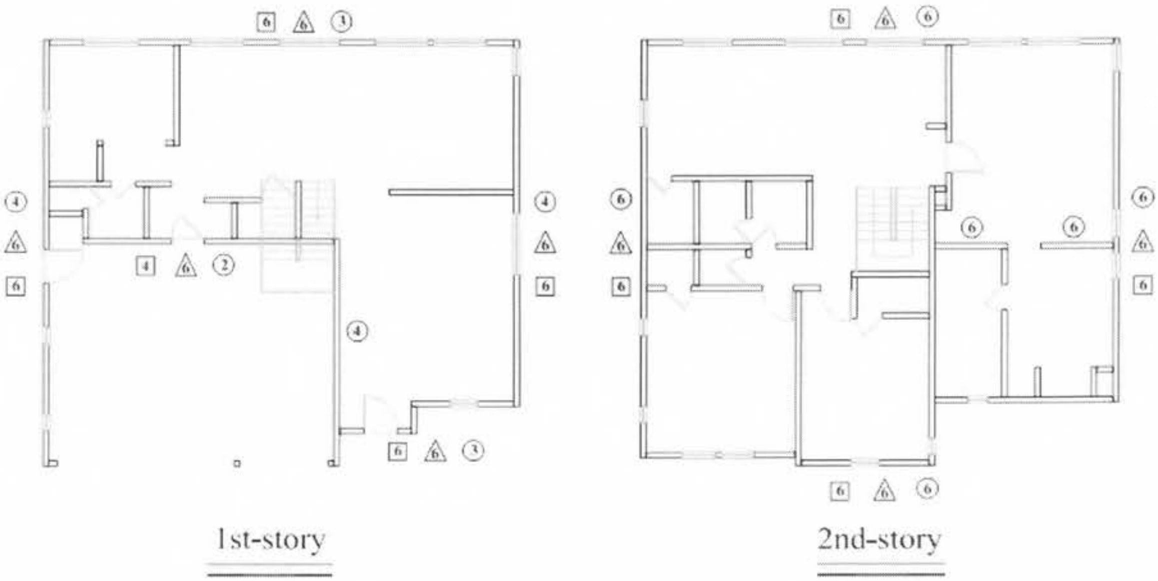

Figure 5-8 Force-based design nail pattern for design example III (square shape)

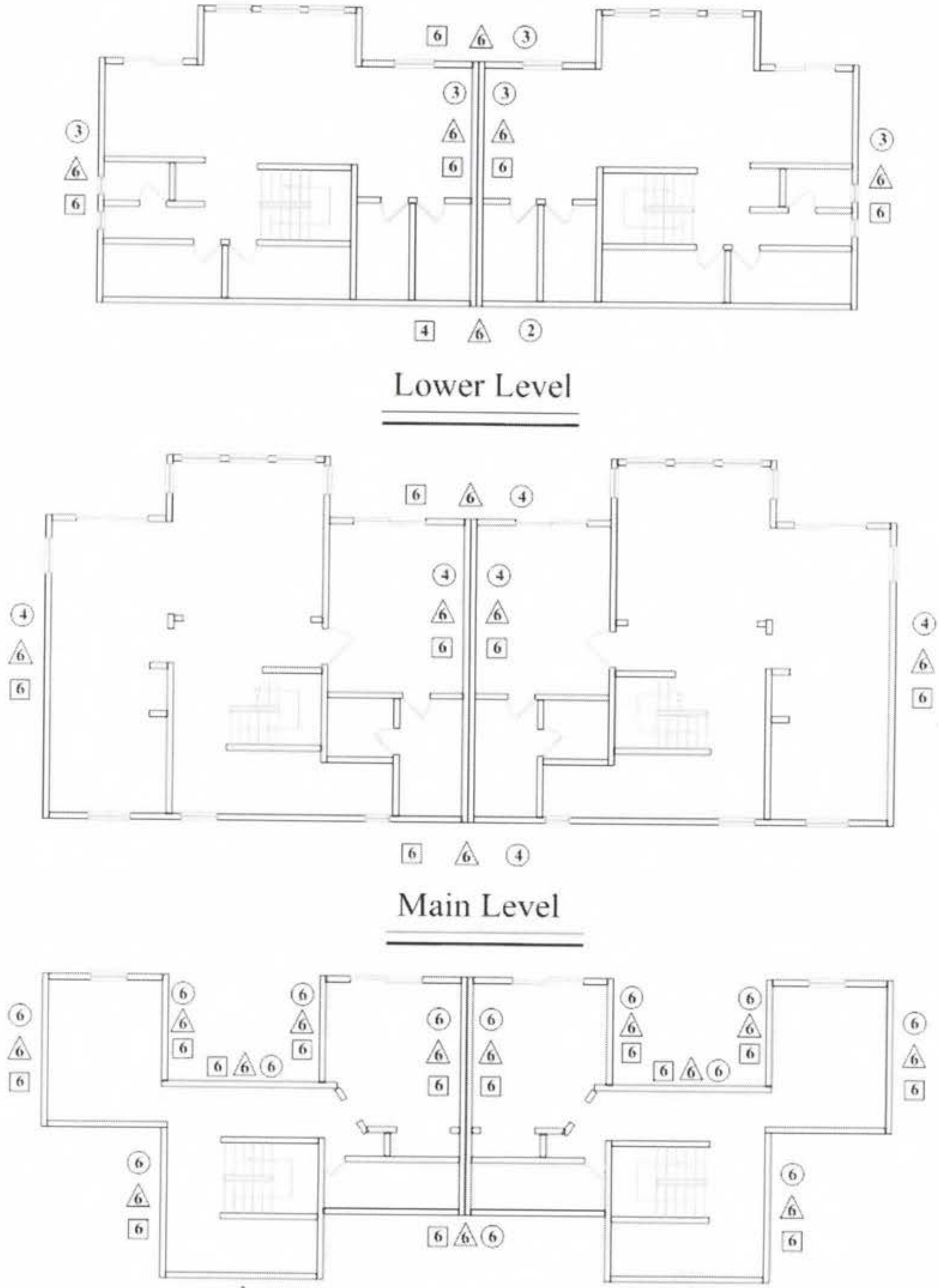

Figure 5-9 Force-based design nail pattern for design example IV (condominium)

5.2.2 Shearwall and partition wall modeling in SAPWood

Based on the preliminary shearwall configuration from force-based design, the individual shearwall can be modeled in SAPNP. Then through cyclic pushover analysis, the hysteresis of each shearwall can be obtained which is needed in system model. This task can be quite time consuming if every shearwall with different configurations, such as nail pattern, the opening, length, etc. was to be modeled first in SAPNP. SAPWood version 2.0 provides a new module which is essentially a shearwall database which is designed to provide an approximate but rapid approach to obtaining wall parameters for shearwalls and partition walls with GWB panels through standard length wall parameters. The shearwall database in SAPWood was set up based on the cyclic nail experiments conducted in the structural lab at the University at Buffalo (UB) listed in Table 5-2. Based on the nail parameters calibrated with the UB experiments, the SAPNP models of shearwalls having lengths of 2', 4' and 8' were used as the standard length shearwall in the database. Four different nail patterns were included in the database, namely 2/12, 3/12, 4/12 and 6/12. In order to obtain the hysteretic parameters for the shearwalls in the floor plan, an input file with the basic wall configuration, such as height, length and nail pattern, will be created and loaded into the database module. The SAPWood program will automatically calculate the wall parameters based on the standard length wall (2', 4' and 8') parameters through interpolation. As for the walls with openings, such as door or windows, only the solid sections without opening were considered in the model set up. This is very slightly conservative. Similarly, for partition walls the database generated parameters for different wall lengths based on a set of 8 ft x8 ft GWB wall parameters calibrated using cyclic GWB wall test data used by Folz and Filiatrault (2004).

Table 5-2 Test Matrix (Hem-fir) from UB

Test Group	Nail Designation	Nail Diameter (in)	Nail Length (in)	Rated Sheathing thickness(in)	Type of Test
A	10d Common	0.148"	3"	7/16"	Parallel
					Perpendicular
B	10d Common	0.148"	3"	5/8"	Parallel
					Perpendicular
C	10d Common	0.148"	3"	3/4"	Parallel
					Perpendicular
D	8d Common	0.131"	2.5"	7/16"	Parallel
					Perpendicular
E	6d Common	0.113"	2"	7/16"	Parallel
					Perpendicular

Note: For each connection type three monotonic and five cyclic tests were conducted

5.2.3 System model in SAPWood

The wall parameters for shearwalls and partition walls were obtained from the database in SAPWood in the previous step. The next step was to set up the system model for the entire building to perform the numerical simulations in PBSD. The input file for system model needs to include wall (including shearwalls and partition walls) position, wall direction, wall height and length, wall parameters, floor diaphragm position and size, seismic weight on each story, hold-down position and parameters and FPS option. As for the input information for walls, floor diaphragm and seismic weight and the basic information, such as wall position, direction etc., can be obtained from the preliminary floor plan designed by force-based seismic design. In SAPWood 2.0 version, vertical stiffness elements can be included to provide the vertical load input needed for the accurate modeling of FPS systems. Since the behavior of hold-down system is not the focus of this study, the behavior of the hold-down element was assumed to be linear in both tension and compression regions. As an illustration, the system model for design example II ('L' shape) was shown in Figure 5-10.

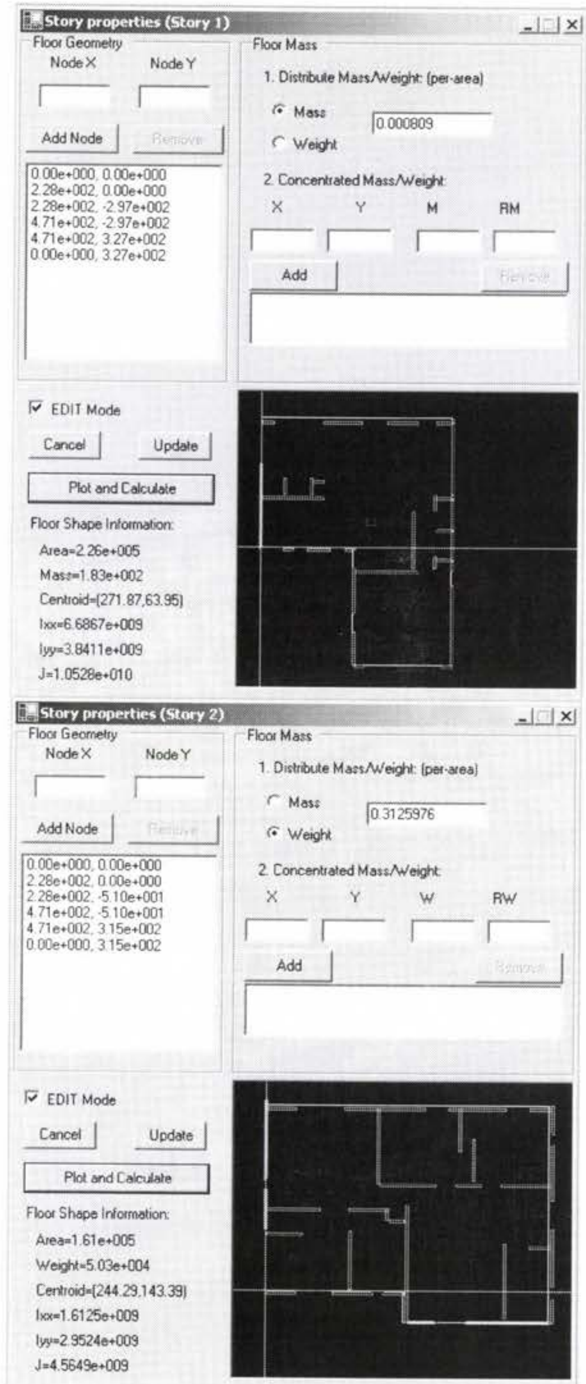

Figure 5-10 SAPWood system model for design example II ('L' shape)

5.2.4 Earthquake ground motion

It was mentioned that M-IDA are required to perform the proposed PBSD method outlined in Section 2.3. Therefore, a suite of recorded earthquake ground motions is needed to conduct the numerical simulations. Note that the PBSD procedure proposed in this study does not require using any specific ground motion suite but requires that the group of ground motions used be representative of the seismic hazard at the building site. In the examples of this study, a ground motion suite used in the ATC-63 project was selected as the earthquake ground motions for the nonlinear time history simulations. There are 22 earthquake ground motions in the ATC-63 classified as the Far-Field earthquake records. These earthquake ground motion records were selected based on several considerations including code (ASCE/SEI 7-05) consistency, the inclusion of very strong ground motions, a relatively large number of records, and structure type/site hazard independency. It was recommended in the ATC-63 report that these earthquake records can be used for nonlinear dynamic analysis (NDA) on buildings and can be considered as a group representing maximum considered earthquake (MCE) ground motions. The ATC-63 study has also provided a systematic procedure to scale these earthquakes to different hazard levels. However, that scaling method is not adopted in this study in order to keep the proposed PBSD procedure general. The detailed information for the 22 earthquake ground motion records used are listed in Table 5-3.

Table 5-3 ATC-63 Far-Field earthquake record information

ID No.	Earthquake				Recorded Motions	
	M	Year	Name	Record Station	PGAmax (g)	PGVmax (cm/s)
1	6.7	1994	Northridge	Beverly Hills	0.52	63
2	6.7	1994	Northridge	Canyon Country	0.48	45
3	7.1	1999	Duzce, Turkey	Bolu	0.82	62
4	7.1	1999	Hector, Mine	Hector	0.34	42
5	6.5	1979	Imperial Valley	Delta	0.35	33
6	6.5	1979	Imperial Valley	El Centro Array #11	0.38	42
7	6.9	1995	Kobe, Japan	Nishi-Akashi	0.51	37
8	6.9	1995	Kobe, Japan	Shin-Osaka	0.24	38
9	7.5	1999	Kocaeli, Turkey	Duzce	0.36	59
10	7.5	1999	Kocaeli, Turkey	Arcelik	0.22	40
11	7.3	1992	Landers	Yermo Fire Station	0.24	52
12	7.3	1992	Landers	Coolwater	0.42	42
13	6.9	1989	Loma Prieta	Capitola	0.53	35
14	6.9	1989	Loma Prieta	Gilroy Array #3	0.56	45
15	7.4	1990	Manjil, Iran	Abbar	0.51	54
16	6.5	1987	Superstition Hills	El Centro Imp. Co.	0.36	46
17	6.5	1987	Superstition Hills	Poe Road	0.45	36
18	7.0	1992	Cape Mendocina	Rio Dell Overpass	0.55	44
19	7.6	1999	Chi-Chi, Taiwan	CHY101	0.44	115
20	7.6	1999	Chi-Chi, Taiwan	Tcu045	0.51	39
21	6.6	1971	San Fernando	LA-Hollywood Stor	0.21	19
22	6.5	1976	Friuli, Italy	Tolmezzo	0.35	31

5.2.5 Performance expectation in current study

In order to use the generalized PBSD procedure in the examples within the current study, the performance expectation (in terms of drift and acceleration levels) and the hazard level (in term of spectral acceleration S_a) was determined/selected in Chapter 2. Based on this configuration, a procedure was taken in this section to determine the probability of non-exceedance (PNE) value at each expectation level incorporating both the end-user expectations and minimal engineering safety consideration. Although there is no explicit requirement on what PNE values can or cannot be used in the proposed PBSD framework, it is natural to assign the PNE values to the target performance curves based on the building location (similar to force-based design) and the owner/user's concern towards different performance expectations for a predefined period of time. A general format of the PNE value for any performance level as function of these factors was proposed as follows:

$$PNE = PNE_F + PNE_T(T) + PNE_u(U) \tag{5-1}$$

where PNE_F is a fixed level of PNE that must be exceeded for this performance level, representing a minimum requirement in PBSD; PNE_T is a function related to exposure period, T, and building location; and PNE_u is a function that reflect the concern of the owner/user at each performance level. These functions can be reasonably assigned by the engineer to reflect the design consideration in the PBSD procedure but have to add up to be less than 1.0. For example, the PNE_F can be obtained from the force-based designed structure's performance if it is assumed that should be the minimum requirement for the engineer. PNE_T can be a function of probability of exceedance of the hazard level at the building site. For the purposes of illustration in this study, the PNE_F for all the performance levels was assumed to be the same with a value of 0.2, which means the design must not exceed the predefined performance levels at their corresponding hazard levels with at least 20% probability. For a given period of time the user wants to design the building for, the probability of an earthquake exceeding a certain hazard level can be obtained based on the USGS hazard curve data. In this study, a 30-year period was used for the period of concern since it is usually the time needed to pay off the mortgage on a typical single family home. The PNE_T for this study was taken as

$$PNE_T = 0.6 \times \frac{\min(2.5, PE_{30} / PE_s)}{3} \tag{5-2}$$

Where PE_{30} is the probability of exceedance for a certain hazard level in 30 years at the building site; PE_s is a standard reference probability of exceedance level for the hazard level. With this formulation, the PNE_T reaches its maximum value if the probability of exceedance at the location is greater than 2.5 times of the standard reference value. The standard reference PE values for each hazard level used in this study were aligned with the performance requirements proposed in ASCE 41 (FEMA 356), namely 50% for IO level, 10% for LS level, and 2% for CP level. Also notice that by using a maximum PE ratio of 2.5 and dividing the ratio by 3, the maximum possible value for PNE_T is 50% rather than 60%, which indicates that the performance always be allowed to be exceeded by a limited percentage (10% in this case) even if the seismic hazard is significant. This also helps to prevent the final PNE value from reaching 100%, which is not realistic for any probabilistic statement. The seismic hazard curves from USGS were obtained for three locations considered in this study. With the hazard curve (annual probability of exceedance) known for different spectral acceleration levels, the probability of earthquake falls in each S_a level (hazard level) interval in 30 years can be calculated using a basic statistical relationship. These probability values of interest were listed in Table 5-4.

Table 5-4 Probability of experiencing earthquake hazard levels in 30-year

Sa @ 0.2 sec (g)	Standard level	Los Angeles	Sacramento	Portland
< 0.4g	5.00E-01	6.88E-01	8.66E-01	9.47E-01
0.4g – 0.8g	3.29E-01	2.07E-01	1.11E-01	3.89E-02
0.8g – 1.2g	1.00E-01	5.76E-02	1.62E-02	8.73E-03
1.2g – 1.6g	6.10E-02	2.36E-02	4.38E-03	3.04E-03
1.6g – 2.0g	2.01E-02	9.36E-03	1.14E-03	9.71E-04

For the PNE_u controlled by the owner/user's concern level, the following calculation was followed in this study:

$$PNE_u = 0.2 \times U \tag{5-3}$$

where U is the concern level between 0 and 1 assigned to each performance level according to the user's concern. Note that only 20% of the PNE was allocated to this mainly due to a potential lack of engineering knowledge. Furthermore, in order to help the owner/user make an informed decision regarding expected building performance, the hazard and performance levels expressed in engineering language (S_a, inter-story drift, acceleration, etc.) has to be re-phrased into lay language based on the assumption that the homeowner is not an engineer. In this study, the following descriptions in Table 5-5 of the hazard and performance levels were adopted.

Table 5-5 Hazard level and performance level description

Hazard Level		Performance Level		
Sa @ 0.2 sec	Description	Drift	Acceleration	Description
< 0.4g	Minor earthquake	< 0.5%	< 0.5g	Very minor damage
0.4g – 0.8g	Moderate earthquake	< 1%	< 0.8g	Slight damage (reparable, low cost)
0.8g – 1.2g	Mid-level earthquake	< 3%	< 1g	Significant damage (reparable, acceptable cost)
1.2g – 1.6g	Large earthquake	< 5%	< 1.5g	Severe damage (non-reparable)
1.6g – 2.0g	Severe earthquake	< 10%	< 2g	Collapse (life safety)

With this terminology for hazard level and performance level as listed in Table 5-4, the engineer can consult the owner's opinion by asking questions such as "On a scale from 0-1, how important it is to you that during a large earthquake and we design the building so that there is no severe damage?" In the examples used for this study, the owner/user's assigned importance factor at three different locations in 30 years were assumed and were listed in Table 5-6. Here in this study, the owner/user's concern for different performance levels at different location was considered. For example, since occurrence of a large earthquake is not common in Portland, the importance factor assigned by owner/user is higher for preventing minor damage to the house during small earthquakes. However, owner/user in Los Angeles area has more concern at the collapse prevention level because of the high seismic zone, while in Sacramento, the focus of the interested of the house owner will be more focused on the repairable level.

Table 5-6 Example owner/user assigned importance factor used in this study

	User assigned importance factor		
	Los Angeles	Sacramento	Portland
$\Pr(Drift < 0.5\% \mid 30\,year)$	20%	20%	80%
$\Pr(Drift < 1\% \mid 30\,year)$	40%	40%	50%
$\Pr(Drift < 3\% \mid 30\,year)$	60%	100%	40%
$\Pr(Drift < 5\% \mid 30\,year)$	80%	80%	30%
$\Pr(Drift < 10\% \mid 30\,year)$	100%	60%	20%

With this information, the PNE values denoted by the user can be calculated based on Equation (5-3). Then the design target curve for PBSD was finally obtained following equation (5-1). It will later be used to compare to the performance curve (or more specifically, the PNE values) obtained from M-IDA numerical simulations. Therefore, the final formula for calculating PNE values at each performance expectation segment can be expressed as:

$$PNE = 0.2 + 0.6 \times \frac{\min(2.5, PE_{30} / PE_s)}{3} + 0.2 \times U \tag{5-4}$$

The minimum PNE requirements for design target curve for these three different locations were calculated and were listed in Table 5-7.

Table 5-7 Target maximum PNE values for design curve at different locations

PNE	Los Angeles	Sacramento	Portland
PNE_{I}	37%	29%	38%
PNE_{II}	34%	29%	31%
PNE_{III}	41%	41%	29%
PNE_{IV}	44%	37%	27%
PNE_{V}	54%	33%	25%

Hence the performance expectation curve pre-defined in Chapter 2 can be completely expressed in Figure 5-11 and 5-12.

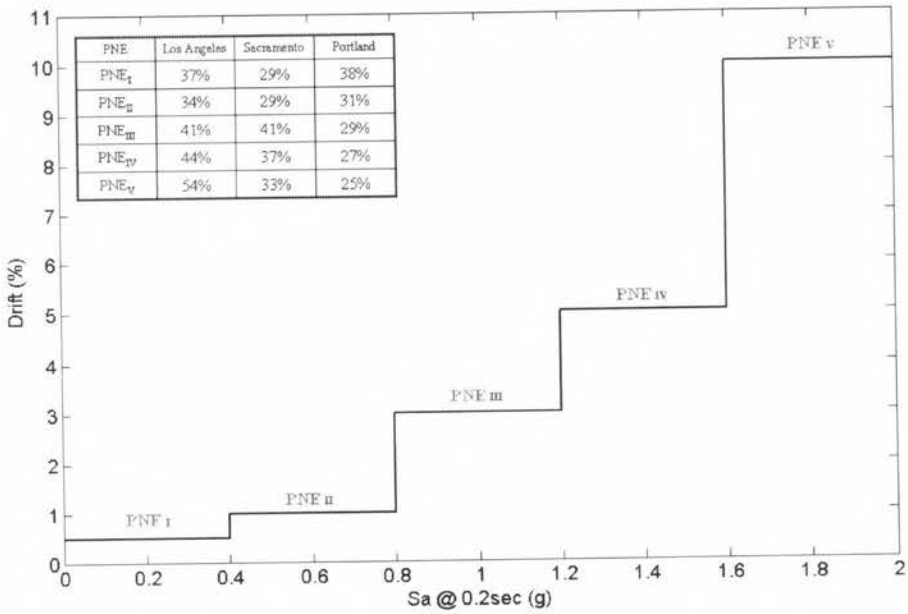

Figure 5-11(a) Performance expectation for inter-story drift

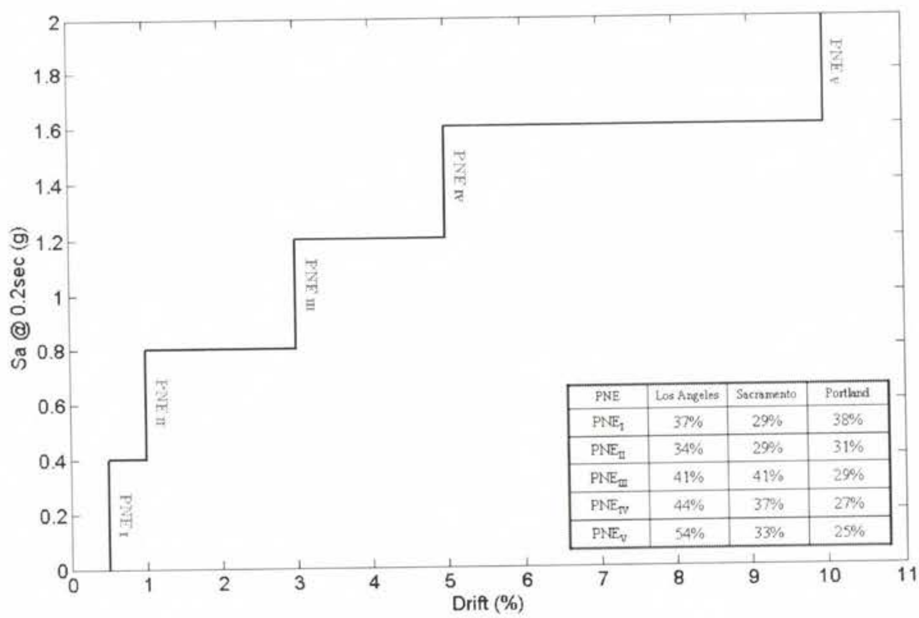

Figure 5-11(b) Performance expectation for inter-story drift (IDA version)

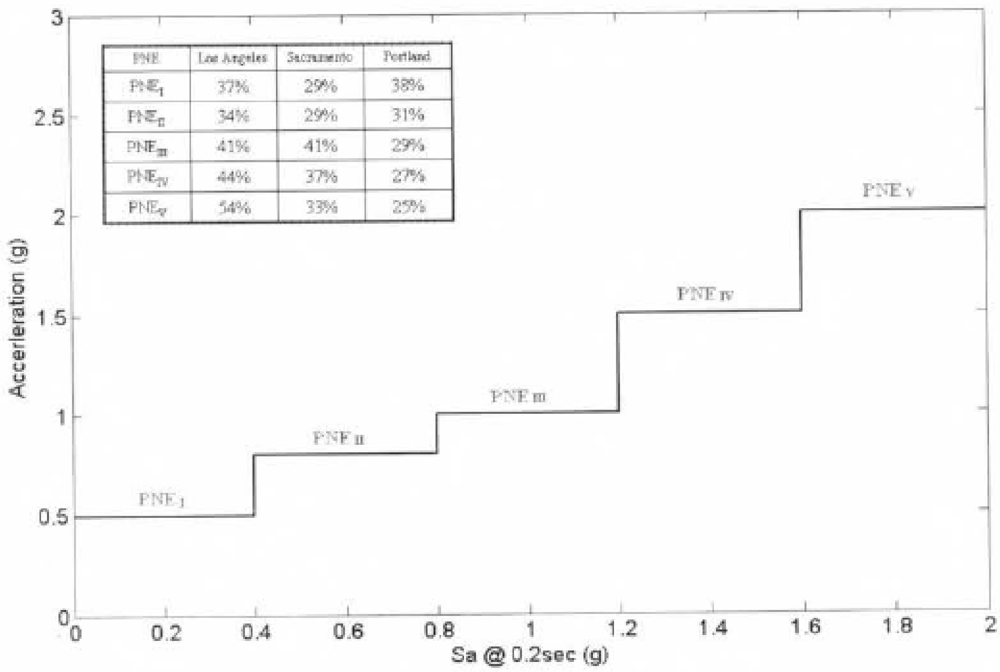

Figure 5-12(a) Performance expectation for acceleration

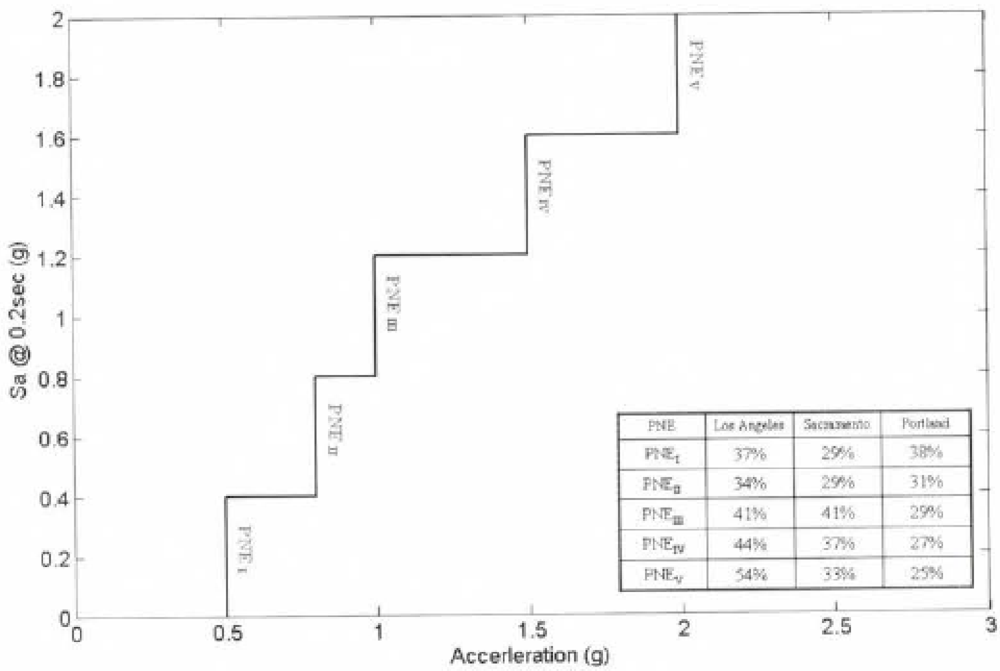

Figure 5-12(b) Performance expectation for acceleration (IDA version)

It is obvious that both the end-user's inputs and the building location have an impact on the design target through Equation (5-4). The resulting target PNE levels make practical sense. In Los Angeles, one can see from the table that the design is stricter (indicated by high PNE values) for larger earthquakes and collapse prevention level because this is the major concern in high seismic hazard regions. While in low seismic activity regions such as Portland, the probability of large earthquakes occurring is not as high as the high seismic zone, the overall requirements only barely exceeds the minimal requirement (20%). The Sacramento case lies in between the two extreme cases. This procedure allows the owner/user to involve/be interactive in the whole design procedure while keeping the concerns of a traditional design to ensure minimal life safety. Although the specific formula used in this study (Equation 5-2, 5-3) were very simplified that might not be generally justifiable, the proposed concept of PNE requirement (Equation 5-1) was felt to be suitable for a wide range of applications. The PNE values listed in Table 5-7 were used for the design of all example structures in this study.

5.2.6 M-IDA numerical simulations in SAPWood

Once the performance expectation with PNE value has been defined and the system model had been built in SAPWood program, M-IDA numerical simulation can be conducted in SAPWood to perform the PBSD procedure proposed in this study. The earthquake ground motion suite was the recorded 22 biaxial earthquake ground motions from the ATC-63 project. The seismic intensity level (represented by S_a at 0.2 second, with 5% damping) of concern in this example ranges from 0 to 2g.

The results of the force-based seismic designed structure performance are then compared to the performance expectation curve and are listed in Table 5-8 and 5-9. In order to satisfy the target curve, the PNE level obtained from the simulation must be equal to or greater than that of the target curve. The PNE values in shaded cell in the following tables indicated that the performance of the current design does not satisfy the performance expectation defined in this Chapter at the hazard levels discussed earlier. The plots of the simulation results versus performance expectation are shown from Figure 5-13 to 5-17.

Table 5-8 M-IDA simulation results of force-based seismic design (inter-story drift)

Los Angeles	Target PNE	**37%**	**34%**	**41%**	**44%**	**54%**
	Example I	64%	36%	59%	36%	41%
	Example II	37%	32%	45%	41%	32%
	Example III	45%	32%	41%	32%	32%
	Example IV	68%	41%	50%	32%	27%
Sacramento	Target PNE	**29%**	**29%**	**41%**	**37%**	**33%**
	Example I	45%	27%	45%	23%	23%
	Example II	27%	18%	27%	23%	23%
	Example III	23%	23%	27%	23%	27%
	Example IV	41%	23%	41%	27%	23%
Portland	Target PNE	**38%**	**31%**	**29%**	**27%**	**25%**
	Example I	45%	36%	59%	27%	23%
	Example II	32%	23%	41%	23%	27%
	Example III	27%	23%	36%	27%	18%
	Example IV	41%	27%	36%	32%	36%

Table 5-9 M-IDA simulation results of force-based seismic design (Acceleration)

Los Angeles	Target PNE	**37%**	**34%**	**41%**	**44%**	**54%**
	Example I	82%	68%	77%	95%	100%
	Example II	82%	82%	73%	95%	100%
	Example III	86%	77%	77%	100%	100%
	Example IV	86%	68%	73%	100%	100%
Sacramento	Target PNE	**29%**	**29%**	**41%**	**37%**	**33%**
	Example I	86%	91%	86%	95%	100%
	Example II	91%	95%	86%	95%	100%
	Example III	82%	91%	91%	100%	100%
	Example IV	86%	91%	77%	91%	100%
Portland	Target PNE	**38%**	**31%**	**29%**	**27%**	**25%**
	Example I	82%	91%	82%	95%	100%
	Example II	91%	95%	86%	95%	100%
	Example III	82%	91%	86%	100%	100%
	Example IV	82%	86%	82%	95%	100%

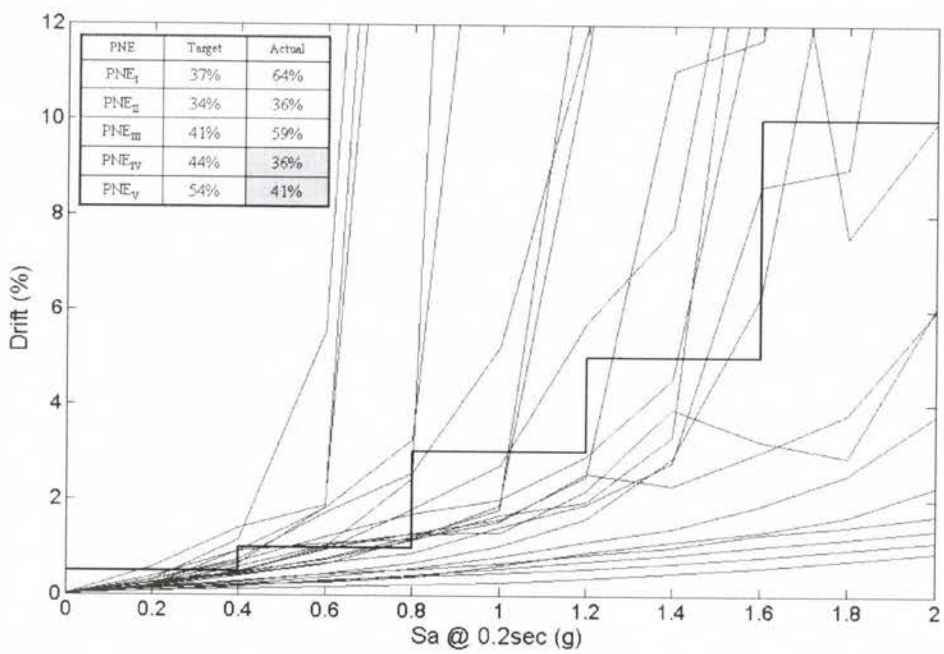

Figure 5-13(a) Inter-story drift comparison of design example I (rectangular) (LA)

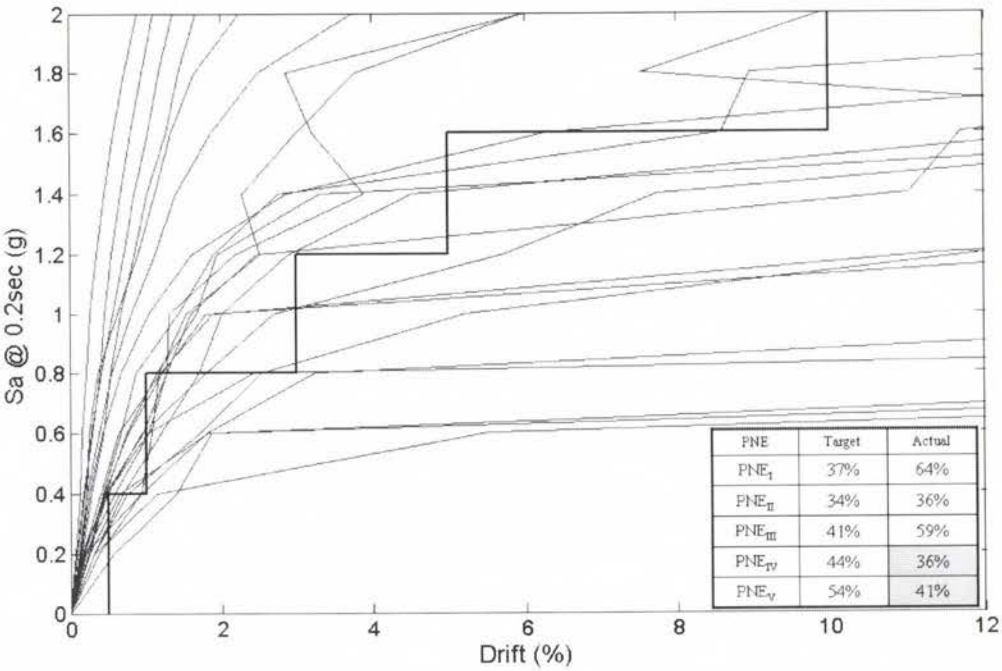

Figure 5-13(b) Inter-story drift comparison of design example I (LA) (IDA version)

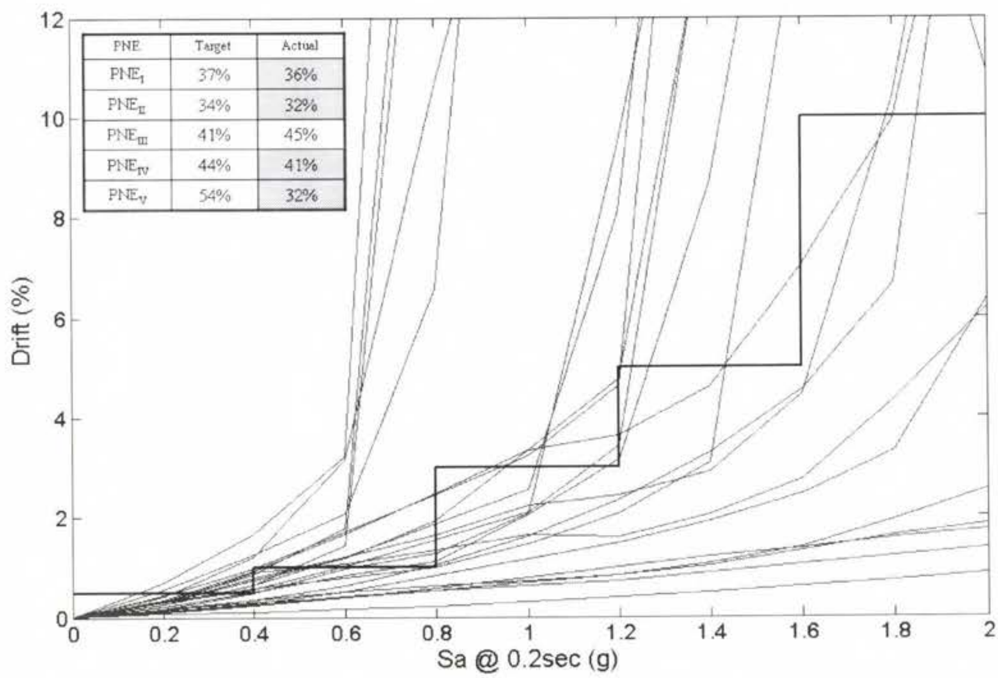

Figure 5-14 Inter-story drift comparison of design example II ('L' shape) (LA)

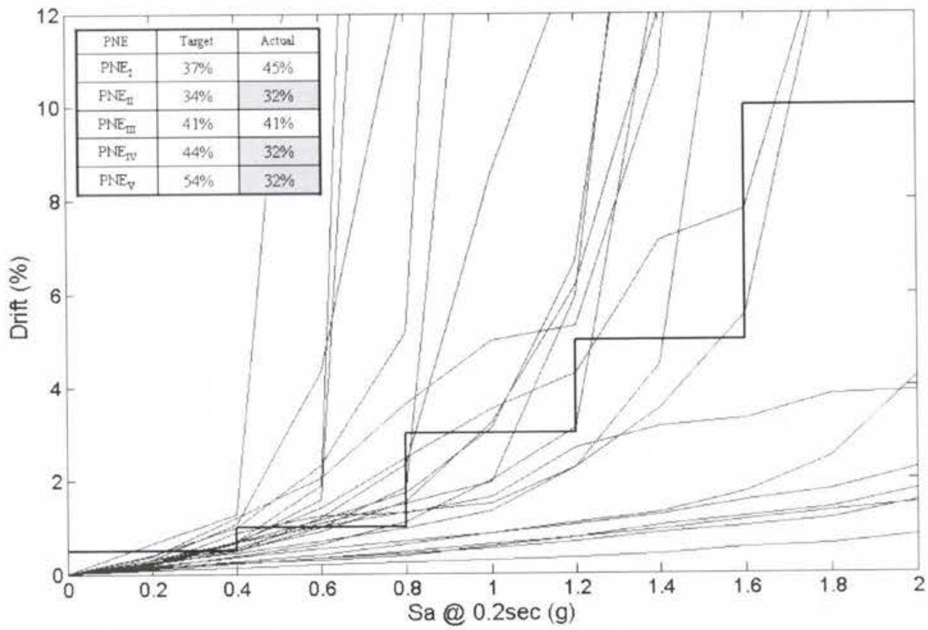

Figure 5-15(a) Inter-story drift comparison of design example III (square) (LA)

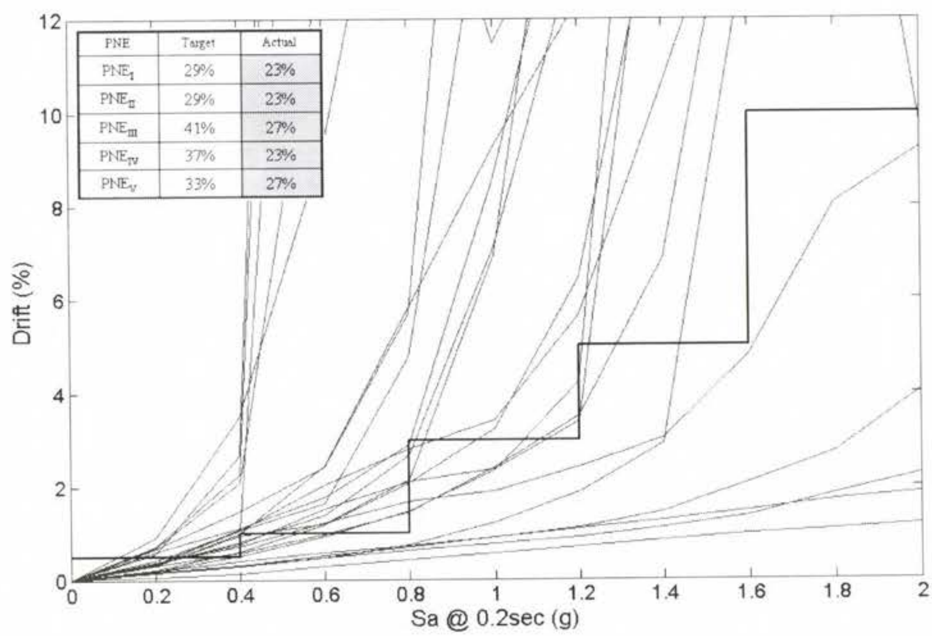

Figure 5-15(b) Inter-story drift comparison of design example III (square)

(Sacramento)

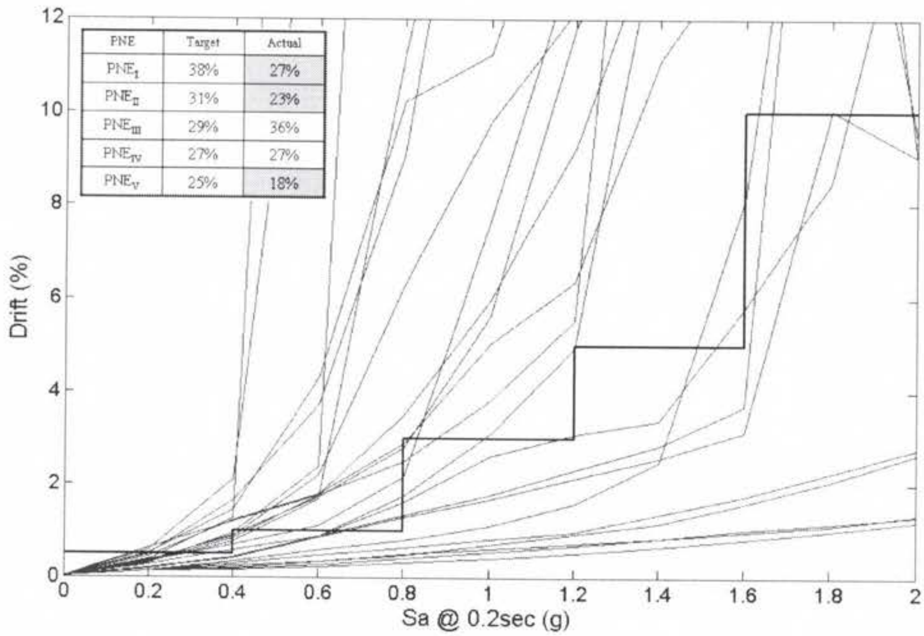

Figure 5-15(c) Inter-story drift comparison of design example III (square) (Portland)

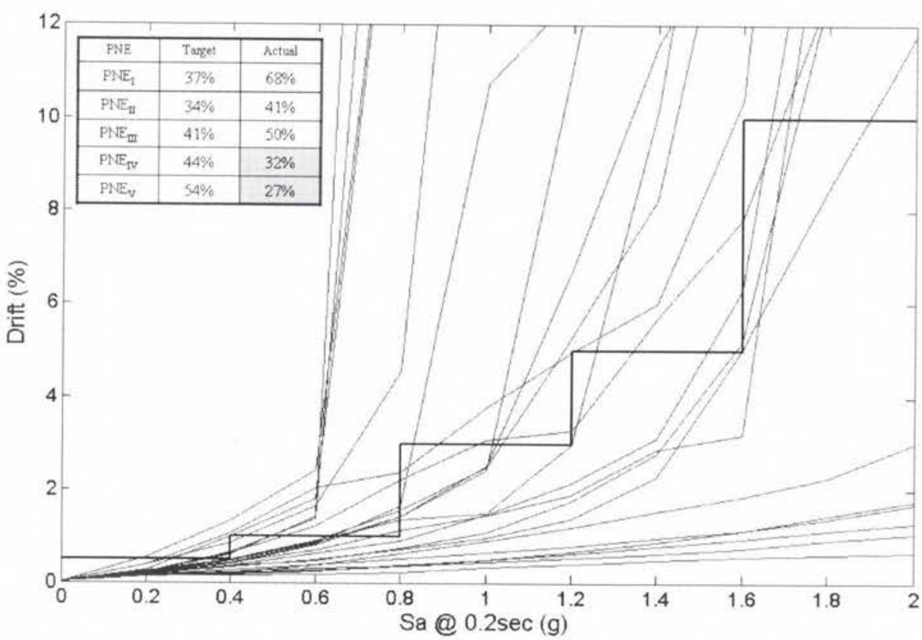

Figure 5-16 Inter-story drift comparison of design example IV (condominium) (LA)

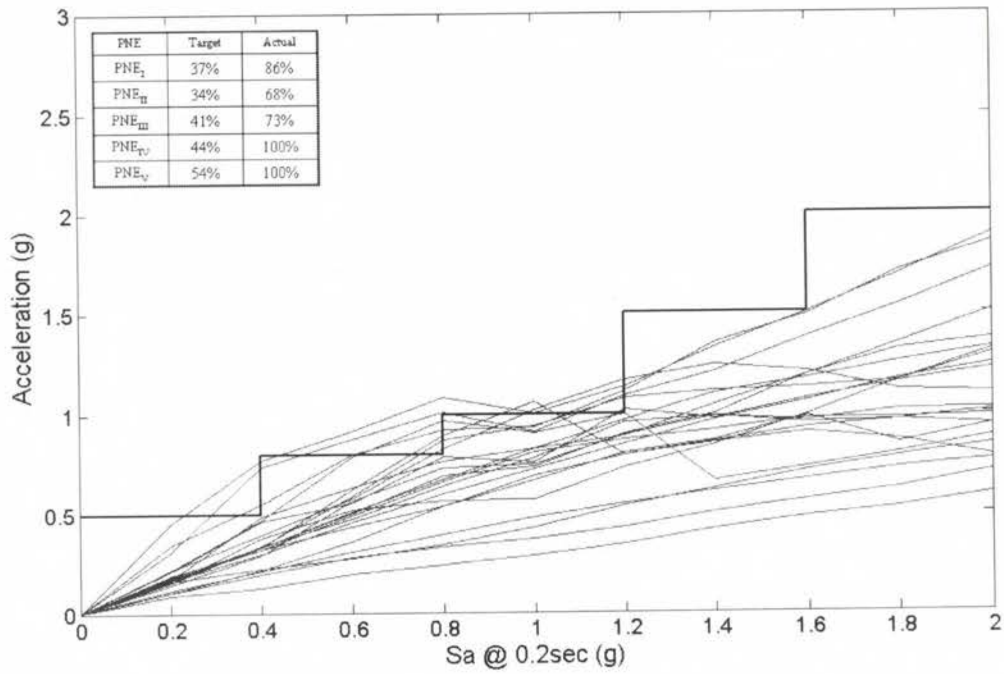

Figure 5-17(a) Acceleration comparison of design example IV (condominium) (LA)

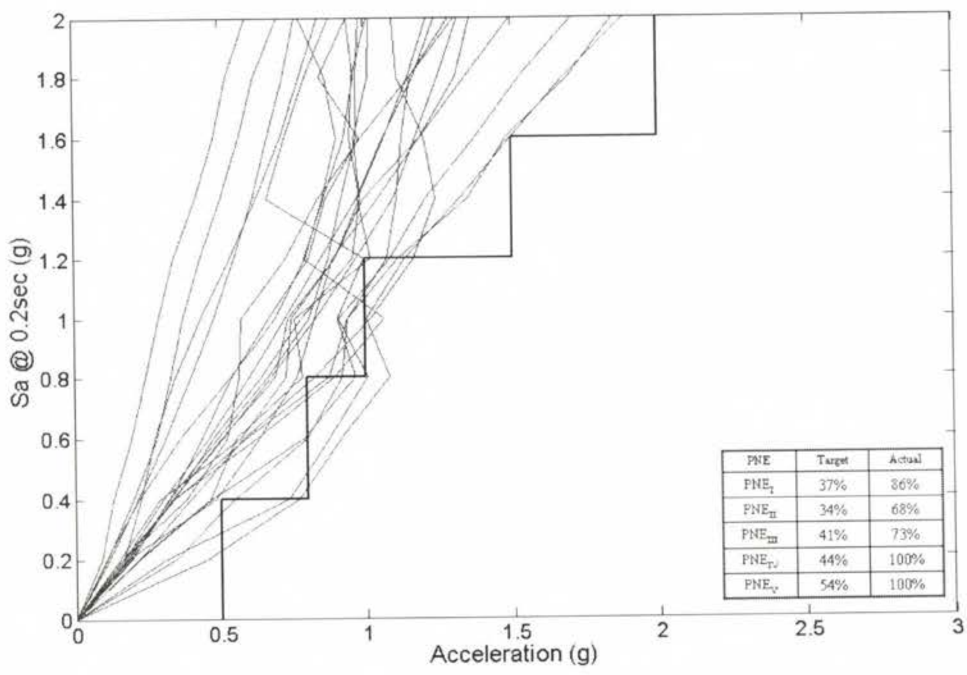

Figure 5-17(b) Acceleration comparison of design example IV (LA) (IDA version)

Based on the simulation results listed in Table 5-8, it is obvious that the preliminary design using the traditional force-based seismic design methodology does not meet the performance expectations defined in this study mainly due to excessive inter-story drifts. The structures do not necessarily collapse and thereby protect life safety which is the objective of force-based design under strong ground motion. Then, following the PBSD design flowchart, the next step is to modify the preliminary design and conduct the M-IDA simulations in SAPWood program with the newly revised model using the same suite of earthquake ground motions until the pre-defined performance expectations can be satisfied. Since even the most strong force-based design, which was the designs using the seismic load values in Los Angeles area, can not meet the least strict performance expectation proposed here (for Portland), the starting point of the revisions for design examples could be safely taken as the force-based design configuration associated with the Los Angeles area design load. A certain procedure was followed during the revision of the structural design. Firstly, if a specific performance level, inter-story drift for example, was not satisfied, the performance of each story of the structure at each direction will be examined in order to identify the problem. Then the shearwalls in the weak direction will be improved. Then the M-IDA was performed again using SAPWood program. In order to illustrate the design procedure conducted for the PBSD procedure, the detailed revision steps adopted for design example III (square shape) are listed as an example in Table 5-10 (for reference, the wall numbers for design example III are shown in Figure 5-18).

Table 5-10 Revision steps for design example III

Trial number	Weak direction	Modification
1	1st-story x-dir	garage wall (I8, I11) double sheathing with nail pattern 2/12 drywall (I13) change to shearwall with nail pattern 2/12
	The performance expectation at Portland was satisfied	
2	1st-story y-dir 2nd-story x-dir	garage wall (I12) double sheathing with nail pattern 4/12 2nd-story x-dir, all shearwalls change nail pattern to 4/12
	The performance expectation at Sacramento was satisfied	
3	1st-story y-dir 2nd-story x-dir	1st-story y-dir, all shearwalls change nail pattern to 3/12 2nd-story x-dir, all shearwalls change nail pattern to 3/12
4	2nd-story y-dir	2nd-story, y-dir, all shearwalls change nail pattern to 4/12
	The performance expectation at Los Angeles was satisfied	

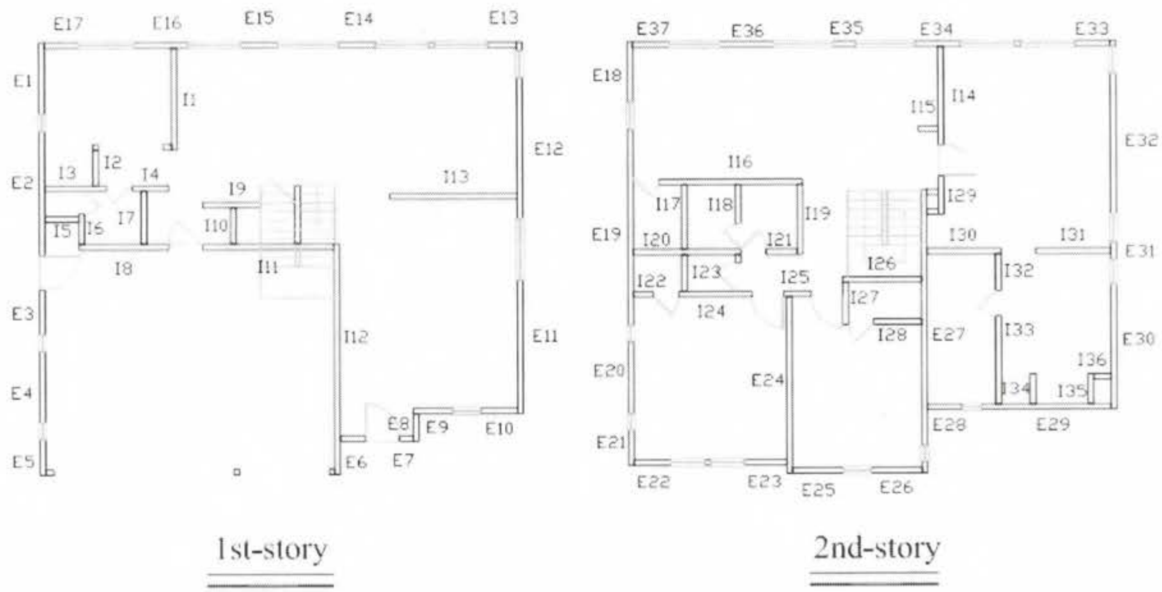

Figure 5-18 Wall numbers for design example III (square shape)

After several revisions for the design examples in this study, the final designs for different locations following PBSD procedure proposed in this study were obtained. The PNE value of final design for design examples at different locations are listed in Table 5-11 and 5-12. In order to briefly illustrate the improvement in M-IDA simulations for the final design, the numerical results of the design example III (square shape) were selected and shown in Figure 5-19.

Table 5-11 M-IDA simulation results of final design (inter-story drift)

Los Angeles	Target PNE	**37%**	**34%**	**41%**	**44%**	**54%**
	Example I	95%	86%	86%	68%	64%
	Example II	95%	77%	86%	73%	55%
	Example III	91%	77%	86%	73%	55%
	Example IV	86%	77%	77%	59%	55%
Sacramento	Target PNE	**29%**	**29%**	**41%**	**37%**	**33%**
	Example I	82%	36%	59%	41%	41%
	Example II	86%	64%	77%	50%	45%
	Example III	86%	55%	68%	50%	36%
	Example IV	82%	68%	68%	59%	36%
Portland	Target PNE	**38%**	**31%**	**29%**	**27%**	**25%**
	Example I	73%	32%	50%	41%	27%
	Example II	68%	32%	50%	32%	27%
	Example III	59%	32%	36%	41%	27%
	Example IV	64%	41%	50%	36%	27%

Table 5-12 M-IDA simulation results of final design (Acceleration)

Los Angeles	Target PNE	**37%**	**34%**	**41%**	**44%**	**54%**
	Example I	77%	82%	86%	100%	100%
	Example II	77%	73%	100%	100%	100%
	Example III	77%	77%	100%	100%	100%
	Example IV	77%	55%	45%	95%	100%
Sacramento	Target PNE	**29%**	**29%**	**41%**	**37%**	**33%**
	Example I	82%	100%	100%	100%	100%
	Example II	77%	77%	100%	100%	100%
	Example III	82%	86%	100%	100%	100%
	Example IV	77%	82%	100%	100%	100%
Portland	Target PNE	**38%**	**31%**	**29%**	**27%**	**25%**
	Example I	100%	100%	100%	100%	100%
	Example II	100%	100%	100%	100%	100%
	Example III	100%	100%	100%	100%	100%
	Example IV	100%	100%	100%	100%	100%

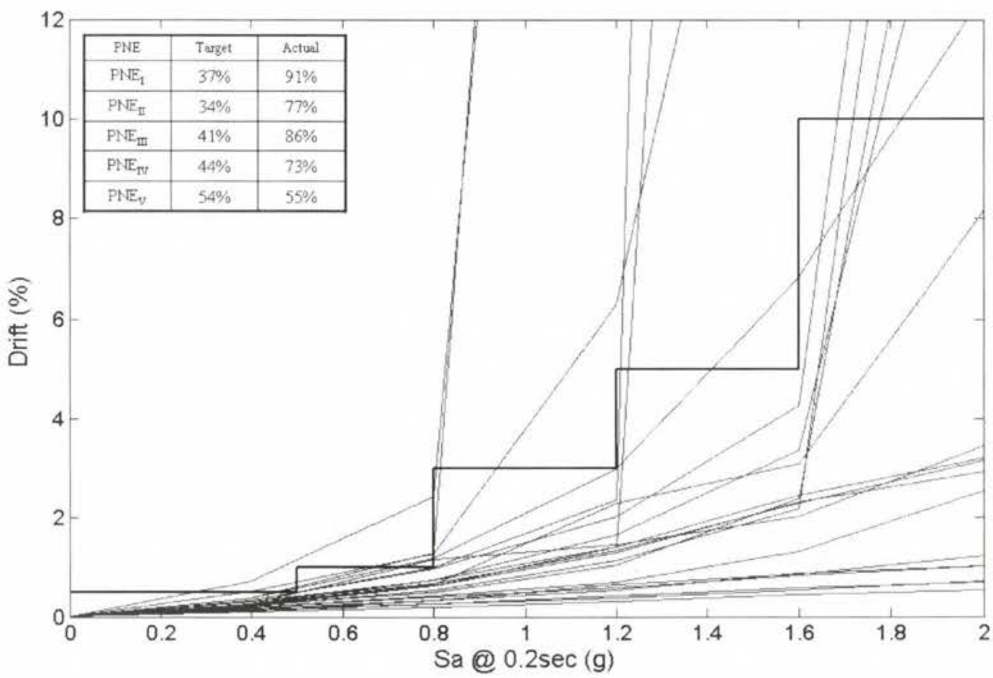

Figure 5-19(a) Inter-story drift comparison of design example III (square) (LA)

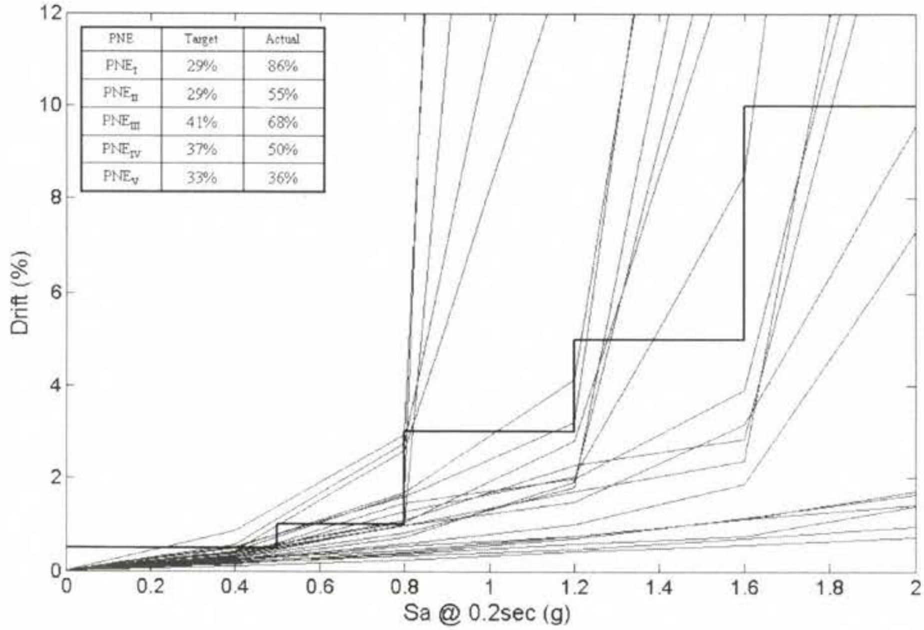

Figure 5-19 (b) Inter-story drift comparison of design example III (square) (Sacramento)

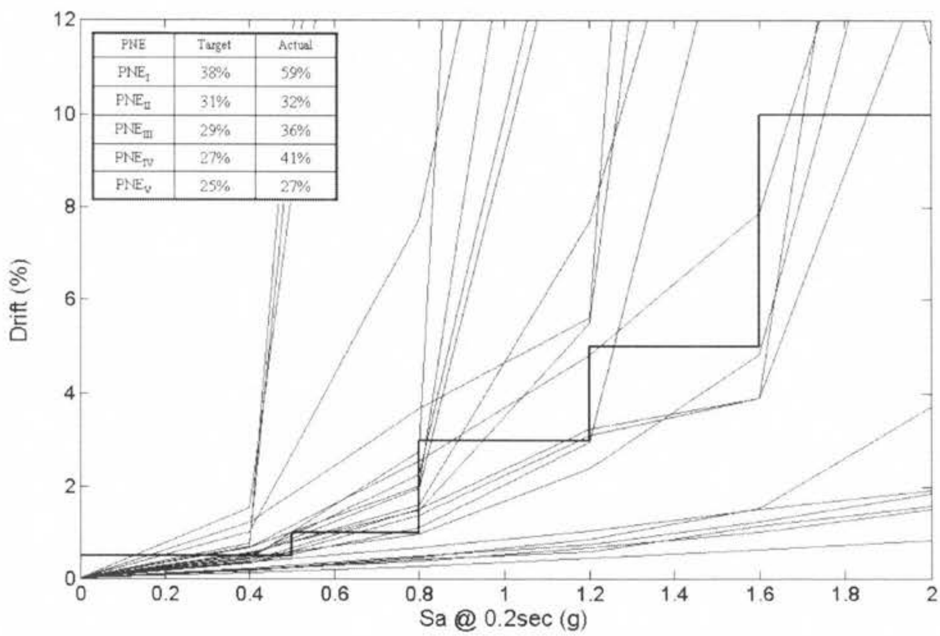

Figure 5-19 (c) Inter-story drift comparison of design example III (square) (Portland)

The final nail pattern for shearwalls in the example buildings at different locations are presented in Figures 5-20 to 5-23. As mentioned, the numbers inside geometric symbols besides walls represent the edge nail spacing used in shearwalls. The nail spacing value in circle stands for the final design in Los Angeles, the value in triangle stands for the final design in Sacramento and the square stands for the final design in Portland. Need to be mentioned that for some shearwalls the geometrical symbols were double edged, which means the shearwall need sheathing on both sides with the nail pattern inside the symbol.

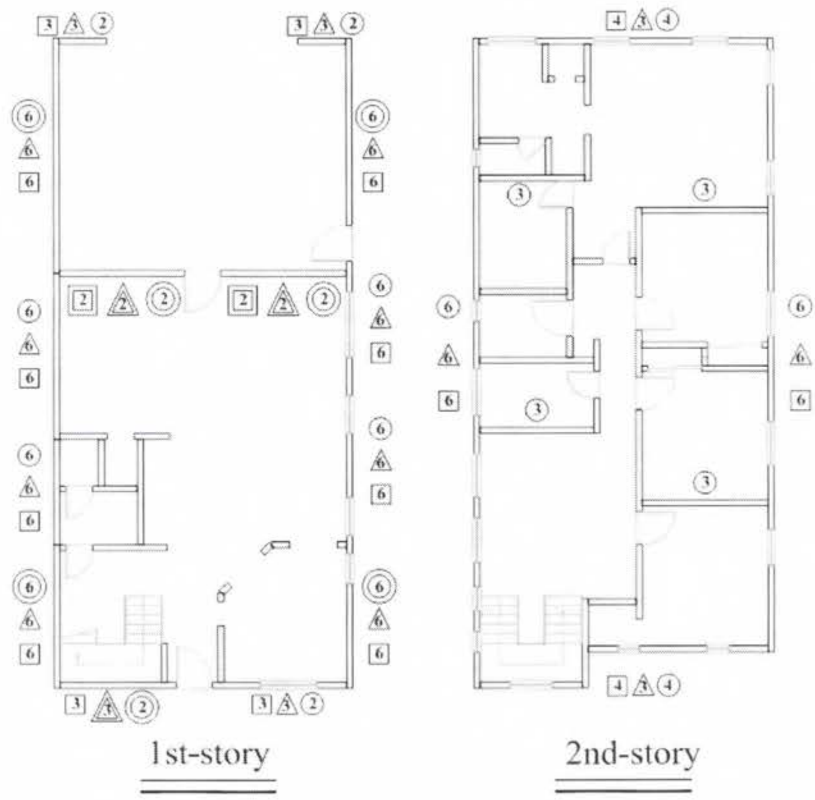

Figure 5-20 Nail pattern for design example I (rectangular shape)

Chapter Six

Mid-rise Woodframe Design Example Using Performance-based Seismic Design Procedure

6.1 Introduction of Capstone building

In this Chapter, the methodology and procedures proposed in Chapter 2 were applied to a mid-rise woodframe building. A six-story woodframe structure, referred to herein as Capstone building, was used as a design example to apply the PBSD procedure proposed in this dissertation. It was mentioned earlier that the design of the Capstone building was one of the tasks conducted within NEESWood project (in a forthcoming paper by Pang et al., 2009). It will be designed using the performance based design philosophy developed as part of that project and then tested on the world largest shake table, E-defense, in Miki City, Japan in 2009. The objective of the NEESWood project is to safely increase the height of light-frame wood buildings height beyond current practices using PBSD philosophy since it is believed that the seismic specifications in the traditional force-based design code may not be fully suitable for woodframe structures

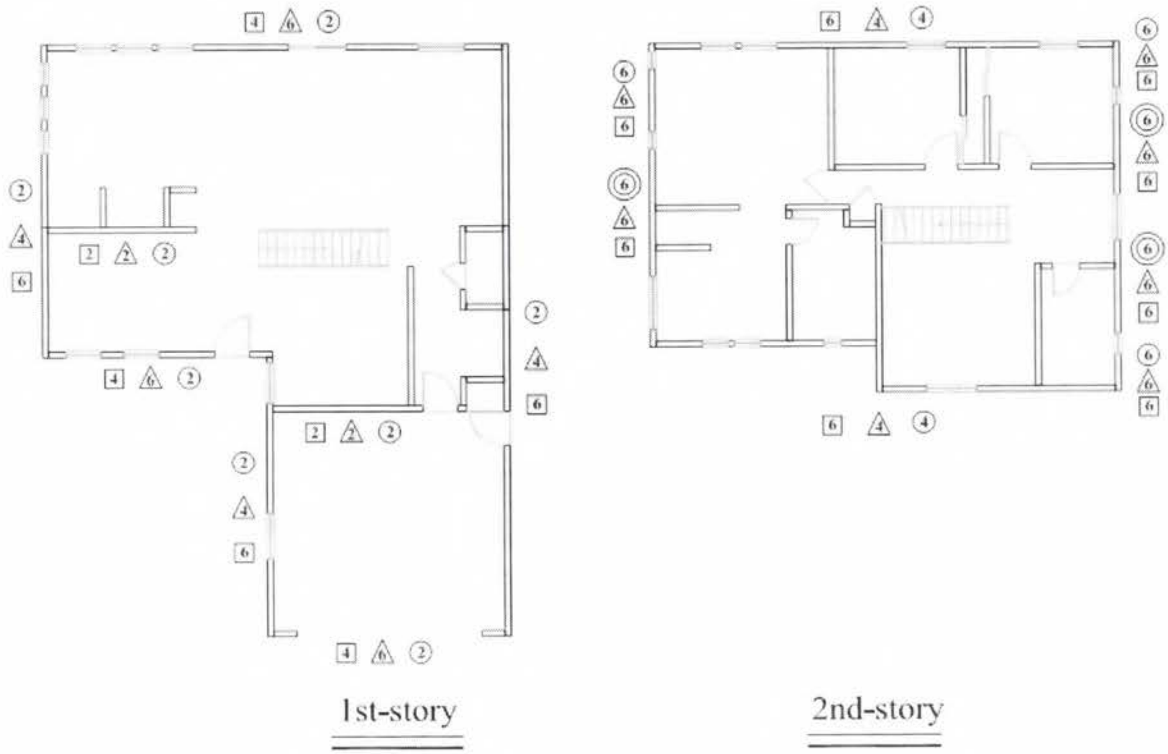

Figure 5-21 Nail pattern for design example II ('L' shape)

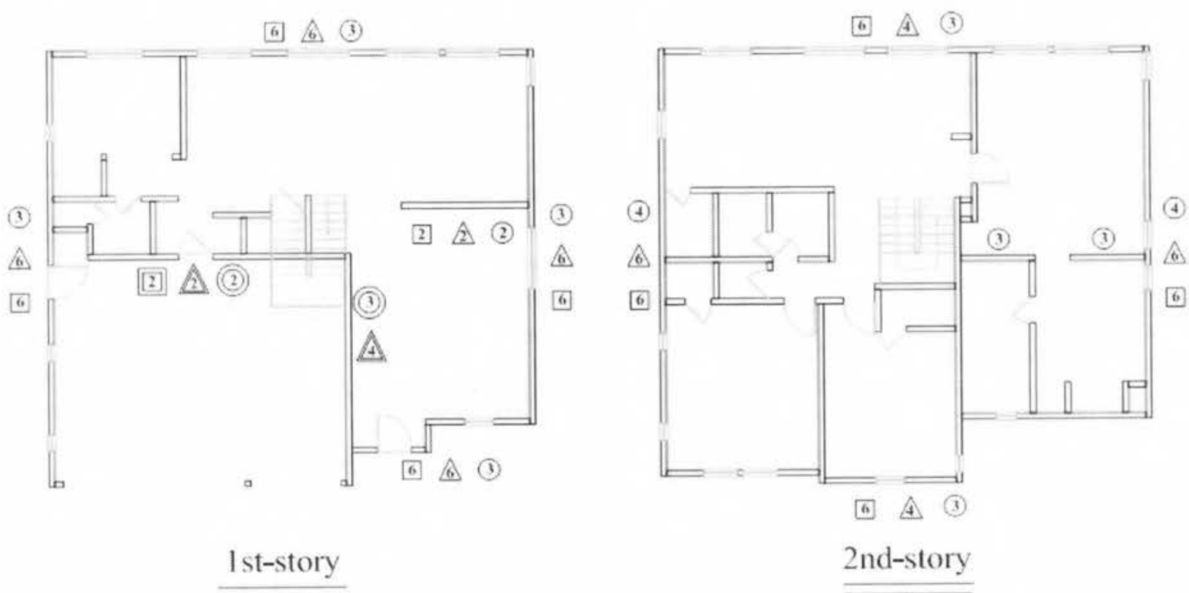

Figure 5-22 Nail pattern for design example III (square shape)

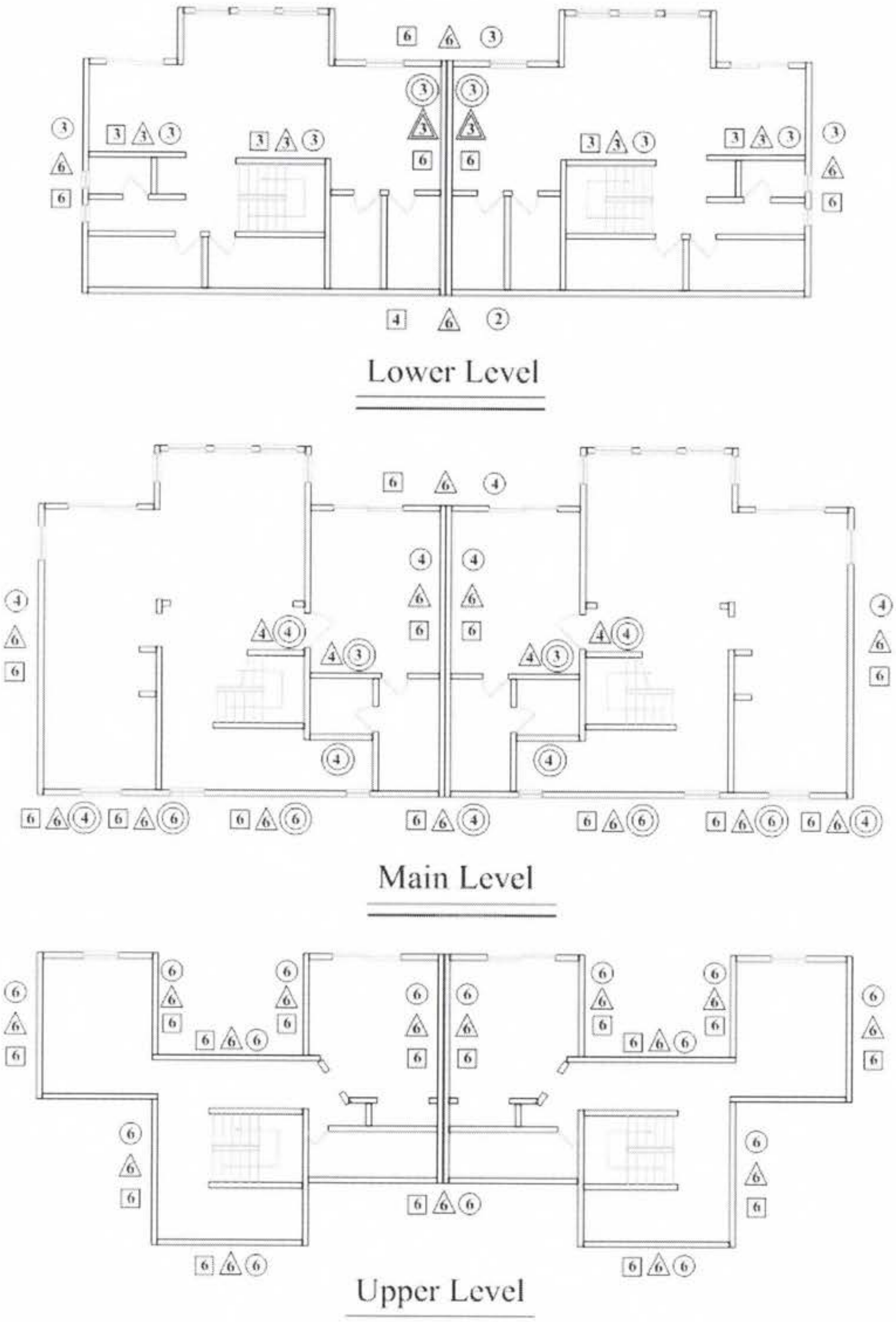

Figure 5-23 Nail pattern for design example IV (condominium)

Each of the final designs from the PBSD had a higher shear capacity than the force-based design requirements. This was decided by the predefined performance target curve. On the other hand, one can see from the design examples that the acceleration requirements did not control the design for low-rise residential buildings most of the time. This is, again, associated with the specific target curve assigned for this study. In other cases where the target curve is different, this situation might change. However, for woodframe buildings with only two stories, the controlling factor is usually the drift based on current studies. Finally, it is also important to point out that the final designs of these buildings are not the only configuration that can achieve the desired performance. The designer may choose to modify the structure in a different fashion (strengthen different wall line, using different nailing pattern, etc.) to achieve the performance target. This freedom is an inherent characteristic of PBSD.

with more than four stories. Basically, the Capstone building was a six-story woodframe structure with a total area of about 14,400 square feet. The Capstone is a condominium building containing 23 living units in which the lower five stories have four units per story and the top story was designed to have three luxury apartments. The floor plan for each story is shown from Figure 6-1 to 6-3 and the elevation views are shown in Figure 6-4 and 6-5.

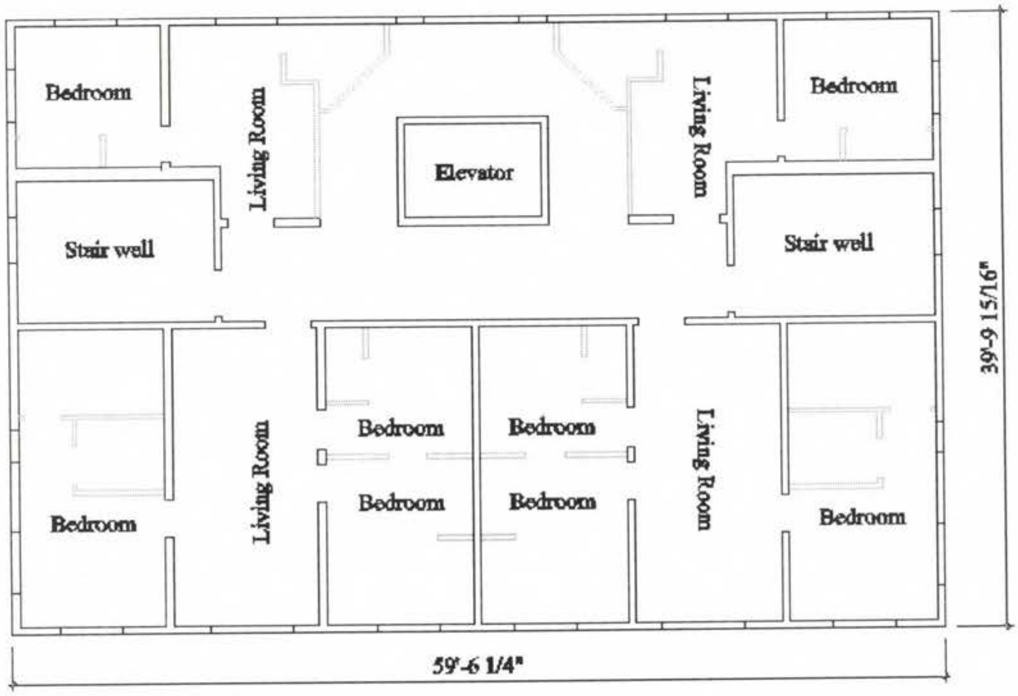

Figure 6-1 Floor plan for the 1st-story of Capstone building

Figure 6-2 Floor plan for the 2nd- to 5th-story of Capstone building

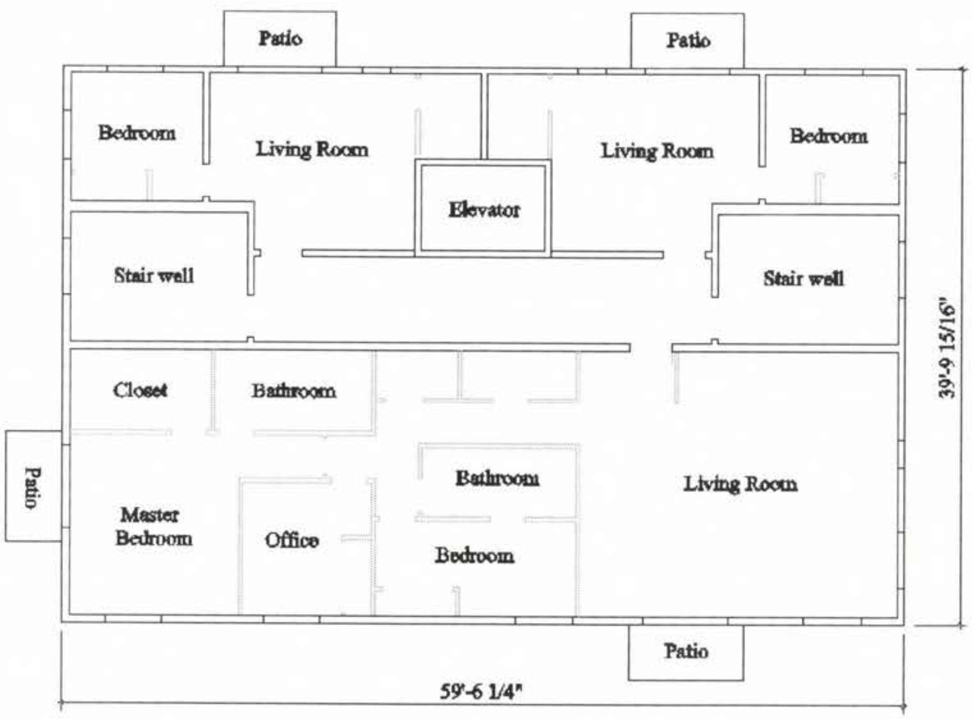

Figure 6-3 Floor plan for the 6th-story of Capstone building

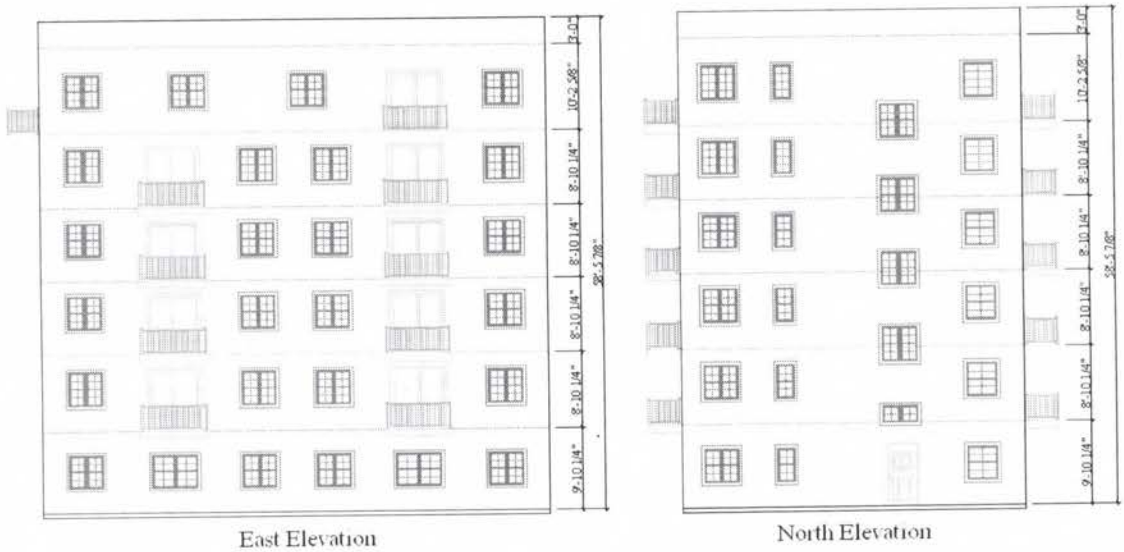

Figure 6-4 East-North elevation view of Capstone building

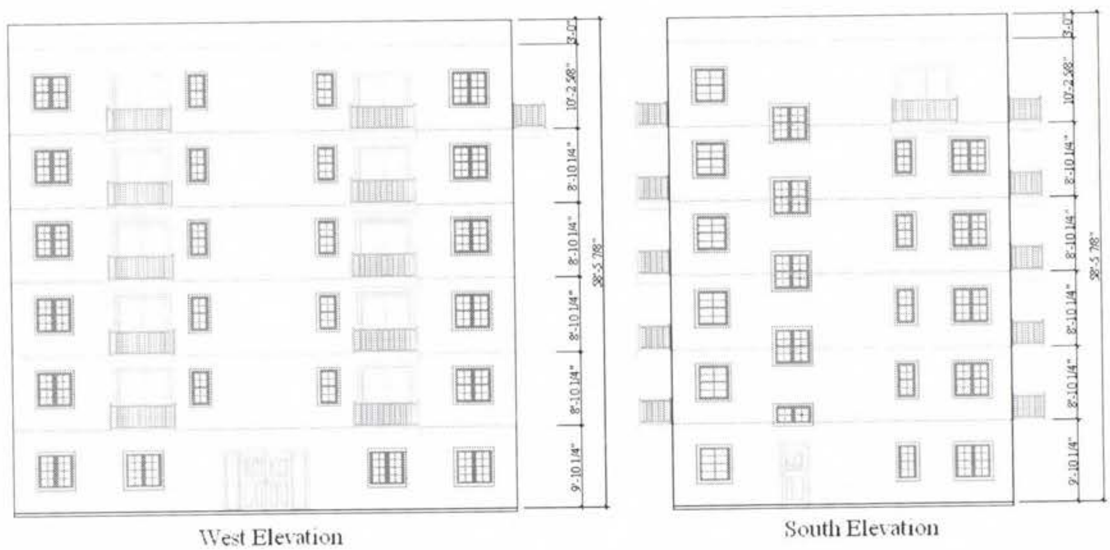

Figure 6-5 West-South elevation view of Capstone building

The clear height of the 1st- and 6th-story is 9 feet and the height in other stories is 8 feet. The shearwalls in the building were built/designed using 2x6 framing members and 15/32 inch thick oriented strand board (OSB) sheathing. The sheathing nails were 10d common nails and 16d common nails were used for framing connections. For partition walls designed using drywall panels, 6d drywall screws with 8 inch spacing were used to attach the drywall panel to the framing. The construction materials and the contents were included in the seismic weight calculations for the whole building. The seismic weight of the n^{th}-story is calculated as the sum of the total weight of the n^{th}-story diaphragm, the total weight of contents on the floor diaphragm and half of the wall weight above and below the story diaphragm. The seismic weight at each story are listed in Table 6-1. More detailed information on the Capstone six-story woodframe building used in this dissertation work can be obtained from the NEESWood website (http://www.engr.colostate.edu/NEESWood/capstone.html). The solid model for the Capstone building is shown in Figure 6-6.

Table 6-1 Total seismic weight at each story of Capstone building

Story #	1	2	3	4	5	Roof	Total
Seismic weight (kips)	122	114	114	114	127	79.5	670.5

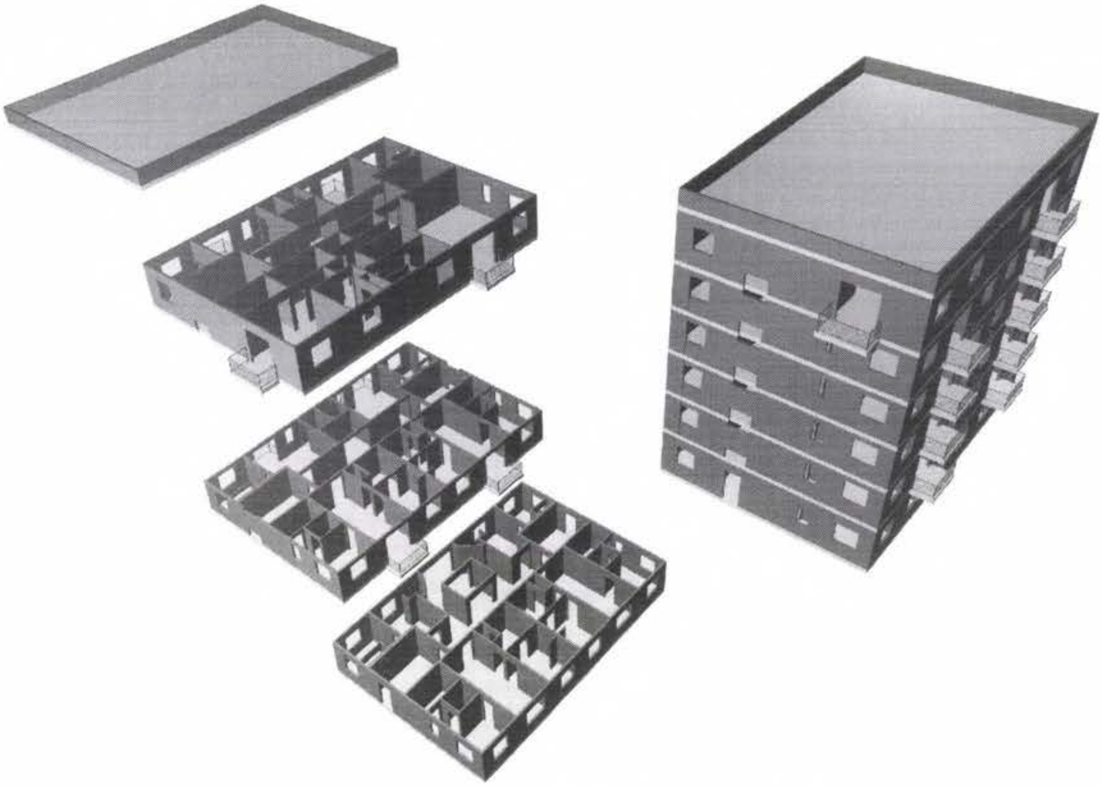

Figure 6-6 Solid model of Capstone building

6.2 Procedure for Capstone building design in this study

6.2.1 Capstone building M-IDA numerical simulations

Following the PBSD procedure discussed in Chapter 5, the numerical simulations of Capstone building were conducted. Since the force-based design was considered to be not sufficient enough for a very large earthquake, i.e. MCE-level, the preliminary design configuration used in this study was obtained from a performance based design philosophy developed in the NEESWood project, namely, Direct Displacement Design method (DDD) (Pang et al., 2007). The DDD which provided the shearwall selection for the Capstone building was conducted at Texas A&M University. The remainder of the PBSD was conducted at Colorado State University. It was illustrated later that the direct displacement designed structure could satisfy the inter-story drift requirements but falls short of the requirements imposed in the present study for acceleration control. The earthquake inputs for the M-IDA simulation were still using the suite of 22 recorded earthquake ground motions from the ATC-63 project. The range of seismic intensity (S_a) was also from 0 to 2g. However, the recorded earthquake ground motions in ATC-63 were different in the x- and y-direction, which is typical of any earthquake. These records were therefore switched and applied to the structure in the reverse orientation. Hence, there are total 44 records used in the M-IDA numerical simulations for the Capstone building in this study.

The method for the PNE calculation for each performance expectation segment (for both inter-story drift and acceleration) in Chapter 5 was adapted in this Section.

$$PNE = PNE_F + PNE_T(T) + PNE_u(U) \tag{5-1}$$

However, because the design structure is a mid-rise structure (six-story apartment building), it is rational to make changes to several details in the calculation of the PNE levels. Here, the PNE_F for all the performance levels was increased to a value of 0.4, which means the design must not exceed the predefined performance levels at their corresponding hazard levels with at least 40% probability, which is more restrictive compared to that of the low-rise construction. The owner/user's input (PNE_u) in the

PBSD design procedure was kept the same as for the low-rise structure which means the factor was kept equal to 0.2. Then the factor for earthquake occurrence (PNE_T) in Equation (5-1) should be 0.4 because they must sum to unity. Therefore, Equation (5-4) should be revised as:

$$PNE = 0.4 + 0.4 \times \frac{\min(2.5, PE_{30} / PE_s)}{3} + 0.2 \times U \tag{6-2}$$

Here, Los Angeles was selected as the building site and the importance factor assigned by owner/user will be the same as the ones in Table 5-6, column 2. Therefore, the PNE can be calculated at each hazard level and the performance expectation curve for inter-story drift and floor acceleration for this mid-rise woodframe building is shown in Figures 6-7 and 6-8.

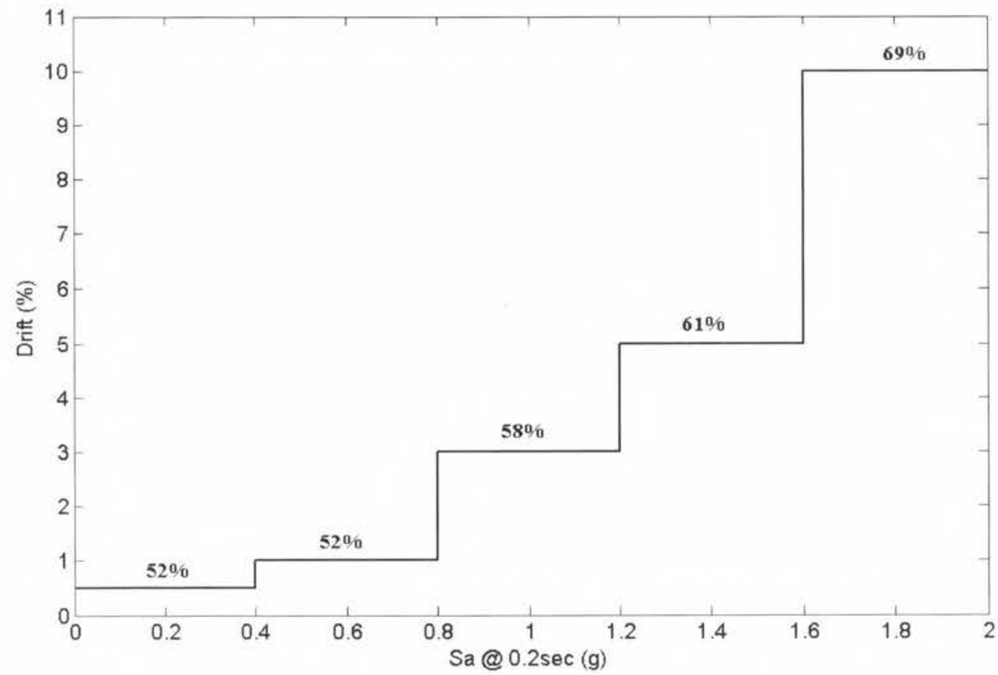

Figure 6-7 Mid-rise woodframe building performance expectation for inter-story drift

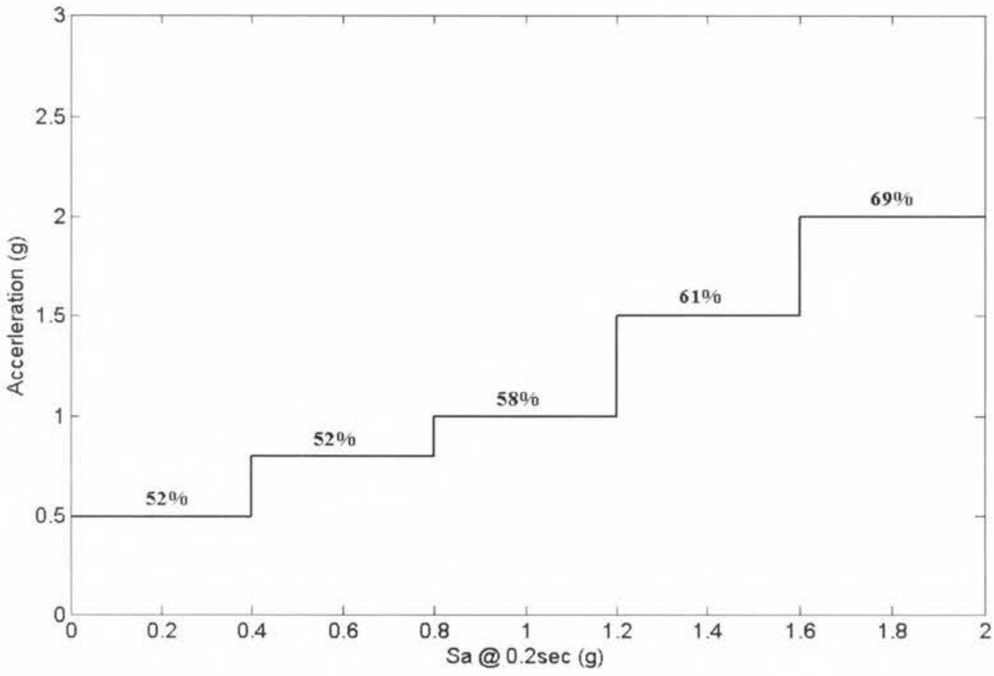

Figure 6-8 Mid-rise woodframe building performance expectation for acceleration

The numerical simulation results for Capstone building comparing to the performance expectation curve were shown in Figure 6-9 and 6-10.

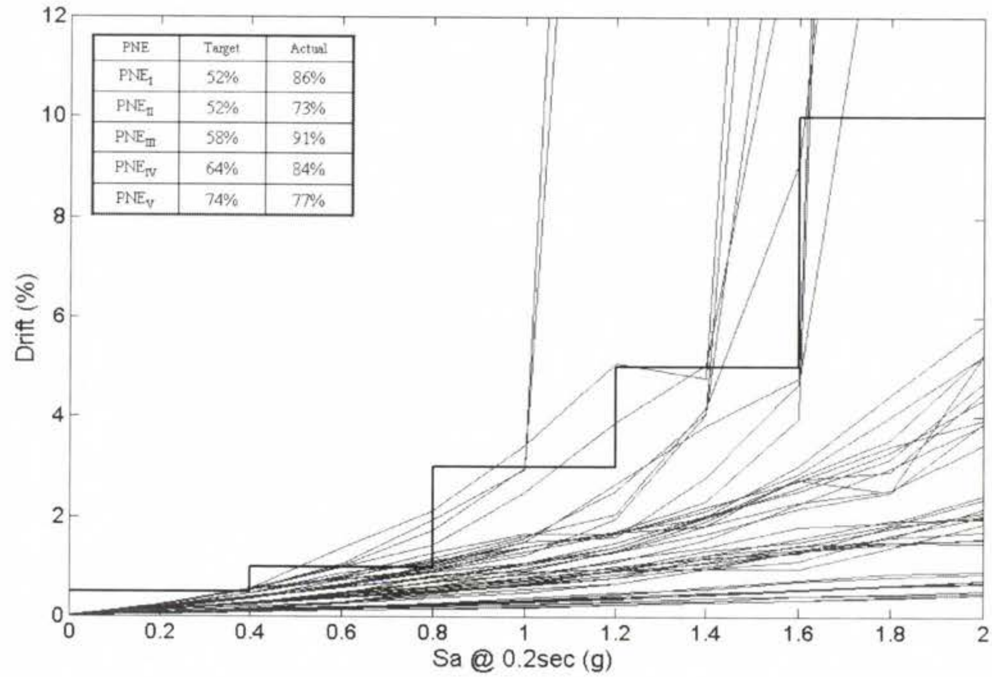

Figure 6-9 Capstone building inter-story drift vs. performance expectation

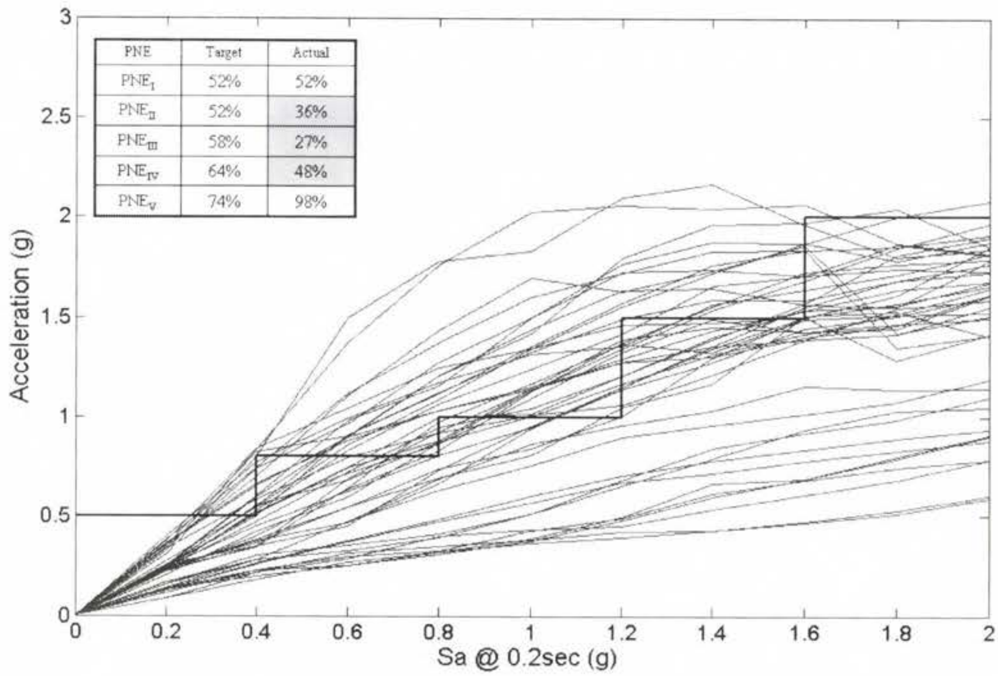

Figure 6-10 Capstone building floor acceleration vs. performance expectation

It was obvious that the inter-story drift of Capstone building can meet the PBSD requirements while the floor acceleration cannot satisfy the performance expectation defined in this Chapter. Based on the numerical simulations conducted in Chapter 5 and 6, it is interesting to note that for mid-rise woodframe buildings, floor acceleration was more likely to control the design while for low-rise woodframe buildings inter-story drift controlled the PBSD.

6.2.2 Capstone building with FP bearings

Based on the numerical simulations for the Capstone building (Figure 6-10), the design of Capstone building using the DDD method cannot satisfy the performance expectation (floor acceleration) curves defined in this dissertation. Since the detailed steps to design a structure using the PBSD procedure have been illustrated in Chapter 5, an alternative design method of applying FP bearings to the Capstone building is conducted as an illustrative design example. However, since the passive seismic control device is considered within the framework of the PBSD procedure, the performance expectation needs to be revised since even better performance should be expected after installing damage mitigation system.

Initially, the target curve should be revised to include not only the performance of the superstructure above the FP device, but also the performance of the FP device itself. Also, considering the additional cost of installing the FP devices, the expected performance should be different (superior) than the cases without this option. Based on the test performance and numerical studies performed on base-isolated structures, it was felt to be reasonable to use a restrictive drift limit for the superstructure. In this case, the inter-story drift for the isolated building was set not to exceed 0.5% for all hazard levels, which essentially prevents the development of even minor damage to most structural and non-structural components and assemblies. The performance expectation of inter-story drift for the structure with FP devices is shown in Figure 6-11. For the acceleration criteria, it was assumed in this study that when the floor acceleration is less than 0.3g, it can be considered as acceptable acceleration; similarly, when the floor acceleration is between 0.3g and 0.5g, it can be considered as noticeable acceleration; and as long as the floor acceleration is below 0.8g, it is assumed that there will not be serious damage and safety threat to the contents and occupants. The performance expectation of floor acceleration for the structures with FP devices is shown in Figure 6-12. The PNE value for both inter-story drift and floor acceleration were arbitrarily assigned to 90% in this study in order to properly reflect the benefit of using the FP device.

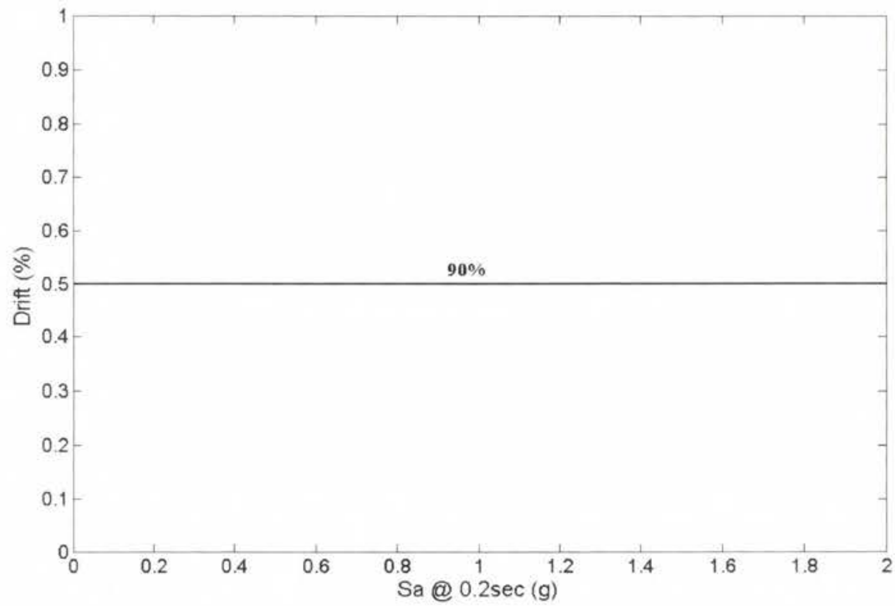

Figure 6-11 Performance expectation of inter-story drift for structure with FP bearings

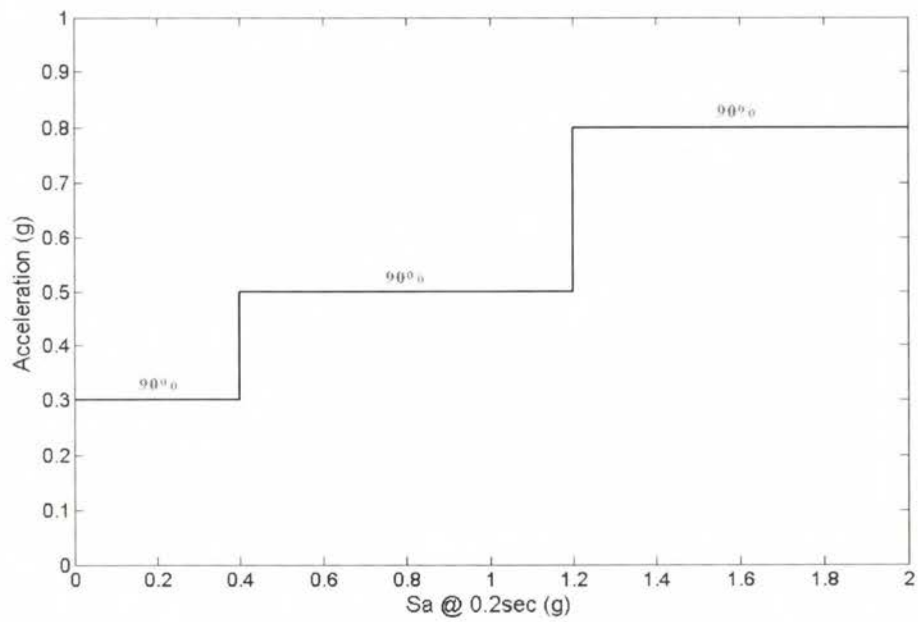

Figure 6-12 Performance expectation of acceleration for structure with FP bearings

As discussed earlier in Chapter 3, the parameters that characterize the behavior of the FP bearing model in SAPWood are controlled by the radius, R, initial stiffness, K_0, the friction coefficient at maximum and minimum velocity f_{max} and f_{min} and the constant for given bearing pressure and condition of interface, a. In this Chapter, the parameters for the FP bearing applied to the Capstone building were assigned to have a radius of curvature equal to 1880 mm (74 in.), the coefficient of friction f_{max} was 0.07 for sliding velocities greater than 50 mm/s (2 in./sec), f_{min} was selected as 0.04 and the constant a was equal to 3.81. These parameters were obtained from a case study for existing San Francisco base isolated structures by Mokha et al. (1996). Also, the displacement capacity of the FP bearing used in this example is 350 mm (13.8 in.). With the FPS devices present, an additional performance expectation for FP bearing needs to be considered so that the movement of the FP bearing during earthquake excitation does not exceed the displacement capacity of the device, which may cause damage to the device itself and superstructure above in the event it hits the hard stop. The performance expectation curve for FP bearing displacement was shown in Figure 6-13.

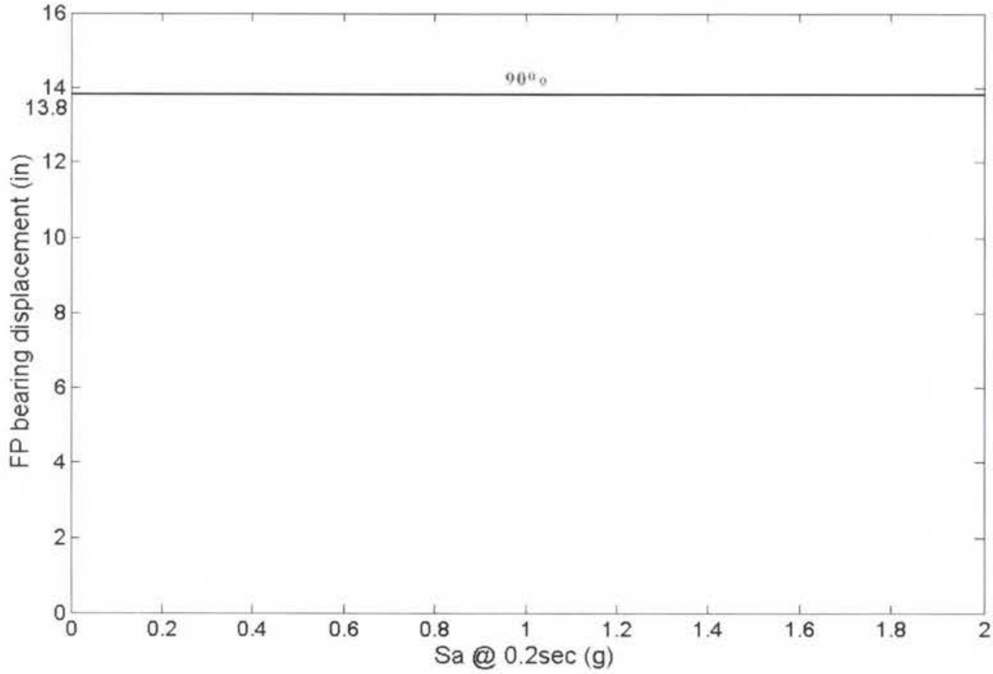

Figure 6-13 Performance expectation of displacement for FPS devices

The total seismic weight of the Capstone building was 2983 kN (670.5 kips) which was far below the working level for vertical load capacity of the FP bearings. There are a total of nine FP bearings modeled/installed under the 1st-story of Capstone building in the numerical system model and the positions of them were shown in the Figure 6-14 with red "+" symbols.

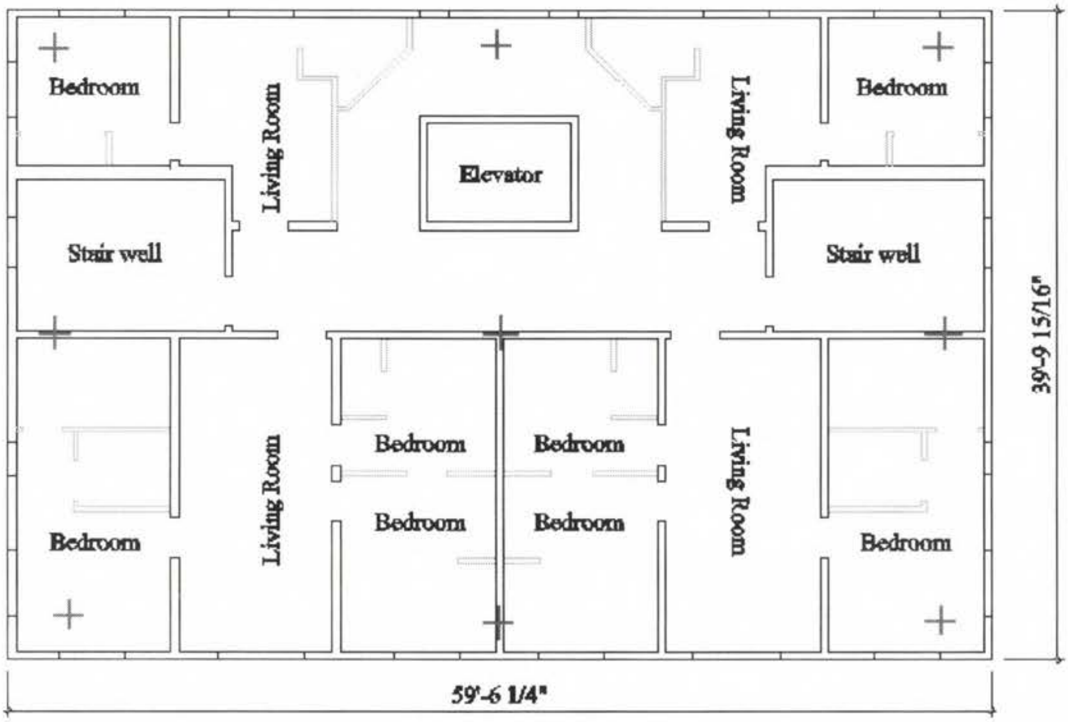

Figure 6-14 Position of FP bearings under Capstone building

The M-IDA were conducted on the system model of the Capstone building with FP bearings using the 44 ATC-63 earthquake ground motion pairs (i.e. the 22 original and 22 switched earthquake records). The results for the superstructure (Capstone building) above the FP bearings, both inter-story drift and floor acceleration, are shown in Figure 6-15 and 6-16.

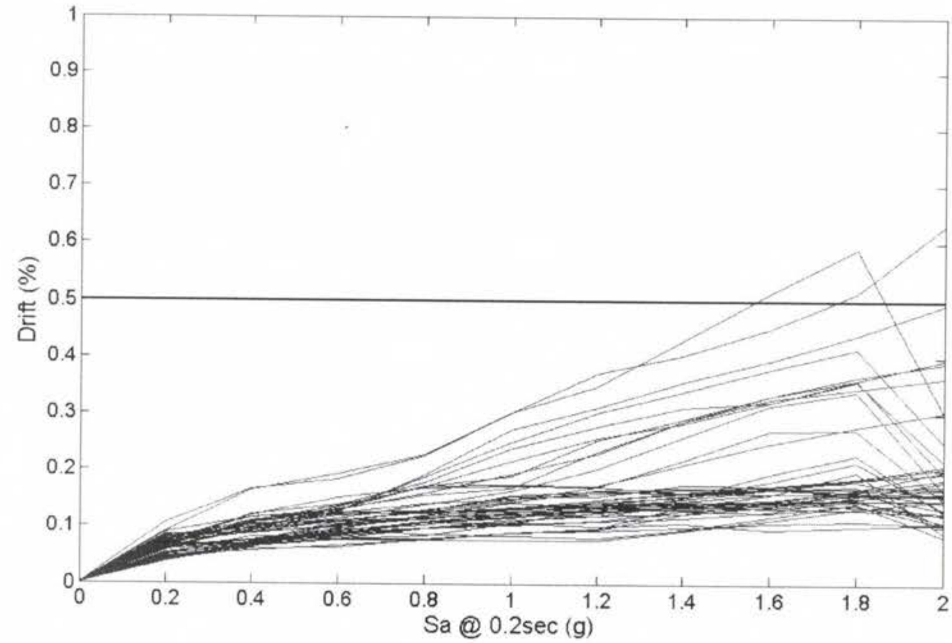

Figure 6-15 Capstone building with FP bearings inter-story drift vs. performance expectation

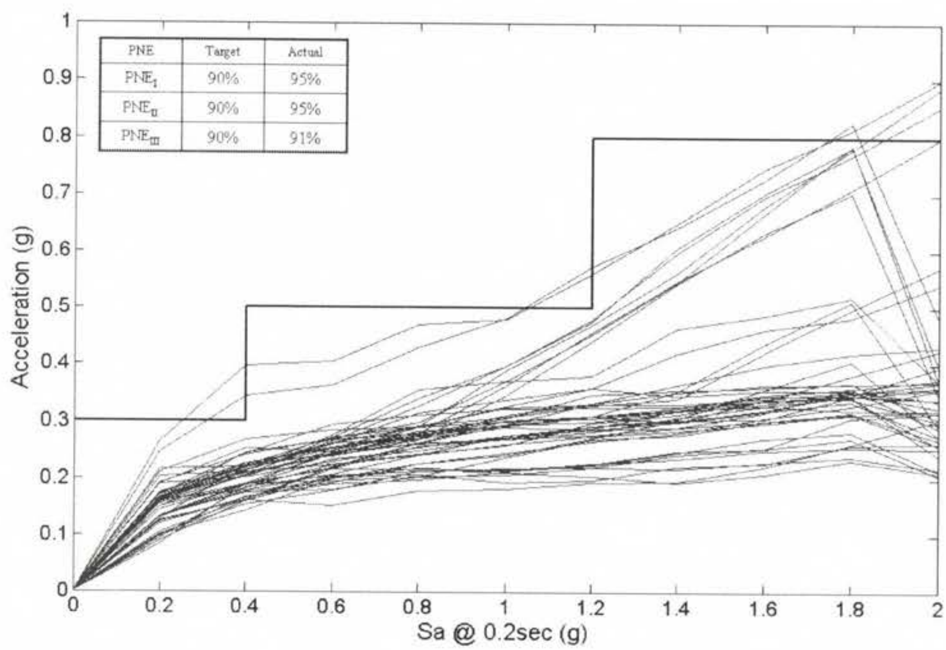

Figure 6-16 Capstone building with FP bearings acceleration vs. performance expectation

It can be seen that for the superstructure, both the inter-story drift and floor accelerations met the performance requirement defined in this study. Recall that in the SAPWood program, FP bearings are allowed to continuously move even after the displacement capacity has been exceeded in the numerical simulations. Thus the failure of the FP system was manually examined after earthquake excitations and indicated by simulated displacement greater than displacement limit. The displacements of FP bearings with 44 earthquake excitations are plotted in Figure 6-17. The FPS displacement requirement set forth previously was not satisfied.

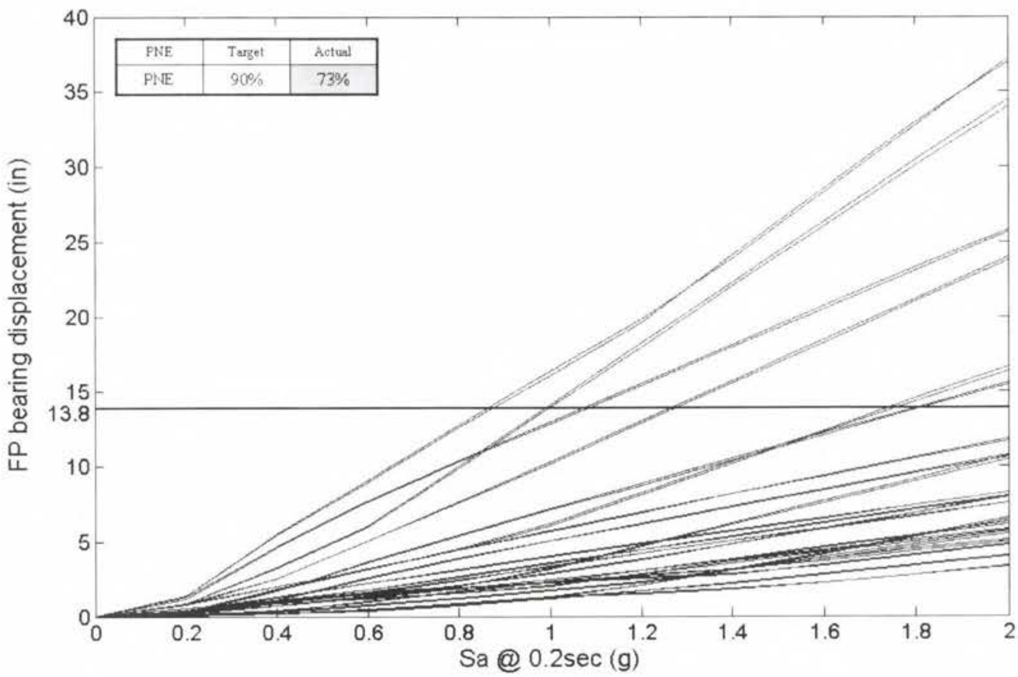

Figure 6-17 FP bearings displacement vs. performance expectation

Recall that there were three ways to modify the FP bearing in Chapter 3 (Figure 3-7) which included changing the radius of the FP bearing, the number and location of the FP bearings, and the displacement capacity. Changing the radius of the FP bearing will affect the response of the superstructure, which has been satisfied with the current configuration. For the Capstone building floor plan, a change in the number and location of the FP bearings will not have significant effect on both the FP bearing and superstructure performance as long as the placement of FP devices is symmetrical, which is the case right now. The most logical method of modification is changing the displacement capacity. Considering the comfort issue for the occupants of the building, the maximum vertical movement of the FP bearing (h in Figure 6-18) was assumed to be 5 inches in this study. Therefore, keeping the radius as 74 inches, the displacement capacity can be calculated as equal to 26.7 inches. Under this new displacement capacity, the displacement requirement of the FP bearings was satisfied. The final comparison of FP bearing movement and the displacement capacity is shown in Figure 6-19.

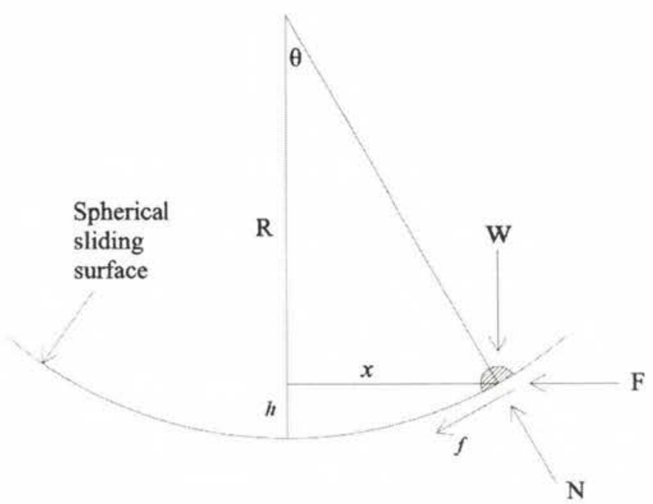

Figure 6-18 FP bearing geometry

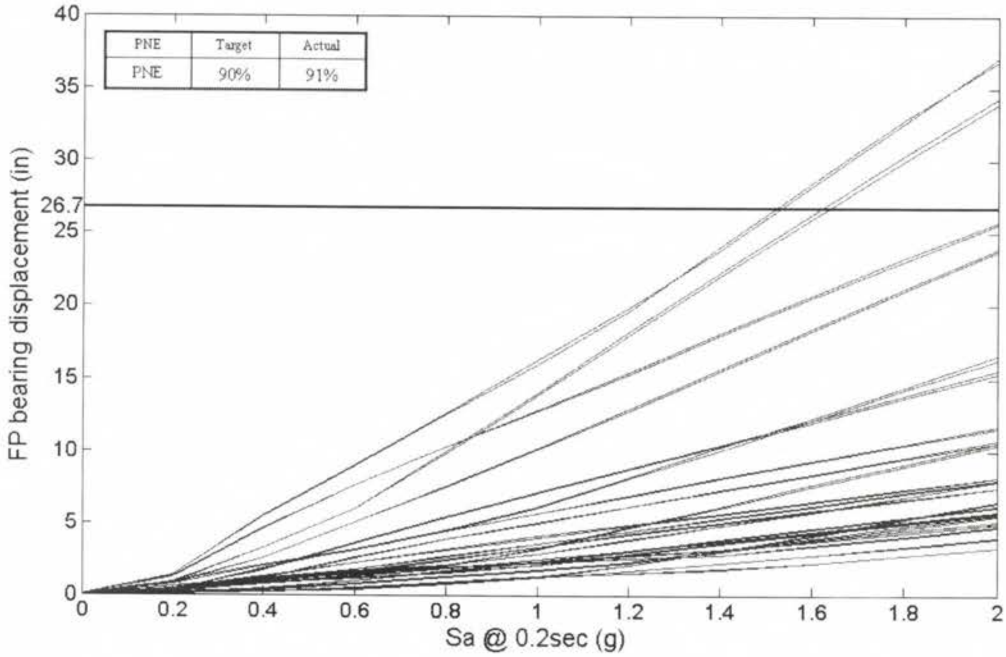

Figure 6-19 FP bearings displacement vs. revised performance expectation

Chapter Seven

Simplified Performance-based Seismic Design Procedure

7.1 Development of simplified PBSD procedure

A comprehensive procedure for conducting the generalized PBSD proposed in this study was illustrated in detail in Chapter 5 and Chapter 6 for both low-rise and mid-rise woodframe buildings. The advantages of using the generalized PBSD procedure can be summarized as follows: first, different from the traditional force-based seismic design procedure, the nonlinear time history analysis was used in the generalized PBSD. Second, the design target in PBSD goes beyond current consideration of solely the sub-assemblies (e.g. shearwalls) capacity and incorporates system-level behavior. Thus, the design objective is extended to a target that the user/engineer can help choose based on their specific building performance needs, which are then related to quantities such as inter-story drift, floor acceleration, etc. At the same time, building performance under multiple hazard levels is also considered. For communication purposes during the design decision process, the return period, spectral acceleration, or other quantities can be used to better communicate the seismic hazard level. Third, earthquake events are considered as random events in the generalized PBSD procedure with their uncertainty explicitly incorporated in the design through the use of earthquake suites. Finally, fourth, the procedure allows the participation of the end-user's opinion, to some degree, in the design target selection as well as the intensity of the earthquake, the occurrence probability of an earthquake, etc.

However, the comprehensive PBSD procedure proposed in this study requires a numerical tool/software to perform NLTHA (non-linear time history analysis). The designer/engineer needs to be familiar with the software and fully understand the modeling procedure so that the revision of the model can be conducted based on proper interpretation of the numerical simulation results until the predefined performance expectation are satisfied. Obviously, the advantages described earlier come at the expense for numerical model development and case-specific analysis of the time history simulation results. Although the final design can be fine-tuned to fit a wide range of PBSD requirements, this procedure is not similar to current design practice which is, obviously, more familiar to engineers and has a specific procedure associated with it. It is for these reasons that a simplified PBSD procedure was developed as part of this dissertation work with the ultimate purpose of being applied in more practical design situations.

It is well accepted in light-frame wood design that the use of design tables and charts is an efficient and practical format for prescriptive design. In this Chapter, a simplified

PBSD procedure is proposed with the help of design tables so that an engineer may design the woodframe structure such that it satisfies the performance curve defined in the generalized procedure. The idea behind the simplified procedure is to use a significant amount of numerical simulation to evaluate a wide range of possible configurations that are commonly used in woodframe building design. Then the performance of these configurations, defined herein based on inter-story drifts and floor accelerations, are adopted as design requirements and arranged into tabular form. The designer can then select from these configurations using the basic design information, including the floor plan, available shear wall length, seismic mass, etc. and predefined design target curve.

However, it is also important to point out that there are certain limitations to this simplified procedure compared to the comprehensive approach outlined earlier in which the non-linear time history analysis of the structure is performed. First, the simulated configurations included in the design tables cannot represent all possible design variations. Next, the design based on the simplified design tables is one option that can be used, but many others are possible as with all design processes. However, by making use of the design tables, the designer can always determine a design that suits their design purpose, that is, satisfying the predefined performance expectations or target curve. Since the majority of residential buildings are low-rise structure, i.e. two stories or under, the simplified design tables generated in this Chapter cover the design of structures having one or two stories.

7.1.1 Design of one story buildings

In order to make the simplified PBSD design tables applicable to typical design configurations, a format similar to the shearwall selection table for force-based design requirements was adopted. Simply speaking, the selection of shearwall nail patterns is also connected to the tributary seismic weight normalized over the shearwall length. A very simple system model with a square shape floor plan and 4 ft walls on both sides of the floor was developed in SAPWood with variants of the seismic mass on the diaphragm. Four feet long wall segments were selected here because these represent a typical structural sheathing panel used in woodframe construction in North America. This simplified system model with different nail patterns was subjected to a suite of earthquake ground motions (22 recorded earthquake ground motions in ATC 63) scaled to the predefined seismic intensity level, similar to the procedure used in the numerical simulations in the generalized PBSD procedure. Finally, a large amount of numerical simulations were performed essentially creating a database. The result was a design table with different combinations of seismic mass and nail pattern at different seismic intensity (hazard) levels and their corresponding performance was obtained and is presented in Table 7-1.

With this table, the simplified design procedure for a one story woodframe building can be conducted following these steps:

(1) Obtain the performance target PNE values based on the building site, designer/engineer consideration and end-user's input;

(2) Calculate the total seismic mass for the one story building which should typically include the mass of the roof and the relevant weight of the walls, e.g. half of total wall weight;

(3) Determine/select the shearwalls for the structure based on the preliminary floor plan and calculate the total shearwall length in each direction;

(4) Calculate the pound per linear foot (PLF) value;

(5) Choose the nail pattern from the PBSD table using the PLF value from Step 4 and target PNE values from Step 1;

(6) If there is no nail pattern under the PLF column that satisfies the defined target PNE values, the wall length called out either needs to be increased to reduce the PLF level, or the designer should consider using double-sheathed walls.

Table 7-1 Design table for single story building (PNE(Drift)/PNE(Acceleration) value), units in percentile

Nail Pattern	Hazard Level	PLF=100	200	400	600	800	1000	1200	1400
2/12	Sa<0.4g	100/100	100/100	100/100	100/95	100/91	100/86	91/82	86/77
	0.4g<Sa<0.8g	100/100	100/95	100/91	100/91	100/82	95/68	91/73	77/55
	0.8g<Sa<1.2g	100/91	100/91	100/82	100/73	100/55	100/36	95/41	91/32
	1.2g<Sa<1.6g	100/95	100/91	100/91	100/86	100/73	95/64	86/51	77/77
	1.6g<Sa<2g	100/100	100/95	100/91	100/91	95/77	86/86	68/-	50/-
3/12	Sa<0.4g	100/100	100/100	100/100	100/91	100/91	95/91	91/86	77/77
	0.4g<Sa<0.8g	100/100	100/95	100/91	100/91	95/82	91/68	82/64	55/64
	0.8g<Sa<1.2g	100/91	100/91	100/86	100/77	100/64	91/45	82/32	64/64
	1.2g<Sa<1.6g	100/95	100/95	100/91	100/82	91/77	73/91	45/-	45/-
	1.6g<Sa<2g	100/100	100/100	100/91	91/82	68/-	50/-	27/-	27/-
4/12	Sa<0.4g	100/100	100/100	100/100	100/91	95/91	91/91	86/86	73/82
	0.4g<Sa<0.8g	100/100	100/95	100/91	100/91	91/77	82/77	59/73	32/77
	0.8g<Sa<1.2g	100/91	100/91	100/86	100/73	95/50	82/50	64/82	55/-
	1.2g<Sa<1.6g	100/95	100/95	100/86	95/77	73/91	55/-	45/-	27/-
	1.6g<Sa<2g	100/100	100/95	100/91	82/-	50/-	36/-	27/-	32/-
6/12	Sa<0.4g	100/100	100/100	100/95	95/91	91/82	77/82	50/82	32/91
	0.4g<Sa<0.8g	100/100	100/95	100/91	91/77	73/77	32/82	27/-	27/-
	0.8g<Sa<1.2g	100/91	100/91	100/77	91/50	73/86	55/-	45/-	27/-
	1.2g<Sa<1.6g	100/95	100/91	95/82	77/-	50/-	27/-	27/-	27/-
	1.6g<Sa<2g	100/95	100/91	86/95	41/-	27/-	32/-	27/-	18/-

Nail Pattern	Hazard level	PLF=1600	1800	2000	2200	2400	2600	2800	3000
2/12	Sa<0.4g	73/73	55/82	45/77	45/68	36/68	23/64	27/55	27/50
	0.4g<Sa<0.8g	55/36	41/36	32/41	27/27	27/32	27/41	27/73	23/-
	0.8g<Sa<1.2g	82/27	77/27	55/32	50/73	45/-	50/-	41/-	41/-
	1.2g<Sa<1.6g	50/-	50/-	50/-	41/100	27/-	27/-	27/-	27/-
	1.6g<Sa<2g	36/-	36/-	27/-	27/-	27/-	27/-	27/-	27/-
3/12	Sa<0.4g	59/82	45/77	36/77	32/82	27/82	27/82	27/86	23/95
	0.4g<Sa<0.8g	32/55	27/82	27/95	27/-	27/-	27/-	27/-	18/-
	0.8g<Sa<1.2g	55/-	45/-	45/-	32/-	27/-	27/-	27/-	27/-
	1.2g<Sa<1.6g	27/-	27/-	27/-	27/-	27/-	27/-	27/-	23/-
	1.6g<Sa<2g	27/-	32/-	27/-	27/-	27/-	23/-	18/-	18/-
4/12	Sa<0.4g	50/82	32/82	32/86	27/86	23/91	27/-	23/-	23/-
	0.4g<Sa<0.8g	27/-	27/-	27/-	27/-	27/-	27/-	23/-	23/-
	0.8g<Sa<1.2g	50/-	36/-	27/-	27/-	27/-	27/-	27/-	27/-
	1.2g<Sa<1.6g	27/-	27/-	32/-	27/-	27/-	27/-	23/-	23/-
	1.6g<Sa<2g	27/-	27/-	27/-	23/-	18/-	18/-	14/-	18/-
6/12	Sa<0.4g	27/95	23/-	23/-	23/-	27/-	23/-	23/-	23/-
	0.4g<Sa<0.8g	27/-	27/-	27/-	23/-	18/-	18/-	18/-	18/-
	0.8g<Sa<1.2g	27/-	27/-	27/-	27/-	23/-	23/-	23/-	23/-
	1.2g<Sa<1.6g	27/-	23/-	23/-	18/-	18/-	18/-	18/-	14/-
	1.6g<Sa<2g	18/-	14/-	14/-	14/-	9/-	9/-	9/-	9/-

7.1.2 Design of two-story buildings

Similar to the simplified PBSD design of a one-story woodframe building discussed in the previous section, the simplified design tables for two-story woodframe buildings were developed based on an even greater number of numerical simulations. Multiple design tables need to be constructed due to the high number of possible combinations of first and second story seismic mass ratios. As mentioned earlier, this simplified design table does not cover all possible cases. However, a representative number of configurations were selected to represent the possible design space. In choosing the configurations represented in the design tables, two assumptions were adopted in this study:

(1) The ultimate strength of the 1^{st}-story (st1) will always be greater than that of the 2^{nd}-story (st2). This assumption was made to eliminate the possibility of a weak and/or soft story.

(2) The length of the shearwalls in both stories is approximately the same. This assumption was made based on the typical construction practice where the shearwalls in upper and lower stories are stacked for many reasons, such as hold-down issue, shear transfer issues, floor collector design, etc.

With these assumptions, a simple system model with a square floor plan and four identical shearwalls (wall length of 4 ft) at each story was built in SAPWood. Non-linear time history analyses with different seismic masses and different nail patterns at each story were run using the earthquake ground motion suite discussed in the previous section for one story buildings. Then the simplified PBSD tables for two-story buildings were developed for different combinations of nail patterns at story 1 and story 2 with the typical seismic mass ratios one might expect in design. These design tables are essentially an expanded version of the one story design table and were organized as Table A, B, C, and D (Table 7-2 to 7-5). Table A, B, C and D represent the nail pattern for shearwalls at the 1st-story being 6/12, 4/12, 3/12 and 2/12.

With these design tables, the simplified PBSD procedure for two-story woodframe buildings can be conducted using the following steps:

(1) Similar to the design of the single story building, the performance target PNE values based on the building site, designer consideration and end-user's input should be obtained;

(2) Calculate the seismic mass at each story: for the 1st-story, the seismic mass is set to the summary of the weight of the floor diaphragm, half weight of the walls at the 1st-story and half weight of the walls at the 2nd-story; for the 2nd-story, the seismic mass was set to the mass of the roof and half the weight of the walls at the second story;

(3) Determine/select the shearwalls for each story based on the architectural floor plan (the assumption in Step (2) should be kept in mind) and calculate the total shearwall length in each direction for each story;

(4) Calculate the PLF value at each story and the ratio of PLF value between the two stories;

(5) Select the nail pattern based on the PLF value and target PNE values;

(6) If there is no nail pattern under the PLF column that satisfies the defined target PNE values, the wall length called out must be increased to reduce the PLF level, or the walls may to be double sheathed (OSB on both sides).

The entire design procedure using the simplified PBSD design tables can be summarized in Figure 7-1.

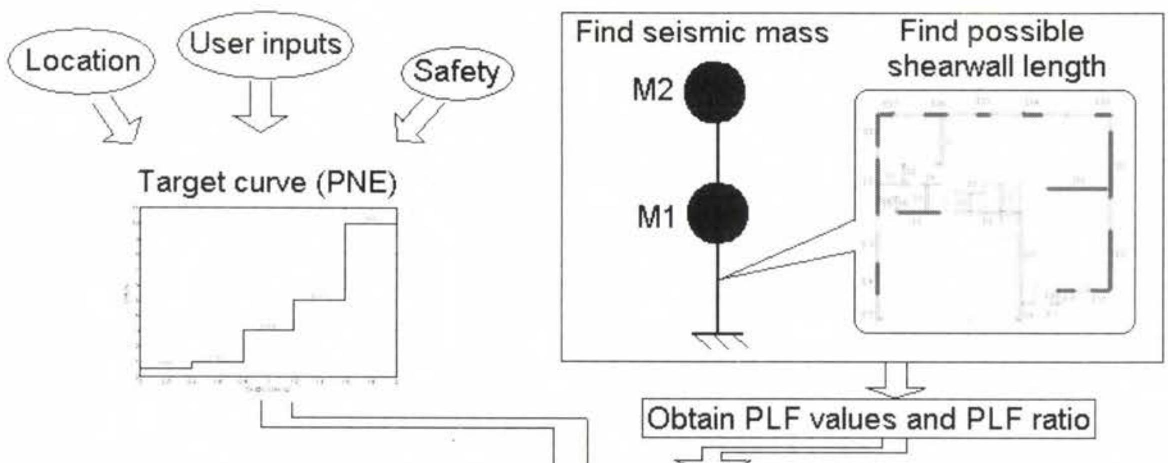

		PLF(st2)/PLF(st1)=1								
Nail Pattern st2//st1	Hazard Level	PLF(st1)=200	400		800	1000	1200	1400	1600	2000
4/12//4/12	Sa<0.4g	100/91	100/91	86/77	64/73	36/64	32/77	27/77	27/82	23/91
	0.4g<Sa<0.8g	100/91	91/73	82/55	36/55	32/68	27/91	23/-	23/-	23/-
	0.8g<Sa<1.2g	100/77	95/36	68/36	59/77	45/-	27/-	32/-	32/-	27/-
	1.2g<Sa<1.6g	100/82	82/73	59/-	32/-	32/-	32/-	23/-	23/-	19/-
	1.6g<Sa<2g	100/82	68/-	36/-	27/-	36/-	19/-	19/-	19/-	14/-
6/12 //4/12	Sa<0.4g	100/95	95/91	86/82	64/68	36/59	32/64	27/77	27/86	23/-
	0.4g<Sa<0.8g	100/91	91/64	64/50	36/59	27/82	27/-	27/-	23/-	19/-
	0.8g<Sa<1.2g	100/73	95/41	73/41	59/77	41/-	32/-	36/-	36/-	23/-
	1.2g<Sa<1.6g	100/82	82/73	59/-	41/-	36/-	36/-	23/-	23/-	14/-
	1.6g<Sa<2g	100/82	64/95	45/-	32/-	27/-	27/-	14/-	14/-	9/-

Obtain the nail pattern (final design)

Figure 7-1 Simplified PBSD design procedure

Table 7-2 Design table A for two-story building (PNE(Drift)/PNE(Acceleration) value), units in percentile

		PLF(st2)/PLF(st1)=1							
Nail Pattern st2// st1	Hazard Level	PLF(st1)=200	400	600	800	1000	1200	1600	2000
6/12 // 6/12	Sa<0.4g	100/91	91/86	68/77	36/73	32/82	27/91	23/-	19/-
	0.4g<Sa<0.8g	100/86	82/73	36/68	27/-	27/-	23/-	19/-	14/-
	0.8g<Sa<1.2g	100/59	82/41	59/95	32/-	32/-	27/-	23/-	23/-
	1.2g<Sa<1.6g	100/77	59/-	32/-	32/-	23/-	19/-	19/-	14/-
	1.6g<Sa<2g	91/82	50/-	27/-	27/-	19/-	14/-	14/-	5/-
		PLF(st2)/PLF(st1)=0.75							
Nail Pattern st2// st1	Hazard Level	PLF(st1)=200	400	600	800	1000	1200	1600	2000
6/12 // 6/12	Sa<0.4g	100/91	95/91	86/77	36/68	27/73	27/82	23/-	23/-
	0.4g<Sa<0.8g	100/91	91/68	45/50	32/86	27/-	27/-	23/-	19/-
	0.8g<Sa<1.2g	100/68	86/36	59/86	32/-	32/-	32/-	27/-	19/-
	1.2g<Sa<1.6g	100/82	64/-	32/-	32/-	27/-	23/-	19/-	14/-
	1.6g<Sa<2g	95/82	41/-	36/-	27/-	19/-	14/-	14/-	9/-
		PLF(st2)/PLF(st1)=0.5							
Nail Pattern st2// st1	Hazard Level	PLF(st1)=200	400	600	800	1000	1200	1600	2000
6/12 // 6/12	Sa<0.4g	100/95	100/91	86/77	64/77	32/68	27/64	27/95	23/-
	0.4g<Sa<0.8g	100/91	91/68	64/59	36/59	27/-	27/-	23/-	19/-
	0.8g<Sa<1.2g	100/82	95/32	64/45	55/-	27/-	32/-	23/-	23/-
	1.2g<Sa<1.6g	100/86	73/91	55/-	27/-	27/-	23/-	19/-	19/-
	1.6g<Sa<2g	100/86	55/-	32/-	27/-	23/-	19/-	14/-	14/-

Table 7-3 Design table B for two-story building (PNE(Drift)/PNE(Acceleration) value) , units in percentile

		PLF(st2)/PLF(st1)=1								
Nail Pattern st2//st1	Hazard Level	PLF(st1)=200	400	600	800	1000	1200	1400	1600	2000
4/12 // 4/12	Sa<0.4g	100/91	100/91	86/77	64/73	36/64	32/77	27/77	27/82	23/91
	0.4g<Sa<0.8g	100/91	91/73	82/55	36/55	32/68	27/91	23/-	23/-	23/-
	0.8g<Sa<1.2g	100/77	95/36	68/36	59/77	45/-	27/-	32/-	32/-	27/-
	1.2g<Sa<1.6g	100/82	82/73	59/-	32/-	32/-	32/-	23/-	23/-	19/-
	1.6g<Sa<2g	100/82	68/-	36/-	27/-	36/-	19/-	19/-	19/-	14/-
6/12 // 4/12	Sa<0.4g	100/95	95/91	86/82	64/68	36/59	32/64	27/77	27/86	23/-
	0.4g<Sa<0.8g	100/91	91/64	64/50	36/59	27/82	27/-	27/-	23/-	19/-
	0.8g<Sa<1.2g	100/73	95/41	73/41	59/77	41/-	32/-	36/-	36/-	23/-
	1.2g<Sa<1.6g	100/82	82/73	59/-	41/-	36/-	36/-	23/-	23/-	14/-
	1.6g<Sa<2g	100/82	64/95	45/-	32/-	27/-	27/-	14/-	14/-	9/-

		PLF(st2)/PLF(st1)=0.75								
Nail Pattern st2//st1	Hazard Level	PLF(st1)=200	400	600	800	1000	1200	1400	1600	2000
4/12 // 4/12	Sa<0.4g	100/95	100/86	91/86	73/77	50/68	27/68	27/73	27/82	23/82
	0.4g<Sa<0.8g	100/91	100/77	86/59	55/50	32/50	27/86	27/-	27/-	23/-
	0.8g<Sa<1.2g	100/86	95/41	82/32	59/50	50/91	32/-	27/-	27/-	27/-
	1.2g<Sa<1.6g	100/86	91/73	59/-	50/-	32/-	32/-	27/-	23/-	23/-
	1.6g<Sa<2g	100/91	82/-	45/-	27/-	32/-	27/-	19/-	19/-	14/-

6/12 // 4/12	Sa<0.4g	100/91	100/86	86/73	82/82	55/73	32/64	32/68	27/77	23/86
	0.4g<Sa<0.8g	100/91	100/82	86/55	50/55	32/59	32/82	27/-	23/-	23/-
	0.8g<Sa<1.2g	100/77	65/36	82/36	68/64	50/77	41/-	32/-	32/-	36/-
	1.2g<Sa<1.6g	100/86	91/64	64/86	50/-	27/-	36/-	36/-	27/-	23/-
	1.6g<Sa<2g	100/91	77/82	50/-	27/-	32/-	27/-	27/-	23/-	19/-
		PLF(st2)/PLF(st1)=0.5								
Nail Pattern st2//st1	Hazard Level	PLF(st1)=200	400	600	800	1000	1200	1400	1600	2000
4/12 // 4/12	Sa<0.4g	100/100	100/91	95/91	86/81	68/77	45/64	32/64	27/59	27/77
	0.4g<Sa<0.8g	100/91	100/77	91/64	77/50	32/41	32/55	27/82	27/-	27/-
	0.8g<Sa<1.2g	100/82	100/45	86/36	68/27	59/59	41/95	27/-	27/-	27/-
	1.2g<Sa<1.6g	100/91	95/68	68/86	55/-	32/-	27/-	27/-	27/-	23/-
	1.6g<Sa<2g	100/91	86/82	50/-	27/-	32/-	27/-	32/-	19/-	19/-
6/12 // 4/12	Sa<0.4g	100/100	100/91	95/91	86/77	64/73	45/64	27/68	27/73	27/77
	0.4g<Sa<0.8g	100/91	100/73	91/64	64/50	32/45	27/68	27/77	27/-	23/-
	0.8g<Sa<1.2g	100/82	100/36	91/32	68/27	59/64	50/95	32/-	27/-	36/-
	1.2g<Sa<1.6g	100/91	95/64	68/77	55/-	32/-	27/-	27/-	27/-	23/-
	1.6g<Sa<2g	100/91	86/86	50/-	36/-	36/-	32/-	27/-	23/-	19/-

Table 7-4 Design table C for two-story building (PNE(Drift)/PNE(Acceleration) value) , units in percentile

		PLF(st2)/PLF(st1)=1				
Nail Pattern st2//st1	Hazard Level	PLF(st1)=200	400	600	800	1000
3/12 // 3/12	Sa<0.4g	100/91	100/73	91/73	73/73	45/73
	0.4g<Sa<0.8g	100/91	100/59	86/45	50/36	32/45
	0.8g<Sa<1.2g	100/77	100/32	86/32	68/41	50/59
	1.2g<Sa<1.6g	100/86	95/59	64/68	41/-	27/-
	1.6g<Sa<2g	100/91	82/82	50/-	32/-	27/-
4/12 // 3/12	Sa<0.4g	100/91	100/73	91/77	73/73	50/73
	0.4g<Sa<0.8g	100/91	95/59	86/55	55/41	36/45
	0.8g<Sa<1.2g	100/77	95/41	86/36	68/32	50/55
	1.2g<Sa<1.6g	100/82	95/59	68/77	45/-	36/-
	1.6g<Sa<2g	100/86	82/73	55/-	36/-	36/-
6/12 // 3/12	Sa<0.4g	100/95	100/77	91/73	77/68	36/68
	0.4g<Sa<0.8g	100/91	95/64	77/45	41/41	27/64
	0.8g<Sa<1.2g	100/77	95/50	82/32	50/64	36/68
	1.2g<Sa<1.6g	100/82	82/59	55/77	32/77	27/95
	1.6g<Sa<2g	100/82	64/86	32/86	27/-	27/-

		PLF(st2)/PLF(st1)=1				
Nail Pattern st2//st1	Hazard Level	PLF(st1)=1200	1400	1600	1800	2000
3/12 // 3/12	Sa<0.4g	27/59	27/73	27/68	23/77	23/77
	0.4g<Sa<0.8g	32/68	27/86	23/95	23/-	23/-
	0.8g<Sa<1.2g	45/95	41/-	32/-	32/-	27/-
	1.2g<Sa<1.6g	32/-	27/-	23/-	23/-	19/-
	1.6g<Sa<2g	23/-	23/-	19/-	14/-	14/-
4/12 // 3/12	Sa<0.4g	32/59	27/59	32/64	23/64	23/77
	0.4g<Sa<0.8g	32/64	27/82	23/-	23/-	23/-
	0.8g<Sa<1.2g	50/-	41/-	36/-	36/-	36/-
	1.2g<Sa<1.6g	32/-	36/-	27/-	23/-	27/-
	1.6g<Sa<2g	23/-	23/-	19/-	19/-	14/-
6/12 // 3/12	Sa<0.4g	27/64	32/68	27/91	23/82	23/86
	0.4g<Sa<0.8g	27/82	23/86	23/86	19/91	14/-
	0.8g<Sa<1.2g	27/68	32/77	27/-	32/-	23/-
	1.2g<Sa<1.6g	27/-	27/-	19/-	14/-	14/-
	1.6g<Sa<2g	19/-	14/-	14/-	14/-	91/-

		PLF(st2)/PLF(st1)=0.75				
Nail Pattern st2//st1	Hazard Level	PLF(st1)=200	400	600	800	1000
3/12 // 3/12	Sa<0.4g	100/95	100/86	91/77	86/77	55/73
	0.4g<Sa<0.8g	100/91	100/64	91/64	68/41	36/41
	0.8g<Sa<1.2g	100/86	100/36	95/32	68/27	50/50
	1.2g<Sa<1.6g	100/91	95/59	77/50	50/-	32/-
	1.6g<Sa<2g	100/91	91/77	50/-	41/-	32/-
4/12 // 3/12	Sa<0.4g	100/95	100/86	91/77	86/73	59/73
	0.4g<Sa<0.8g	100/91	100/73	86/59	68/41	36/32
	0.8g<Sa<1.2g	100/86	100/36	95/32	77/27	64/45
	1.2g<Sa<1.6g	100/91	95/59	77/64	50/-	36/-
	1.6g<Sa<2g	100/91	86/82	50/-	36/-	32/-
6/12 // 3/12	Sa<0.4g	100/91	100/86	95/73	91/77	64/64
	0.4g<Sa<0.8g	100/91	100/73	91/45	59/32	32/41
	0.8g<Sa<1.2g	100/77	100/32	91/32	73/36	55/45
	1.2g<Sa<1.6g	100/91	95/59	77/55	45/86	32/-
	1.6g<Sa<2g	100/91	86/73	45/91	36/-	32/-

		PLF(st2)/PLF(st1)=0.75				
Nail Pattern st2//st1	Hazard Level	PLF(st1)=1200	1400	1600	1800	2000
3/12 // 3/12	Sa<0.4g	32/68	27/59	27/64	27/73	23/64
	0.4g<Sa<0.8g	27/59	27/68	27/86	23/95	23/-
	0.8g<Sa<1.2g	50/91	41/-	27/-	27/-	32/-
	1.2g<Sa<1.6g	27/-	27/-	27/-	23/-	23/-
	1.6g<Sa<2g	27/-	23/-	23/-	19/-	14/-
4/12 // 3/12	Sa<0.4g	36/73	27/59	27/59	27/64	23/64
	0.4g<Sa<0.8g	27/45	27/68	27/77	23/95	23/-
	0.8g<Sa<1.2g	50/73	41/-	32/-	32/-	36/-
	1.2g<Sa<1.6g	27/-	32/-	27/-	23/-	23/-
	1.6g<Sa<2g	27/-	27/-	23/-	19/-	19/-
6/12 // 3/12	Sa<0.4g	41/59	32/45	32/59	32/68	27/68
	0.4g<Sa<0.8g	27/50	27/82	23/-	23/95	23/-
	0.8g<Sa<1.2g	45/91	36/95	27/-	32/-	32/-
	1.2g<Sa<1.6g	27/-	32/-	27/-	23/-	19/-
	1.6g<Sa<2g	27/-	23/-	19/-	14/-	14/-

		PLF(st2)/PLF(st1)=0.5				
Nail Pattern st2//st1	Hazard Level	PLF(st1)=200	400	600	800	1000
3/12 // 3/12	Sa<0.4g	100/100	100/86	100/82	86/73	82/73
	0.4g<Sa<0.8g	100/91	100/77	91/50	86/45	59/36
	0.8g<Sa<1.2g	100/86	100/50	85/32	82/32	64/27
	1.2g<Sa<1.6g	100/91	100/64	86/59	59/91	50/-
	1.6g<Sa<2g	100/91	95/77	68/-	45/-	27/-
4/12 // 3/12	Sa<0.4g	100/100	100/86	95/82	86/73	82/73
	0.4g<Sa<0.8g	100/91	100/77	91/55	86/41	50/41
	0.8g<Sa<1.2g	100/86	100/55	95/32	86/32	64/27
	1.2g<Sa<1.6g	100/91	100/64	86/55	64/91	50/-
	1.6g<Sa<2g	100/91	100/73	64/-	45/-	32/-
6/12 // 3/12	Sa<0.4g	100/100	100/82	100/68	86/73	86/68
	0.4g<Sa<0.8g	100/91	100/77	91/45	86/50	50/41
	0.8g<Sa<1.2g	100/86	100/45	95/36	86/27	73/27
	1.2g<Sa<1.6g	100/91	100/59	86/45	68/73	50/-
	1.6g<Sa<2g	100/91	95/77	82/95	45/-	27/-

		PLF(st2)/PLF(st1)=0.5				
Nail Pattern st2//st1	Hazard Level	PLF(st1)=1200	1400	1600	1800	2000
3/12 // 3/12	Sa<0.4g	50/68	32/68	27/50	27/59	27/64
	0.4g<Sa<0.8g	36/36	27/41	27/64	27/64	23/-
	0.8g<Sa<1.2g	50/50	50/95	32/-	27/-	27/-
	1.2g<Sa<1.6g	27/-	27/-	27/-	27/-	23/-
	1.6g<Sa<2g	32/-	27/-	27/-	23/-	19/-
4/12 // 3/12	Sa<0.4g	50/73	36/68	27/55	27/59	27/68
	0.4g<Sa<0.8g	32/36	27/50	27/73	27/68	27/95
	0.8g<Sa<1.2g	55/55	50/95	36/-	27/-	27/-
	1.2g<Sa<1.6g	32/-	27/-	27/-	27/-	27/-
	1.6g<Sa<2g	32/-	27/-	23/-	23/-	19/-
6/12 // 3/12	Sa<0.4g	45/73	41/55	27/55	27/50	27/55
	0.4g<Sa<0.8g	32/27	27/36	32/59	27/68	23/95
	0.8g<Sa<1.2g	64/27	50/59	41/-	32/-	32/-
	1.2g<Sa<1.6g	32/-	27/-	32/-	27/-	27/-
	1.6g<Sa<2g	32/-	27/-	32/-	23/-	23/-

Table 7-5 Design table D for two-story building (PNE(Drift)/PNE(Acceleration) value) , units in percentile

		PLF(st2)/PLF(st1)=1					
Nail Pattern st2//st1	Hazard Level	PLF(st1)=200	400	600	800	1000	1200
2/12 // 2/12	Sa<0.4g	100/91	100/59	91/50	86/64	59/68	27/68
	0.4g<Sa<0.8g	100/82	100/45	95/50	68/41	41/32	27/27
	0.8g<Sa<1.2g	100/82	100/27	95/23	86/27	73/27	64/27
	1.2g<Sa<1.6g	100/86	100/41	91/36	73/36	50/82	50/-
	1.6g<Sa<2g	100/91	95/64	77/73	50/-	32/-	36/-
3/12 // 2/12	Sa<0.4g	100/86	100/55	95/59	86/64	64/64	41/55
	0.4g<Sa<0.8g	100/82	100/45	95/45	73/41	41/27	27/27
	0.8g<Sa<1.2g	100/82	100/27	95/27	86/27	55/27	55/27
	1.2g<Sa<1.6g	100/86	100/41	86/41	59/45	45/82	32/-
	1.6g<Sa<2g	100/91	95/64	73/64	36/91	32/95	27/-
4/12 // 2/12	Sa<0.4g	100/91	100/59	95/64	86/73	73/68	41/59
	0.4g<Sa<0.8g	100/82	100/50	91/59	68/45	36/27	27/36
	0.8g<Sa<1.2g	100/82	100/36	95/36	77/32	55/32	45/59
	1.2g<Sa<1.6g	100/91	95/59	82/45	50/73	41/64	27/64
	1.6g<Sa<2g	100/91	95/68	59/73	41/82	27/91	27/-
6/12 // 2/12	Sa<0.4g	100/95	100/73	86/77	64/68	50/64	27/64
	0.4g<Sa<0.8g	100/91	95/64	77/50	36/50	27/68	27/73
	0.8g<Sa<1.2g	100/82	95/36	77/36	50/55	27/55	32/45
	1.2g<Sa<1.6g	100/86	91/55	50/77	27/77	27/64	27/59
	1.6g<Sa<2g	100/91	64/86	32/91	27/77	23/82	14/-

		PLF(st2)/PLF(st1)=1					
Nail Pattern st2//st1	Hazard Level	PLF(st1)=1400	1600	1800	2000	2200	2400
2/12 // 2/12	Sa<0.4g	27/50	27/45	27/45	19/50	19/59	19/55
	0.4g<Sa<0.8g	27/41	27/50	23/64	23/55	23/91	19/95
	0.8g<Sa<1.2g	45/32	41/73	36/95	36/-	32/-	32/-
	1.2g<Sa<1.6g	36/-	32/-	32/-	27/-	27/-	27/-
	1.6g<Sa<2g	32/-	27/-	27/-	27/-	19/-	19/-
3/12 // 2/12	Sa<0.4g	27/45	27/50	27/55	23/50	19/59	23/68
	0.4g<Sa<0.8g	32/36	27/50	23/55	23/95	23/-	23/95
	0.8g<Sa<1.2g	50/32	36/86	27/86	27/-	27/-	32/-
	1.2g<Sa<1.6g	27/-	27/-	32/-	36/-	27/-	23/-
	1.6g<Sa<2g	27/-	27/-	23/-	19/-	14/-	14/-
4/12 // 2/12	Sa<0.4g	27/50	27/59	27/55	23/59	23/68	23/82
	0.4g<Sa<0.8g	27/59	27/73	23/73	23/68	19/73	19/82
	0.8g<Sa<1.2g	27/50	27/55	27/59	27/59	27/95	27/-
	1.2g<Sa<1.6g	27/95	27/-	27/-	32/-	23/-	14/-
	1.6g<Sa<2g	23/-	19/-	14/-	14/-	14/-	14/-
6/12 // 2/12	Sa<0.4g	27/68	27/77	23/82	14/91	14/91	19/86
	0.4g<Sa<0.8g	19/68	23/59	19/68	9/64	14/64	14/64
	0.8g<Sa<1.2g	27/45	27/41	23/41	23/50	19/77	19/95
	1.2g<Sa<1.6g	23/82	19/-	14/-	14/-	14/-	14/-
	1.6g<Sa<2g	14/-	14/-	9/-	9/-	9/-	9/-

		PLF(st2)/PLF(st1)=0.75					
Nail Pattern st2//st1	Hazard Level	PLF(st1)=200	400	600	800	1000	1200
2/12 // 2/12	Sa<0.4g	100/100	100/64	91/59	91/59	82/59	91/59
	0.4g<Sa<0.8g	100/95	100/55	91/50	86/41	50/41	86/41
	0.8g<Sa<1.2g	100/82	100/23	95/27	95/27	86/27	95/27
	1.2g<Sa<1.6g	100/91	100/41	95/36	41/82	45/64	82/32
	1.6g<Sa<2g	100/91	100/64	86/45	64/-	41/-	55/-
3/12 // 2/12	Sa<0.4g	100/95	100/64	91/55	91/55	77/68	59/64
	0.4g<Sa<0.8g	100/95	100/64	91/50	86/41	55/41	36/27
	0.8g<Sa<1.2g	100/82	100/23	95/27	95/27	86/23	64/27
	1.2g<Sa<1.6g	100/91	100/45	95/36	86/32	55/64	50/86
	1.6g<Sa<2g	100/91	100/64	86/27	59/86	45/-	36/-
4/12 // 2/12	Sa<0.4g	100/95	100/59	100/59	91/59	86/68	64/59
	0.4g<Sa<0.8g	100/95	100/64	95/45	86/41	59/32	36/32
	0.8g<Sa<1.2g	100/82	100/32	100/27	86/32	82/23	55/27
	1.2g<Sa<1.6g	100/91	100/59	91/45	77/36	50/64	41/86
	1.6g<Sa<2g	100/91	100/68	82/73	50/77	36/-	27/-
6/12 // 2/12	Sa<0.4g	100/95	100/77	91/64	91/59	73/68	45/59
	0.4g<Sa<0.8g	100/91	100/68	86/55	64/41	27/36	27/50
	0.8g<Sa<1.2g	100/82	100/41	91/32	68/27	41/32	36/55
	1.2g<Sa<1.6g	100/91	95/64	73/59	45/73	27/64	27/50
	1.6g<Sa<2g	100/91	91/64	50/82	27/77	27/77	23/-

		PLF(st2)/PLF(st1)=0.75					
Nail Pattern st2//st1	Hazard Level	PLF(st1)=1400	1600	1800	2000	2200	2400
2/12 // 2/12	Sa<0.4g	27/59	27/50	27/41	23/45	19/45	23/55
	0.4g<Sa<0.8g	27/32	27/41	27/45	19/55	23/55	19/59
	0.8g<Sa<1.2g	55/27	45/32	45/55	36/95	27/-	27/-
	1.2g<Sa<1.6g	41/-	32/-	32/-	32/-	32/-	27/-
	1.6g<Sa<2g	32/-	32/-	27/-	27/-	27/-	19/-
3/12 // 2/12	Sa<0.4g	27/59	27/41	27/50	27/41	27/45	23/55
	0.4g<Sa<0.8g	27/27	27/32	27/32	23/50	23/59	23/86
	0.8g<Sa<1.2g	59/27	50/27	45/59	41/-	36/-	32/-
	1.2g<Sa<1.6g	50/-	41/-	32/-	36/-	36/-	32/-
	1.6g<Sa<2g	36/-	32/-	27/-	27/-	27/-	27/-
4/12 // 2/12	Sa<0.4g	36/50	27/45	27/41	27/59	27/50	23/59
	0.4g<Sa<0.8g	27/27	27/32	27/41	27/68	23/82	23/91
	0.8g<Sa<1.2g	55/32	41/55	36/77	27/73	27/95	27/-
	1.2g<Sa<1.6g	27/-	27/-	27/-	27/-	32/-	27/-
	1.6g<Sa<2g	27/-	27/-	23/-	23/-	19/-	14/-
6/12 // 2/12	Sa<0.4g	27/45	27/55	27/59	23/68	19/86	19/82
	0.4g<Sa<0.8g	27/77	27/73	23/64	19/64	19/64	14/73
	0.8g<Sa<1.2g	27/41	32/41	27/36	27/45	27/82	14/-
	1.2g<Sa<1.6g	27/82	27/-	23/-	19/-	14/-	14/-
	1.6g<Sa<2g	19/-	14/-	14/-	14/-	14/-	9/-

		PLF(st2)/PLF(st1)=0.5					
Nail Pattern st2//st1	Hazard Level	PLF(st1)=200	400	600	800	1000	1200
2/12 // 2/12	Sa<0.4g	100/100	100/86	100/68	91/64	77/64	77/64
	0.4g<Sa<0.8g	100/100	100/73	95/45	91/45	86/36	50/32
	0.8g<Sa<1.2g	100/91	100/59	100/27	95/27	91/23	77/27
	1.2g<Sa<1.6g	100/91	100/68	95/36	86/32	77/36	55/73
	1.6g<Sa<2g	100/91	100/73	95/68	82/64	45/-	36/-
3/12 // 2/12	Sa<0.4g	100/100	100/82	100/64	91/73	86/64	77/68
	0.4g<Sa<0.8g	100/100	100/73	100/45	91/45	82/36	45/32
	0.8g<Sa<1.2g	100/91	100/59	100/27	95/27	91/23	82/23
	1.2g<Sa<1.6g	100/91	100/68	95/36	86/32	77/36	55/68
	1.6g<Sa<2g	100/91	100/77	91/68	77/68	50/-	41/-
4/12 // 2/12	Sa<0.4g	100/100	100/82	100/64	91/64	91/64	82/55
	0.4g<Sa<0.8g	100/100	100/73	100/45	91/45	82/41	50/32
	0.8g<Sa<1.2g	100/91	100/59	100/23	95/82	95/23	77/27
	1.2g<Sa<1.6g	100/91	100/73	95/41	91/36	77/27	59/55
	1.6g<Sa<2g	100/91	100/82	91/64	77/55	55/-	45/-
6/12 // 2/12	Sa<0.4g	100/100	100/77	100/45	95/64	91/55	86/59
	0.4g<Sa<0.8g	100/91	100/77	100/45	91/41	77/36	50/32
	0.8g<Sa<1.2g	100/91	100/50	100/23	91/23	77/27	59/27
	1.2g<Sa<1.6g	100/91	100/59	95/41	77/45	45/50	41/73
	1.6g<Sa<2g	100/91	100/73	82/64	45/68	27/86	27/-

		PLF(st2)/PLF(st1)=0.5					
Nail Pattern st2//st1	Hazard Level	PLF(st1)=1400	1600	1800	2000	2200	2400
2/12 // 2/12	Sa<0.4g	50/59	32/64	27/45	27/36	27/41	23/45
	0.4g<Sa<0.8g	27/27	27/27	27/32	27/36	23/50	19/50
	0.8g<Sa<1.2g	50/27	55/27	50/27	45/32	36/86	27/95
	1.2g<Sa<1.6g	50/-	36/-	27/-	27/-	36/-	32/-
	1.6g<Sa<2g	36/-	27/-	27/-	32/-	23/-	23/-
3/12 // 2/12	Sa<0.4g	50/55	32/59	27/45	27/41	27/41	27/36
	0.4g<Sa<0.8g	32/27	27/27	27/27	27/32	27/36	19/45
	0.8g<Sa<1.2g	59/27	55/27	50/27	41/41	41/91	32/-
	1.2g<Sa<1.6g	55/-	45/-	27/-	27/-	27/-	27/-
	1.6g<Sa<2g	27/-	27/-	27/-	32/-	32/-	23/-
4/12 // 2/12	Sa<0.4g	55/64	32/55	27/45	27/41	27/45	27/32
	0.4g<Sa<0.8g	36/27	27/27	27/27	27/32	27/32	23/45
	0.8g<Sa<1.2g	64/27	55/27	50/27	50/27	41/55	41/95
	1.2g<Sa<1.6g	55/86	50/-	32/-	32/-	27/-	36/-
	1.6g<Sa<2g	27/-	32/-	32/-	27/-	27/-	27/-
6/12 // 2/12	Sa<0.4g	64/55	45/45	27/41	27/32	27/32	27/45
	0.4g<Sa<0.8g	27/27	27/27	27/32	27/55	27/73	23/73
	0.8g<Sa<1.2g	50/27	32/55	27/55	27/59	27/95	27/-
	1.2g<Sa<1.6g	27/86	27/-	27/-	27/-	27/-	23/-
	1.6g<Sa<2g	27/-	23/-	19/-	14/-	14/-	14/-

7.2 Design examples using simplified PBSD procedure

With the simplified PBSD design tables at hand, several design examples are outlined using the simplified procedure in this section, including the design for a typical residential building floor plan in North America such as Example II ('L' shape) and Example III (square shape) in Chapter 5.

7.2.1 Design examples with square shape floor plan

The floor plan and wall numbers are shown in Figure 7-2. Also, based on the numerical simulations done in Chapter 5, the floor acceleration did not control the design for most low-rise woodframe buildings, thus the inter-story drift was the only design target considered in this Section.

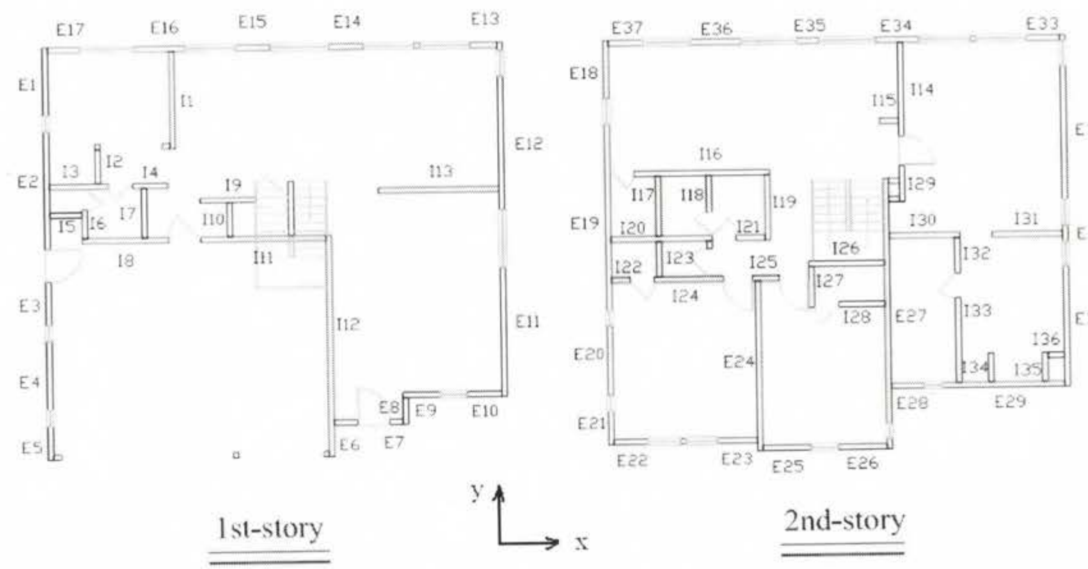

Figure 7-2 Floor plan and wall numbers for square shape design example

In single family dwellings the exterior walls are often designated as available for shearwalls. Hence, the wall number and wall length for the exterior walls in both stories are summarized in Table 7-6. It should be mentioned that the total wall length in the x-dir at the 1st-story is very short due to the large number of openings in that direction including the garage wall. Therefore the interior walls I8 and I11 were added as likely shearwalls. The total available shearwall length in each direction at both stories is also shown in the last row of Table 7-6. As one can see from Table 7-6, consideration of a minimum shearwall aspect ratio was not accounted for since the assumption is that the numerical model is accurately accounting for uplift and bending, if present.

Table 7-6 Shearwall length calculation for square shape design example

1st-story x-dir		1st-story y-dir		2nd-story x-dir		2nd-story y-dir	
Wall number	Wall length (ft)	Wall number	Wall length (ft)	Wall number	Wall length (ft)	Wall number	Wall length (ft)
E6	2.25	E1	6.5	E22	3.25	E18	5.5
E7	1.25	E2	11.25	E23	3.75	E19	17.5
E9	3.5	E3	4	E25	4.5	E20	6.5
E10	3.25	E4	6.5	E26	4.5	E21	3.25
E13	2.5	E5	3.25	E28	3	E30	11.25
E14	3.25	E8	2.5	E29	11.25	E31	1.5
E15	3.25	E11	12	E33	3	E32	12.75
E16	4.75	E12	12.75	E34	4		
E17	3			E35	2		
I8	8			E36	4.75		
I11	11.75			E37	3.25		
Total wall length (ft)	46.75		58.45		47.25		58.25

Based on the shearwall details listed in Table 7-6, the shearwall length in x-dir at 1st-story was selected as the design criteria to calculate the PLF value in the simplified PBSD procedure since it is the shortest overall. The seismic mass at the 1st-story was assumed to be equivalent to 30 psf and evenly distributed over the floor diaphragm. Hence the PLF at the 1st-story can now be calculated as:

$$PLF(st1) = \frac{30\,psf \times 1550\,ft^2}{46.75\,ft} = 995\,plf \approx 1000\,plf \tag{7-1}$$

Three different locations for the floor plan above were selected as three design example variants to illustrate the simplified PBSD procedure and are listed in Table 7-7. The target PNE values for the performance expectation for the inter-story drifts at those three locations would be the same as the ones in Chapter 5 and are listed in Table 7-8.

Table 7-7 Design examples using simplified PBSD design tables

Design Case	Design conditions of the design examples
I	Los Angeles, PLF(st2)/PLF(st1)=0.75
II	Sacramento, PLF(st2)/PLF(st1)=1
III	Portland, PLF(st2)/PLF(st1)=0.5

Table 7-8 Target PNE values for inter-story drift at different locations

PNE	Los Angeles	Sacramento	Portland
PNE_{I}	37%	29%	38%
PNE_{II}	34%	29%	31%
PNE_{III}	41%	41%	29%
PNE_{IV}	44%	37%	27%
PNE_{V}	54%	33%	25%

With all the information above, by choosing a shearwall nail pattern based on Table 7-2 to 7-5, the design for these three examples is demonstrated. The final shearwall configurations were listed in Table 7-8 with the shearwalls select for both stories shown shaded in Figure 7-3. It should be mentioned that the shearwall length in the design examples was using the length in x-dir at 1st-story which was the shortest one in both directions for both stories, the final design using design tables is therefore slightly conservative overall. Therefore, when comparing the PNE values listed in Table 7-2 to 7-5 to the design expectations (Table 7-8), the nail pattern combination may still be selected even if the PNE values fall a bit short of the design expectations (it is arbitrarily adopted in this study that a difference of 5% in PNE values is acceptable). Another thing that should be mentioned is that the designer may actually have multiple options to design the structure if the purpose is to exceed the performance requirements. For example, if the design in the Portland area and the PLF ratio was equal to 0.5, the designer can select any of the nail pattern combination (st2//st1): 6/12//6/12, 4/12//4/12, 6/12//4/12, 6/12//3/12…etc. Obviously, the final choice (6/12//6/12) listed in Table 7-9 is the most economical design from the available options. The actual PNE values resulting from the designed structure are shown in Table 7-10 (obtained from time history simulation with the designed configurations using the suite of earthquakes discussed throughout this dissertation). One can see that the performance exceeds the requirements, with one of the hazard intensity region controlling the design for each location shown shaded in Table 7-10.

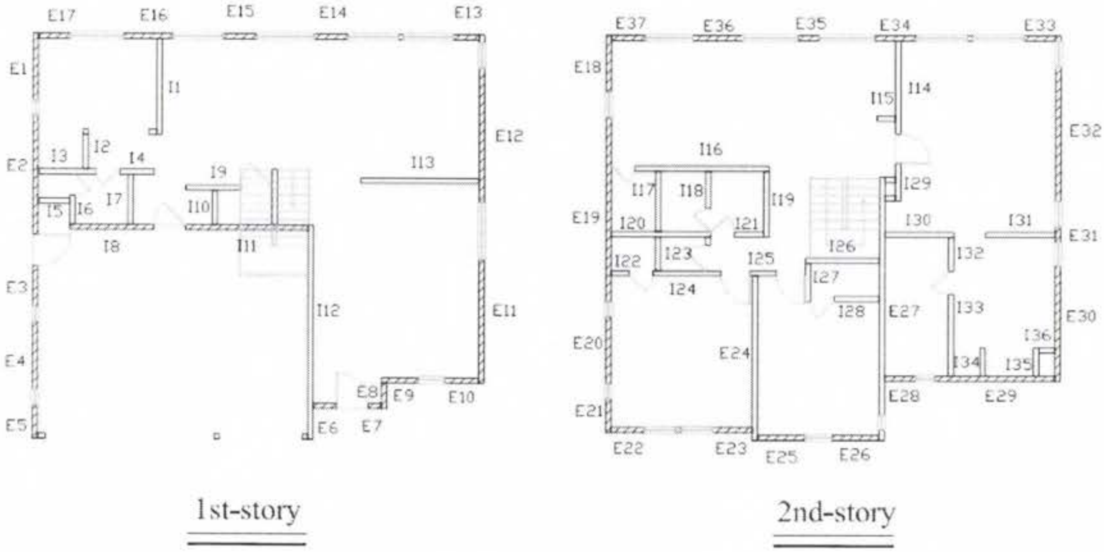

Figure 7-3 Shearwalls for design examples

Table 7-9 Design results for design examples using simplified PBSD design tables

Design Case	Design results of the design examples
I	Shearwalls at 1st-story were using nail pattern 2/12 and shearwalls at 2nd-story were using nail pattern 3/12
II	Shearwalls at 1st-story were using nail pattern 3/12 and shearwalls at 2nd-story were using nail pattern 4/12
III	Shearwalls at both stories were using nail pattern 6/12

Table 7-10 Resulted PNE values for inter-story drift from simplified design

	Los Angeles		Sacramento		Portland	
PNE	Target	Actual	Target	Actual	Target	Actual
PNE_I	37%	95%	29%	64%	38%	50%
PNE_{II}	34%	86%	29%	55%	31%	32%
PNE_{III}	41%	91%	41%	73%	29%	45%
PNE_{IV}	44%	82%	37%	50%	27%	36%
PNE_V	54%	68%	33%	41%	25%	36%

7.2.2 Design examples with 'L' shape floor plan

In order to illustrate the application of the simplified procedure to various floor plans, a non-square floor plan (the Example II in Chapter 5, 'L' shape) design example was also conducted and is presented in this Chapter. The floor plan and wall numbers are shown in Figure 7-4.

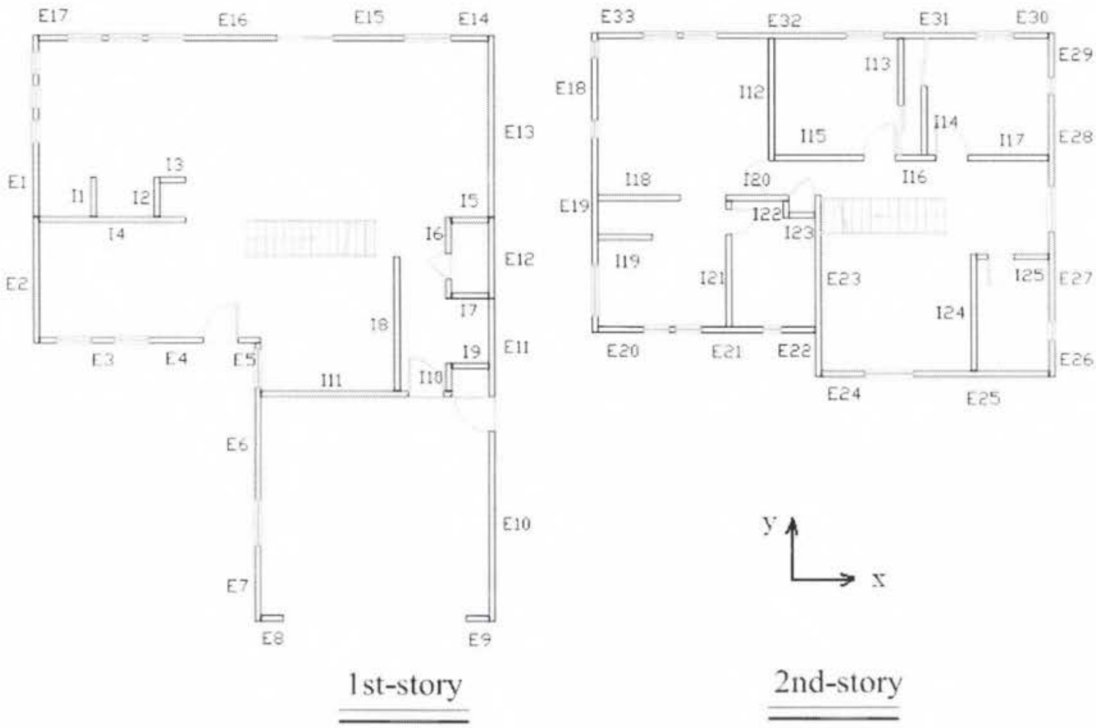

Figure 7-4 Floor plan and wall numbers for 'L' shape design example

Similarly, the wall number and wall length for the shearwalls in both stories are summarized in Table 7-11. Note that the interior walls I4 and I11 in the first story were called out as shearwalls also. The total available shearwall length in each direction at both stories is also shown in the last row of the Table 7-11.

Table 7-11 Shearwall length calculation for design example

1^{st}-story x-dir		1^{st}-story y-dir		2^{nd}-story x-dir		2^{nd}-story y-dir	
Wall number	Wall length (ft)	Wall number	Wall length (ft)	Wall number	Wall length (ft)	Wall number	Wall length (ft)
E3	2	E1	6.5	E20	4	E18	5.5
E4	4.75	E2	11.25	E21	5.5	E19	11.25
E5	2	E6	9.75	E22	3	E23	16.25
E8	2	E7	6.75	E24	3.75	E26	3.25
E9	2	E12	7.25	E25	11.75	E27	8
E14	3.25	E13	16	E30	3	E28	8
E15	6.25			E31	8	E29	4
E16	8.25			E32	11.25		
E17	2.5			E33	4		
I4	12.75						
I11	13						
Total wall length (ft)	58.75		57.5		54.25		56.25

The floor plan area is approximately 1570 sq. ft for story 1 and 1120 sq. ft for story 2. The seismic mass at the 1^{st}-story was assumed to be equivalent to 35 psf and evenly distributed over the floor diaphragm. The roof distributed mass was assumed to be 25 psf. Hence the PLF at the 1^{st}-story and 2^{nd} story can now be calculated as:

$$PLF(st1) = \frac{35 psf \times 1570 ft^2}{55 ft} = 999 plf \approx 1000 plf \tag{7-2}$$

$$PLF(st2) = \frac{25 psf \times 1120 ft^2}{55 ft} = 508 plf \approx 500 plf \tag{7-3}$$

Thus the PLF ratio of this structure is about 0.5. Using the target PNE values for the performance expectation in the Los Angeles area, the final shearwall configuration was selected to be 3/12 for story 2 and 2/12 for story 1. The final design performance was evaluated using non-linear time history analysis as with the previous example. The result show that actual PNE values satisfied the design target (see Table 7-12), and again the hazard intensity region controlling the design shown shaded in the Table 7-12.

Table 7-12 Resulted PNE values for inter-story drift from simplified design

	Los Angeles	
PNE	Target	Actual
PNE_I	37%	100%
PNE_{II}	34%	91%
PNE_{III}	41%	96%
PNE_{IV}	44%	82%
PNE_V	54%	55%

Chapter Eight

Conclusions, Contributions, and Recommendations

8.1 Summary and conclusions

As the standard design practice in current engineering practice, force-based design is mainly developed from component behavior. That is, components and sub-assemblies are designed and the building is assumed to perform as good or better at the system level. It has been shown to be reliable in most situations. However, the lessons learned from past catastrophic events (earthquakes, hurricanes, etc.) have also proven the need for the next generation of design philosophy and procedures which allow explicit consideration of system behavior. There is also a need for explicitly incorporating the probabilistic nature of extreme loading conditions and structural responses into engineering design philosophy. Because of the limitations of traditional force-based seismic design approaches and the increasing focus on system performance in modern structures, the concept of performance-based seismic design (PBSD) is considered a promising candidate of the next generation design methodology. The goal of PBSD is to design for the specific performance of the structure during earthquake loading, usually at the system-level. Of course, the components and sub-assembly performance is considered also as a subset of the methodology.

The accurate prediction of woodframe system performance under earthquake loading was needed for the proposed generalized PBSD procedure presented herein. The structural response prediction relies on numerical models and this necessitates the application of suitable numerical tools that can perform nonlinear time history analysis of woodframe buildings. A state-of-the-art nonlinear model capable of performing time history analysis was adopted in this study to conduct numerical simulations. Most of these models and numerical tools were developed during the CUREE-Caltech wood frame research project and expanded upon during the NSF-funded NEESWood research project. The SAPWood software package was selected for use in the present study because it is a three-dimensional model. This dissertation work extended the modeling capabilities of the SAPWood program by adding the ability to include FP bearings. Specifically, a half-scaled two-story woodframe building was built and base-isolated with four FP bearings on the uni-axial shake table. Practical issues related to the ability to construct full-scale prototypes using FP bearings were also investigated. Particularly the issues related to stiffening the floor diaphragm to ensure proper shear transfer from the base isolation points to the shear walls.

A generalized PBSD procedure was proposed in this dissertation which utilizes these state-of-art numerical models. The proposed design method utilizes a target curve which is a combination of the multiple hazard levels and the expected building performance levels. However, it is important to note that the proposed procedure is more generalized in a sense that a wide range of hazard and performance levels can be used to construct the design target (instead of only concentrating on inter-story drift as is the current state-of-the-art) depending on what is desired in the way of performance. For example, the performance level can be peak floor acceleration which is also an important concern when designing buildings above two stories. As an improvement to existing performance requirements in PBSD, a probability of non-exceedance (PNE) value is assigned to each combination of hazard and performance level which is linked to the building site information, end-user input, and minimum (life) safety requirements. Through this PNE value, the uncertainty of the earthquake ground motion was incorporated into the design by using earthquake suites and time history simulation.

The generalized PBSD procedure was then applied to different woodframe buildings at several different locations. The design examples used in this study include typical low-rise residential buildings in North America and a mid-rise woodframe condominium building. For the first time in the PBSD of woodframe structures, both inter-story drift and floor acceleration were selected as performance targets. Although only illustrative, the method used in defining the PNE values for the example structures was the first time a method has the ability to incorporate the end-user (e.g. owner) wishes into the structural performance expectations. Architecturally this has been done since the beginning of building construction, but once model building design codes were developed performance choices for woodframe buildings were severely reduced and even eliminated. The design procedure was shown to be viable through traditional measures (add/move shearwalls, change the nail pattern, etc.) for these design examples. An alternative and effective way to satisfy a much more strict design target using the FP bearing system was also shown in this study.

Since the generalized PBSD procedure requires a significant amount of numerical simulation using nonlinear time history models, and would therefore be quite tedious for engineers in practice, a simplified procedure for PBSD of low-rise woodframe buildings was developed based on numerical simulation results using strategically selected structural configurations.

The conclusions that can be drawn from this study include:

1) With the addition of the FP slider base isolation element, the SAPWood program can be used to perform numerical analysis on base isolated woodframe structures with FP bearings. The accuracy of the numerical model was verified through multiple shake table experiments.
2) The use of FP isolation system is a viable option for passive seismic protection of woodframe structures.
3) The generalized PBSD procedure, and particularly the PNE value, proposed in this study gives more freedom to design engineers to explicitly improve the performance expectation of a woodframe building beyond what is currently provided by force-based design.

4) It was more logical to develop the performance target used in PBSD based on multiple influential factors such as site/hazard condition, end-user concerns, and minimum engineering requirements.

5) The floor acceleration does not typically control the design for low-rise buildings. For mid-rise buildings, it must have some consideration in a performance based seismic design.

6) The simplified, or prescriptive procedure, was verified using nonlinear time history analysis and therefore proved that the simplified procedure was a viable option for design of one- and two-story woodframe buildings.

8.2 Contributions

The contributions of this dissertation work to the woodframe research and design community are the following:

1. This study is the first time that an FP bearing system has been tested on a shake table under a woodframe building in the United States. The study verified the effectiveness of this technique on woodframe buildings and also resulted in numerical tools to analyze and predict the behavior of base isolated woodframe buildings.

2. The generalized PBSD procedure proposed in this dissertation is the most general form developed to date. It expanded the current focus on inter-story drift to multiple performance targets including peak floor acceleration. The idea of incorporating

end-user's input and design minimum requirements into the PBSD target curve is novel and supports the original intent of performance-based design.

3. The simplified PBSD procedure developed in this study provides an efficient and reliable approach to low-rise woodframe building design. This type of prescriptive approach may be able to provide a tool that provides designers the benefits of performance-based seismic design without the requirement or need for knowledge of the details of nonlinear time history analysis.

8.3 Recommendations

Based on the results and conclusions obtained from this study, there are several potential areas of study that can further improve the effectiveness of woodframe PBSD research and applications. These are as follows:

1. Although the numerical model of the FP isolation bearing used in this study was able to model three-dimensional ground excitation situation, it was only verified using the uni-axial shake table test at CSU. More application of base isolation systems on woodframe structures and experimental investigation with more realistic ground motion at full scale will help to further verify the FP bearing numerical model in SAPWood and probably provide opportunities to improve the numerical model for better prediction. In order to make base isolation economically viable for residential structures, additional practical and detailing issues should be examined.

2. Although the formula for defining the PNE value for each segment of the performance curve was proposed in this study, the illustrative examples utilized arbitrary assumptions to incorporate the building site/location and the end-user's wishes. Therefore, a study towards an appropriate method to obtain the performance PNE values that are compatible to current design safety levels should be conducted. The specific format for this conceptual formula needs to be further studied.

3. Finally, the simplified PBSD design tables presented in this study are limited to one- and two-story woodframe buildings. While these are the most common buildings in North America, the design tables should be expanded to buildings three stories and up for a wider range of applications. There are challenges in developing simplified or tabulated procedures for structures higher than two stories and other procedures may be needed.

References

Almazan J. L., De la Llera J. C. and Inaudi J. A. Modelling aspects of structures isolated with the frictional pendulum system. *Earthquake Engineering and Structural Dynamics*, v 27, 1998, p 845-867

ASCE 41 Seismic Rehabilitation of Existing Buildings. ASCE Standard No. ASCE/SEI 41-06. *American Society of Civil Engineers* 2007

ASCE 7 Minimum Design Loads for Buildings and Other Structures. ASCE Standard No. ASCE/SEI 7-05. *American Society of Civil Engineers* 2006

ASD supplements of NDS for wood construction. *American Forest and Paper Association and the American Wood Council* 2001

ATC63 project report (90% draft) Quantification of Building Seismic Performance Factors. FEMA P695, April, 2008

Bertero, V., Aktan, A. E., Charney F. and Sause R. Earthquake simulator tests and associated experimental analytical and correlation studies of one-fifth scale model. *Earthquake Effects on Reinforced Concrete Structures – U.S.-Japan Research*, SP-84, American Concrete Institute, 1985, p 375-424

Caccese, V. and Harris H.G. (1990) Earthquake simulation testing of small-scale reinforced concrete structures. *ACI Structural Journal (American Concrete Institute)*, v 87, n 1, Jan-Feb, 1990, p 72-80

Christovasilis, I.P., Filiatrault, A. and Wanitkorkul A. Seismic test of a full-scale two-story light-frame wood building: NEESWood benchmark test. NEESWood project report NW01, 2007

Constantinou M.C.. Properties of sliding bearings: Theory and Experiments. Passive and Active Vibration Control in Civil Engineering, Springer Verlag Wien – New Your, 1994, p 97-109

Constantinou, M., Mokha, A. and Reinhorn, A. Teflon bearings in base isolation II: modeling. *Journal of Structural Engineering*, v 116, n 2, February, 1990, p 455-474

Ellingwood, B.R., Rosowsky, D.V. Li, Y. and Kim, J.H. Fragility assessment of light-frame wood construction subjected to wind and earthquake hazards. *Journal of Structural Engineering*, v 130, n 12, December, 2004, p 1921-1930

Federal Emergency Management Agency (FEMA) (2000a). Prestandard and Commentary for Seismic Rehabilitation of Buildings, FEMA356, Federal Emergency Management Agency, Washington, DC.

Filiatrault A. and Folz B. Performance-based seismic design of woodframed buildings. *Journal of Structural Engineering*, v 128, n 1, January, 2002, p 39-47

Foley C.M. Optimized Performance-based Design for Buildings. *Recent Advances in Optimal Structural Design*. Burns S.A. (editor) ASCE, Structural Engineering Institute, Reston , VA 2002 (Chapter 8)

Folz, B. and Filiatrault, A. Cyclic analysis of wood shear walls. Journal of Structural Engineering, v 127, n 4, p 433-441, 2001

Folz, B. and Filiatrault, A. Seismic analysis of woodframe structures. II: Model implementation and verification. *Journal of Structural Engineering*, v 130, n 9, p 1361-1370, 2004

Foschi, R.O. Estimating reliability and implementing performance based design for shearwall. *Proceeding Structure Congress 2003*, Seattle, WA.

International Code Council, International Building Code, 2006 version, Washington DC, 2006

ICBO, (1998). *Uniform Building Code*, 1998 edition, International Conference of Building Officials, Whittier, California.

Iiba M., Midorikawa M., Yamanouchi Y., Ikenaga M. and Machida K. Construction of a base-isolated house for observation of isolation effects during earthquake and wind. *Proceedings of the Joint Meeting of the U.S.-Japan Cooperative Program in Natural Resources Panel on Wind and Seismic Effects*, v 32, 2001, p 203-211

Krawinkler, H., F. Parisi, L. Ibarra, A. Ayoub, and R. Medina. Development of a Testing Protocol for Woodframe Structures, CUREE Publication No. W-02, Richmond, CA., 2000

Lippke, B. and Edmonds, L. Environmental performance improvement in residential construction: the impact of products, biofuels and processes. *Forest Products Journal*, v 56, n 10, October, 2006, p 58-63

Liu M. Seismic Design of Steel Moment-Resisting Frame Structures Using Multiobjective Optimization. Earthquake Spectra, v 21, n 2, May 2005, p 389-414

Liu M., Burns, A. S. and Wen Y. K. Multiobjective optimization for performance-based seismic design of steel moment frame structures. *Earthquake Engineering and Structural Dynamics*. v 34, 2005, p 289-306

Mokha, A.S., Amin, N., Constantinou, M.C. and Zayas, V. Seismic isolation retrofit of large historic building. *Journal of Structural Engineering*, v 122, n 3, March, 1996, p 298-308

Mosqueda, G., Whittaker, A.S., Fenves, G.L. Characterization and modeling of friction pendulum bearings subjected to multiple components of excitation. *Journal of Structural Engineering*, v 130, n 3, March, 2004, p 433-442

Naeim Farzad, Kelly J. M. Design of seismic isolated structures. John Wiley & Sons, INC 1999

Noor F A, Boswell L F. Small scale modeling of concrete structures, *Taylor & Francis Books Ltd* 1998

Pang, W. and Rosowsky, D. Direct displacement procedure for performance-based seismic design of multistory woodframe structures. NEESWood project report NW02, 2007

Pang, W.C., Rosowsky, D.V., Pei, S. and van de Lindt, J.W. Evolutionary parameter hysteretic model for wood shear walls. *Journal of Structural Engineering*, v133, n8, 2007, p1118-1129

Pei, S. and van de Lindt, J.W. Methodology for earthquake-induced loss estimation: An application to woodframe buildings. *Structural Safety*. In press, 2008.

Pei, S. Loss Analysis and Loss Based Seismic Design for Woodframe Structures. Doctoral dissertation, 2007, Colorado State University, Fort Collins, CO

Porter, K.A., Beck J.L., Seligson H.A., Scawthorn C.R., Tobin L.T., Young R. and Boyd T. Improving loss estimation for woodframe buildings. CUREE Publication No. W-01, CUREE-Caltech Woodframe Project, Department of Structural Engineering, University of California, San Diego.

Priestley, M.J.N. Displacement-based approaches to rational limit states design of new structures. Keynote Address, *Proceedings of the 11th European Conference on Earthquake Engineering*, Paris, France, 1998

Rosowsky, D.V. and Ellingwood, B.R. Performance-based engineering of wood frame housing: a fragility analysis methodology. *Journal of Structural Engineering*, v 128, n 1, January, 2002, p 32-38

Ryan, K.L. and Chopra A.K. Estimating the seismic displacement of friction pendulum isolators based on non-linear response history analysis. *Earthquake Engineering and Structural Dynamics*, v 33, 2004, p 359-373

Samli B., Li J., Mayol E., Wu Y. M. System identification of a five storey benchmark model using modal analysis. *The Proceedings of the International Conference on Applicatiions of Modal Analysis*. Dec, Gold Coast, Australia, 1999.

Shinde, J.K., Symans, M.D., Liu, H. and van de Lindt, J.W. Seismic performance assessment of woodframed structures with energy dissipation systems. *Proceeding of Eighteenth Conference on Analysis and Computation* held in Conjunction with ASCE/SEI Structures Congress 2008, Vancouver, Canada, April,2008.

Symans M. D., Cofer W. F., and Fridley K. J. Base isolation and supplemental damping systems for seismic protection of wood structures: literature review. *Earthquake Spectra*, v 18, n 3, August, 2002, p 549-572

Vamvatsikos D. and Cornell C.A. Incremental dynamic analysis. *Earthquake Engineering and Structural Dynamics*, v 31, 2002, p 491-514

van de Lindt, J. W. Damage-based seismic reliability concept for woodframe structures. *Journal of Structural Engineering*, v 131, n 4, April, 2005, p 668-675

van de Lindt J. W., Liu H. Nonstructural elements in performance-based seismic design of wood frame structures. *Journal of Structural Engineering*, v 133, n 3, Mar, 2007 p 432-439

van de Lindt J. W., Liu H. and Pei S. Performance of a woodframe structure during full-scale shake table tests: drift, damage and effect of partition wall. *Journal of Performance of Constructed Facilities*, v 21, n 1, Jan-Feb, 2007 p 35-43 van de Lindt, J. W., Pei, S. and Liu, H. Performance-based seismic design of wood frame buildings using a probabilistic system identification concept. *Journal of Structural Engineering*, v 134, n 2, 2008, p 240–247

van de Lindt, J.W., Rosowsky, D.V., Filiatrault, A., Symans, M.D., Davidson, R.A. The NEESWood Project: Progress on the Development of a Performance-Based Seismic Design Philosophy for Mid-Rise Woodframe Construction. *World Conference on Timber Engineering*, Portland, OR., 2006

van de Lindt, J. W., and Walz, M. A. Development and application of wood shear wall reliability model. *Journal of Structural Engineering*, v 129, n 3, 2003, p 405–413

van de Lindt, J.W. Energy-Based Similitude for Dynamic Scaling of Woodframe Structures. *Journal of Earthquake Engineering*, v 12 , n 2, 2008, p281-292

Wu Y. M., Samali B. Shake table testing of a base isolated model. *Engineering Structures*, v 24, n 9, September, 2002, p 1203-1215

Zarnic R., Gostic S., Crewe A. J. and Taylor C. A. Shaking table tests of 1:4 reduced-scale models of masonary infilled reinforced concrete frame buildings. *Earthquake Engineering and Structural Dynamics*, v 30, n 6, June, 2001, p 819-834

Zhang, J. and Foschi, R.O. Performance-based design and seismic reliability analysis using designed experiments and neural networks. *Probabilistic Engineering Mechanics*, 2004, v 19, p 259-267